PREDICTION OF THE FORMATION OF DENSITY CURRENTS FOR THE MANAGEMENT OF RESERVOIR SEDIMENTATION

GR Basson · A Oosthuizen · H Wicht · SP van der Walt

WRC Report No. 911/1/03

Water Research Commission

PREDICTION OF THE FORMATION OF DENSITY CURRENTS FOR THE MANAGEMENT OF RESERVOIR SEDIMENTATION

Report to the

Water Research Commission

by

G R Basson, A Oosthuizen, H. Wicht and S P van der Walt

Department of Civil Engineering

University of Pretoria

WRC Report No. 911/1/03

ISBN No. 1-77005-071-X

August 2003

Disclaimer

This report emanates from a project financed by the Water Research Commission (WRC) and is approved for publication. Approval does not signify that the contents necessarily reflect the views and policies of the WRC or the members of the project steering committee, nor does mention of trade names or commercial products constitute endorsement or recommendation for use.

Printed by Silowa Printers: 012 804 7565

Summary

Reservoir sedimentation causes an average annual loss in storage capacity of 130 million m³ in South Africa. In a semi-arid country such as South Africa measures to limit the rate of reservoir sedimentation such as flushing is in most cases not feasible due to the lack of excess water. Density current venting is however one management technique whereby high river sediment loads can be transported through a reservoir and released to the downstream river through bottom outlets, without water level draw-down of over-year storage reservoirs. If sufficient fine sediment is available with suitable boundary conditions, the turbulent river flow plunges to the reservoir bottom to transport the sediment at the bed in a density current.

This study investigated the use of a new theory based on minimum stream power at the plunge point, to predict the formation of a density current. Laboratory tests were carried out with sediment transport to verify the theory. Clear water flume tests were also carried out to investigate the velocity distribution at the plunge point and the critical hydraulic conditions required for stable density current formation.

Field data of three dams were used to verify the theory. The density current formation and location of plunging could be forecasted with the minimum input stream power theory.

The generally used densimetric Froude number theory indicates a wide range of values based on the laboratory data of this study. It s however related to the density difference ratio created by the sediment load of the river, and it is proposed that the densimetric Froude number is used as recommended in this report as alternative to the minimum stream power approach.

Capacity building:

This study was used for three undergraduate student dissertations at the University of Pretoria and the University of Stellenbosch, and also currently forms part of one MSc study.

The guidelines provided in this study to determine density current formation should be used for all planning, feasibility and detail design studies by the Department of Water Affairs and Forestry, and is important not only as possible sediment management technique, but also to determine the spatial distribution of sediment deposition in the reservoir and to design suitable outlet works.

The methodology proposed in this study has already been used in the design of the Mohale Dam (Lesotho Highlands Water Project) outlet works and to evaluate the Mohale-Katse tunnel intake location.

Table of Contents

Table of Contents (cont.)

Table of Contents (cont.)

List of Figures

List of Figures (cont.)

List of Tables

List of Symbols

B_D	flow width of density current
B_R	flow width of river
d	density current flow depth
D	plunge point water depth
E	Specific energy
Fr	Froude number
Fr_D	Densimetric Froude number
g	gravitational acceleration
γ	specific weight of water
Δγ	density difference
γ'	specific weight of density current
h_0	water depth at plunge point
k_s	bed roughness
κ	von Kármán coefficient
ρ	water density
ρ_D	density current density
ρ_R	river water density
ρ_w	clear water density
Δρ	water density difference
$\frac{d\rho}{\rho}$	density difference ratio
q	unit discharge
Q	discharge
Re	Reynolds number
s_o	bed slope assuming a uniform density current
s_f	energy slope
τ	shear stress
$\tau\frac{dv}{dy}$	applied unit stream power
μ	dynamic viscocity
v	flow velocity
y	point depth or flow depth

Acknowledgements

The study team wishes to thank the South African Water Research Commission (Project Leader, Mr H. Maaren) for sponsoring this research project.

Thanks are also due to the Steering Committee members for their role in steering this project to its successful completion:

Mr H Maaren	-	Water Research Commission (Late Chairman)
Mr DS van der Merwe	-	Water Research Commission
Prof GR Basson	-	University of Pretoria
Dr Harry Swart	-	LHA
Prof A Rooseboom	-	University of Stellenbosch
Prof CS James	-	University of the Witwatersrand
Mr W van Wyk	-	BKS (Pty) Limited

1. INTRODUCTION

1.1 Background

The Water Research Commission project: Dealing with Reservoir Sedimentation (Basson and Rooseboom, 1997), studied the various modes of sediment transport through a reservoir in detail.

A density current (also known as gravity current or turbidity current) may form at the upstream end of a reservoir in the delta region, due to the higher inflowing river's suspended sediment concentration during floods than that of the relatively clear water in the reservoir. At the point where the inflowing river dives to the bottom of the reservoir to form a density current, the plunge point (or plunge line) is observed which is indicated in the field by floating stationary debris. A schematic diagram of this phenomenon is shown in Figure 1.1-1.

A new theory was derived during the 1997 study to describe the formation of sediment induced density currents in a reservoir, which was also successfully verified against data of Akiyama and Stefan (1987). The data obtained from the experiments of Akiyama were however for density currents formed by temperature differences, and there was therefore a need to verify the new theory against sediment induced density currents.

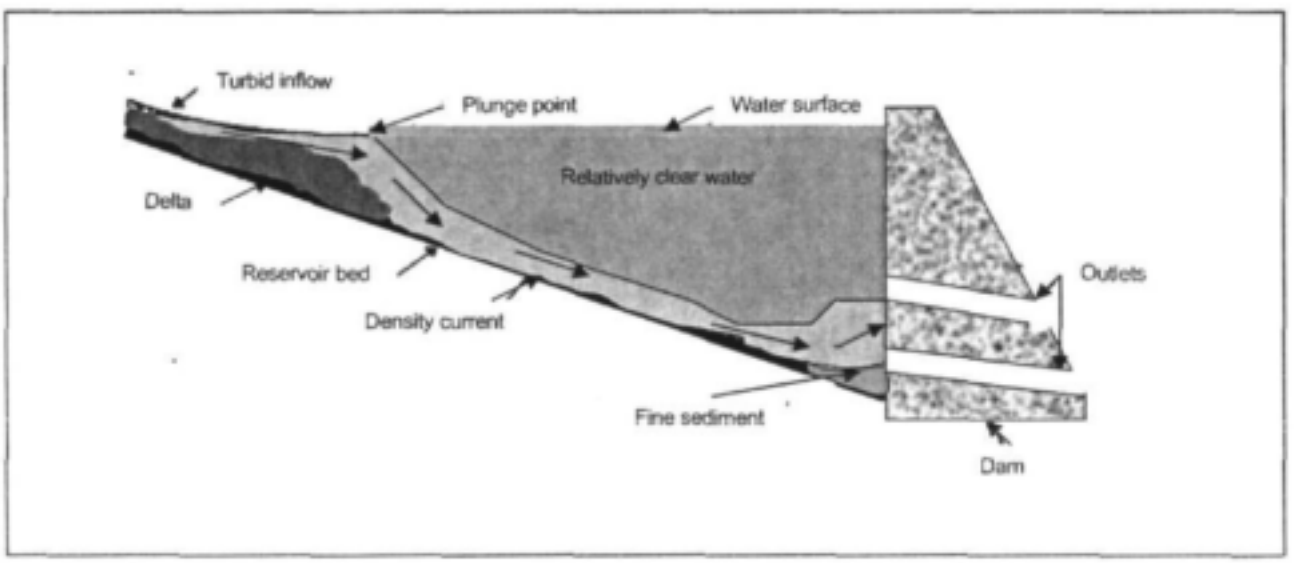

Figure 1.1-1 Schematic diagram of density current formation

This relatively small study commenced in January 1998 and was scheduled for completion in December 1998. However, due to the difficulty experienced in obtaining reservoir field data from international sources and additional tests carried out on the plunge line in the laboratory, the study duration was extended.

1.2 Objectives of the study

This research project was originally proposed in 1997 to:

- verify the minimum input stream power theory to describe sediment induced density current formation (derived in WRC project K5/580), against sediment induced density currents forming in a laboratory flume.

- investigate the reliability and possible constraints of the new input stream power theory, also verifying it against the densimentric Froude number theory generally used.

- verify the prediction of density current formation against observed reservoir field data

- investigate the possibility of forcing density current formation in a reservoir as management technique to limit reservoir sedimentation.

All of the above objectives have been addressed during the study.

1.3 Motivation

Reservoir sedimentation in South Africa causes an average annual loss of 130 million m^3 storage capacity, which is a medium sized reservoir and replacement cost is very high, especially if the social and environmental costs are considered. The historical growth in storage capacity in South Africa is shown in Figure 1.3-1. In future more storage capacity would be required to cater for future sedimentation, as indicated in Figure 1.3-1, or improved management techniques have to be developed. One such measure that can be considered is density current venting which is especially applicable with over-year storage operation and fine sediment transport conditions that are generally found in South Africa.

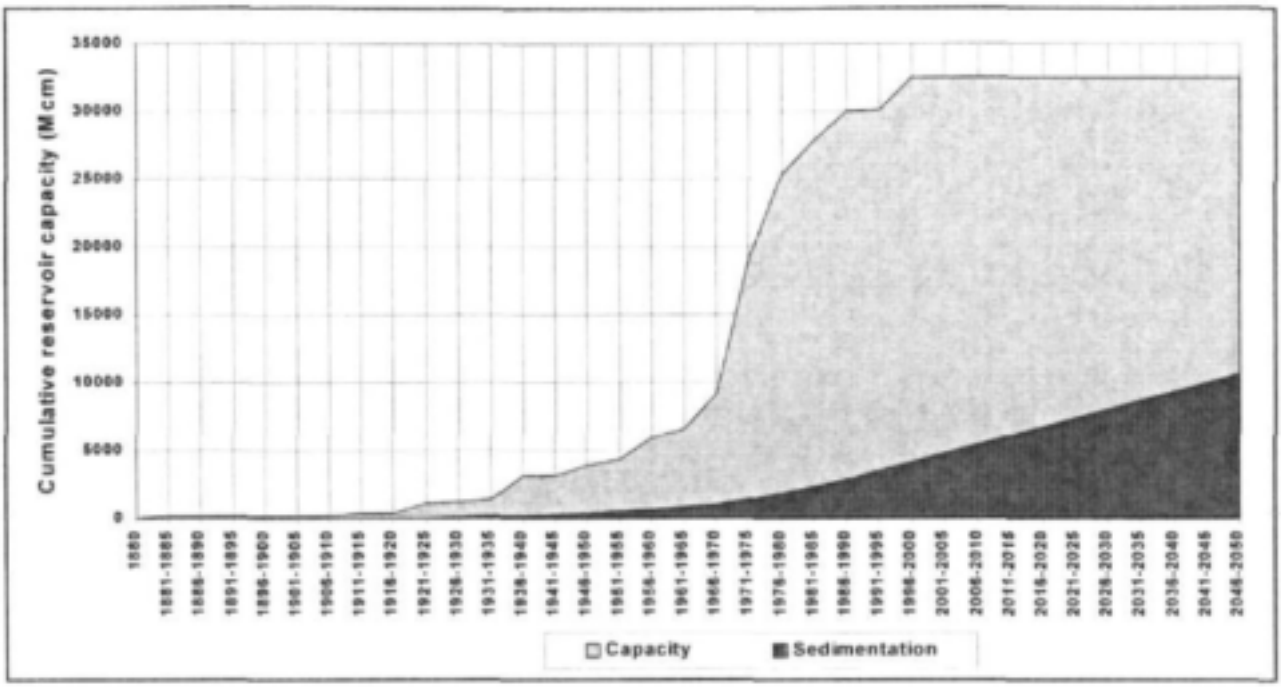

Figure 1.3-1 Historical growth in storage capacity and projected future reservoir sedimentation in South Africa

Existing theory (Fan, 1960) to describe density current formation only provides a rough indication whether sediment would be transported through the reservoir in turbulent suspended sediment transport mode or in a density current. Since many reservoirs in South Africa are relatively large compared to the mean annual runoff (MAR) with over-year storage, most of the sediment transported into these reservoirs are trapped. Not enough excess water is available for sediment flushing or sluicing during floods, with water level draw-down to pass high sediment yields through, and therefore the mode of operation of these reservoirs are often storage operation. The management measures that could be employed to limit or control the rate of reservoir sedimentation when a reservoir storage capacity/MAR ratio is large are:

- Soil-water conservation programmes in the catchment
- density current venting through bottom outlets
- dredging or hydrosuction (siphon)
- raising of the dam
- construction of a new dam
- bypassing by tunnel or canal
- off-channel storage dams

Dredging, the raising of a dam and new dam construction, often have serious environmental and economic consequences and should in most cases not be considered in sustainable dam development, when there is an option such as the venting of density currents. With the latter operational mode, it should be possible under specific boundary conditions to release high sediment loads from the reservoirs, without water level draw down (storage operation), thereby minimizing reservoir sedimentation and changes in both the upstream and the downstream river morphology.

Reservoirs where density current venting of sediment would be useful (not enough excess water available for flushing), typically have a capacity-MAR ratio larger than 0.2, as classified in Figure 1.3-2 (Basson and Rooseboom, 1997).

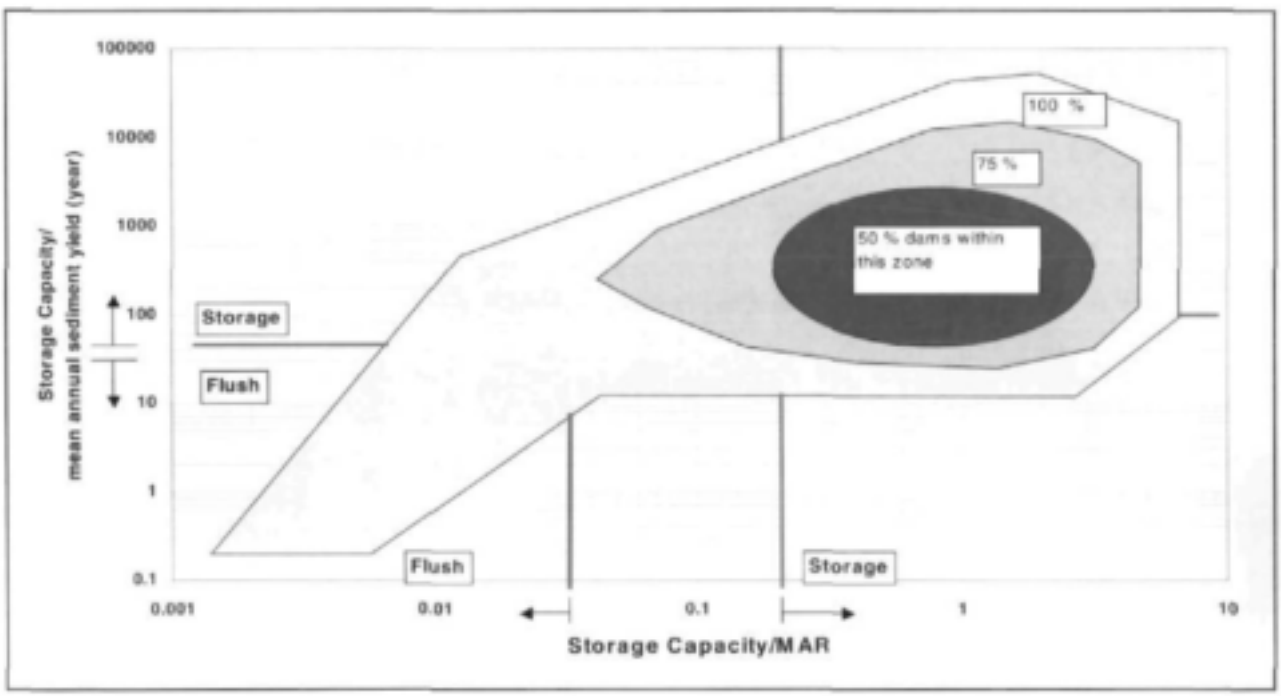

Figure 1.3-2 Reservoir operation and sedimentation

Accurate prediction whether a density current would form in a reservoir, is very important to determine:

- the need for density current venting and for the design and judicious operation of low level outlets
- the spatial distribution of sediment deposition in a reservoir, and impacts on offtake structures
- the long-term rate of sedimentation of a reservoir, in the dead or live storage zones
- sustainable development and operation of a reservoir
- the sediment balance in the reservoir-river system.

1.4 Methodology

The methodology adopted for this study included:

- Laboratory flume tests on sediment induced density currents
- Verification of the minimum input stream power against these test results
- Laboratory tests on clear water plunge line hydraulics
  Modification of the theory if required
- Analysis of reservoir field data using case studies where density currents have been observed (international dams), as well as a local reservoir with turbulent suspended sediment transport

1.5 Layout of the report

Chapter 1: Provides the motivation and background to the study

Chapter 2: Existing and proposed new theory on density current formation

Chapter 3: Laboratory flume tests on density current formation and verification of the proposed theory

Chapter 4: Verification of the theory against field data

Chapter 5: Provides data on sediment size requirements to form a density current

Chapter 6: Viewpoint on forced density current formation as management technique

Chapter 7: Gives a typical proposed calculation procedure to determine density current formation

Chapter 8: Conclusions and Recommendation

2. DENSITY CURRENT FORMATION THEORY

2.1 Description of density current formation

If for example, a river carrying an appreciable amount of suspended sediment enters a quiet body of clear water, the turbid water could plunge beneath the mass of clear water and travel by gravity along the bed of the standing body of water. A density (or gravity) current can be simply defined as a current that carries fine-grained sediment in suspension. Water charged with fine suspended particles is denser than clear water of the same temperature and salinity, and, because of its greater density, the water that carries suspended sediment can flow beneath less dense clear water.

The location where the density current dives to the reservoir bed is called the plunge point, although plunging actually occurs across the river at what is known as a plunge line. On the water surface a line of floating stable debris is typically observed, indicating the plunge line, which is curved according to the river surface flow velocity. The debris seems to be trapped by the slowly upstream movement of reservoir surface water. A typical example of a plunge line as observed at Eril Emda Reservoir, Algeria, is shown in Figure 2.1-1.

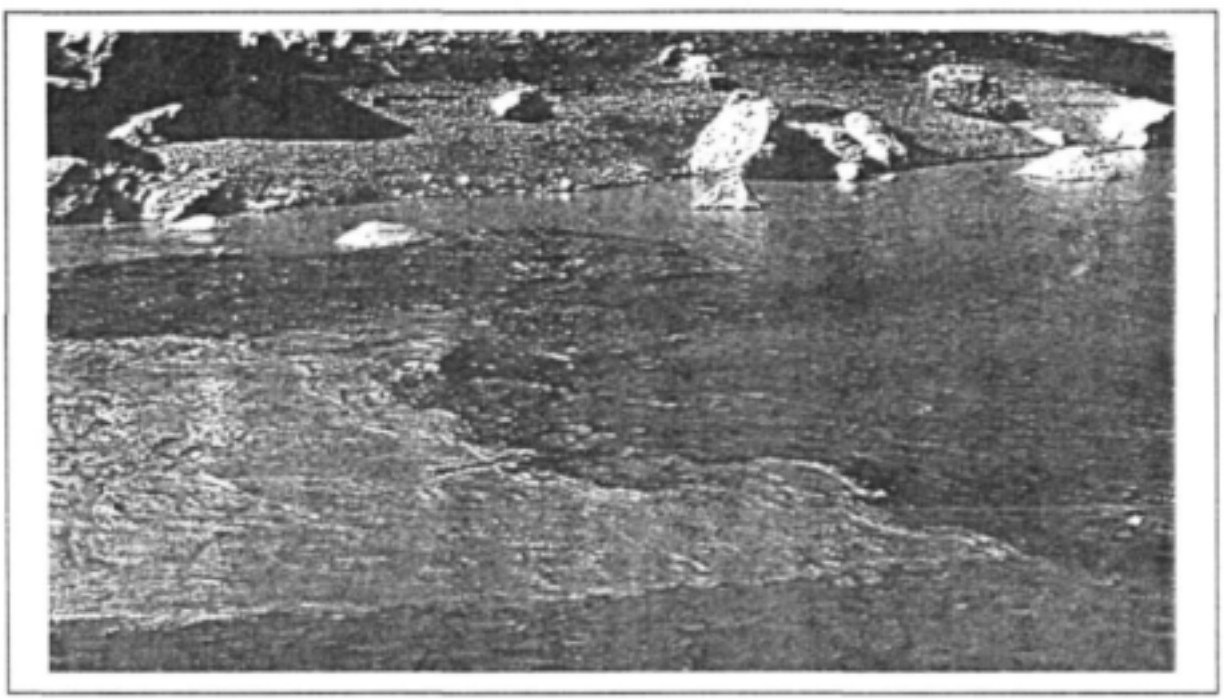

Figure 2.1-1 Observed plunge line at Eril Emda Reservoir, Algeria (Dequennois, 1956)

2.2 Formation theory

Various theories to describe density current formation have been derived (Refer to Basson and Rooseboom, 1997, for a discussion). In this report only the widely used densimetric Froude number and minimum stream power concepts have been investigated, however.

2.2.1 Densimetric Froude number theory (Fan, 1960)

Upstream of the plunge point, the velocity decreases as the depth increases in the transition zone from open channel flow to the reservoir flow, and the velocity becomes a minimum and the depth of water approaches a maximum at the spot of plunge of the muddy water (Figure 2.2-1). Therefore the specific energy (E) (equation 2.2-1) (Fan, 1960):

$$E = h_0 + \frac{v^2}{2\frac{\Delta\gamma}{\gamma} g h_0} \qquad (2.2\text{-}1)$$

with h_0 = water depth at plunge point
v = flow velocity
γ = specific weight of water
$\Delta\gamma$ = $\gamma' - \gamma$
γ' = specific weight of density current
g = gravitational acceleration

has a minimum value at the spot where the inflowing turbid water begins to plunge, or

$$\frac{\partial E}{\partial h_0} = 1 - \frac{q^2}{\frac{\Delta\gamma}{\gamma} g h_0^3} = 0 \qquad (2.2\text{-}2)$$

with q = unit discharge

Once the density current is formed, the bed slope controls the underflow conditions.

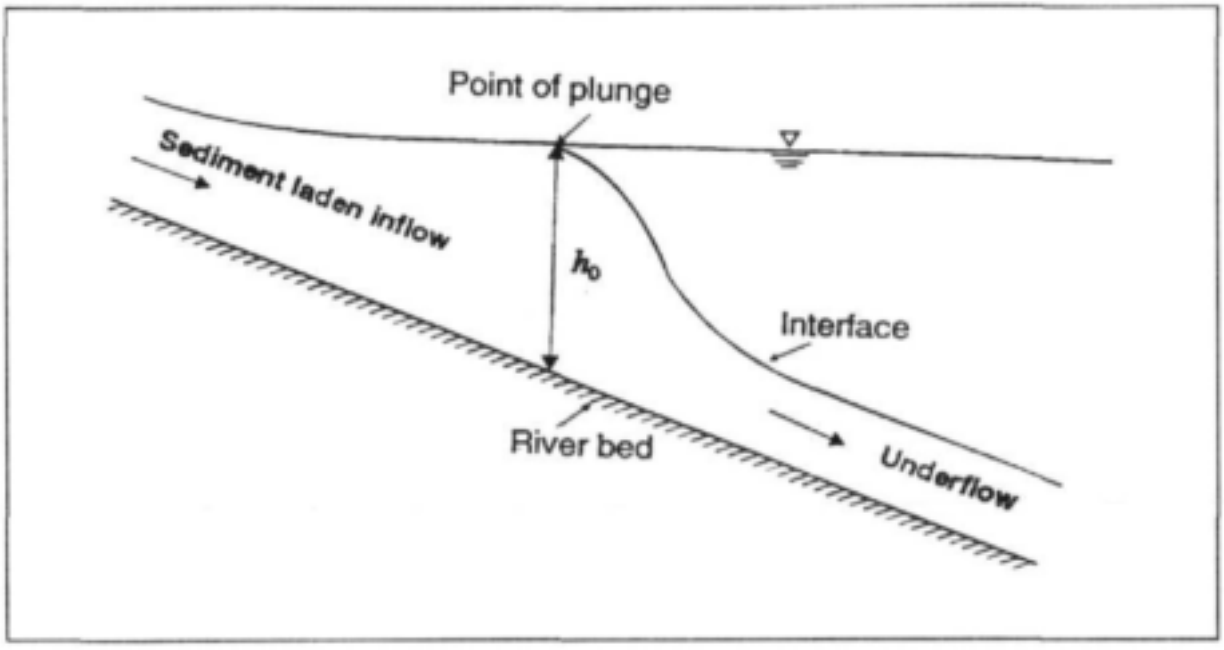

Figure 2.2-1 Schematic diagram of density current formation (Fan, 1960)

Based on experimental data, Fan (1960) calibrated equation 2.2-2 and proposed the relationship:

$$\frac{v_o}{\sqrt{\frac{\Delta\gamma}{\gamma} g \quad h_o}} = 0{,}78\ (<1) \qquad (2.2\text{-}3)$$

where v_o = velocity at the plunge point

and h_o = depth of flow at the plunge point

g = gravitional acceleration

Equation 2.2.-3 (left hand side) is known as the densimetric Froude number (Fr_D) and the experimental data used by Fan (1960) is shown in Figure 2.2-2.

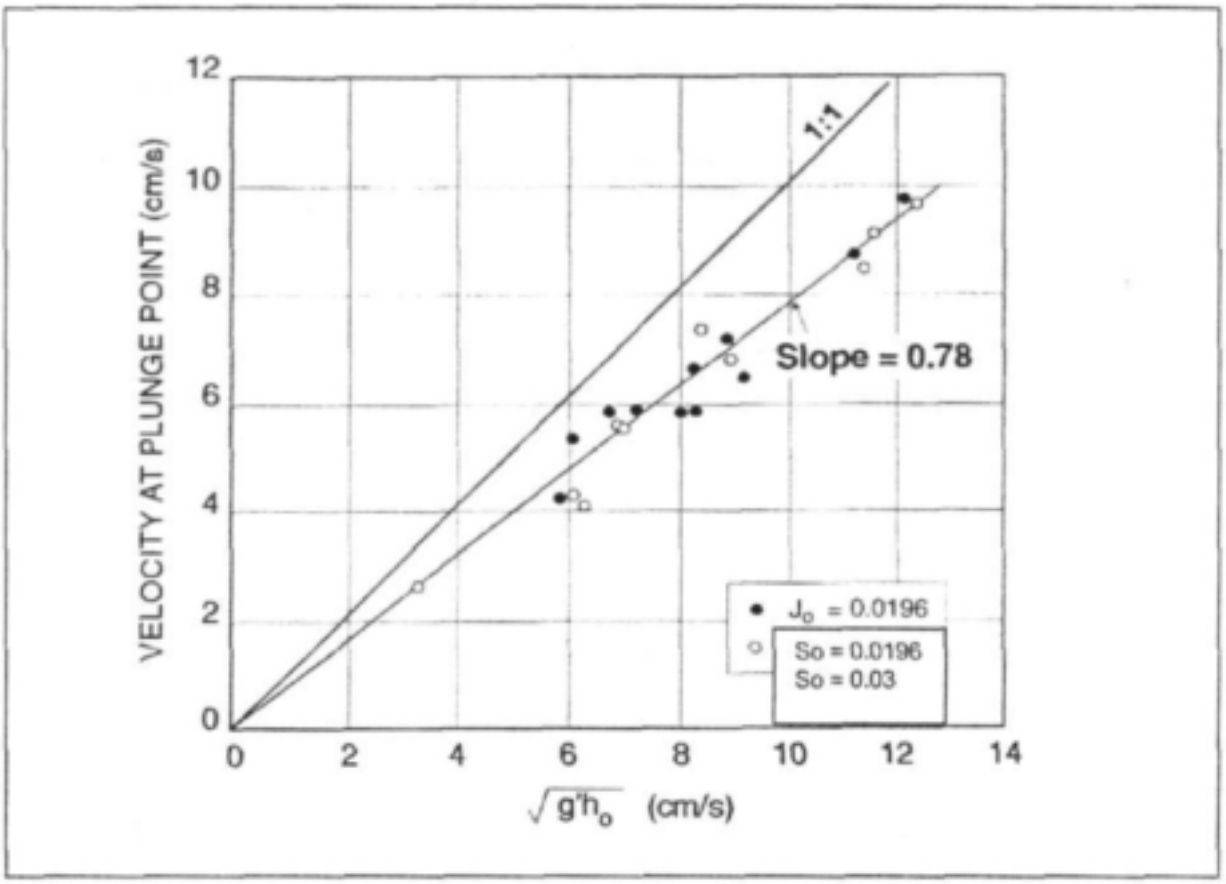

Figure 2.2-2 Densimetric Froude number and density current formation (Fan, 1960)

The constant in equation 2.2-3 was found less than unity, and Fan explained this by arguing that the streamline at the interface possesses a point of inflection which is located downstream of the plunging point. Fan stated: "It is evident that the control section where $v^2/(\Delta\gamma/\gamma)g\,h_0 = 1$ occurs at the point of inflection . . . "

Fan (1986) found that the formation of density currents could be forecasted by means of equation 2.2-3 for concentrations < 100 kg/m^3. It was, however, found that the densimetric Froude number also depends on the inflow sediment concentration and decreases with increasing concentration. This helps to explain why different researchers have found a wide range of densimetric Froude numbers that predict density current formation, from their experiments.

Cao (1992) published a relationship between Fr_D and the density difference ratio. (Figure 2.2-3) It appears that when sediment concentrations are < 40 kg/m^3, Fr_D is approximately 0,78. As the sediment concentration increases the density current changes from turbulent to laminar with hyperconcentrations above 300 kg/m^3.

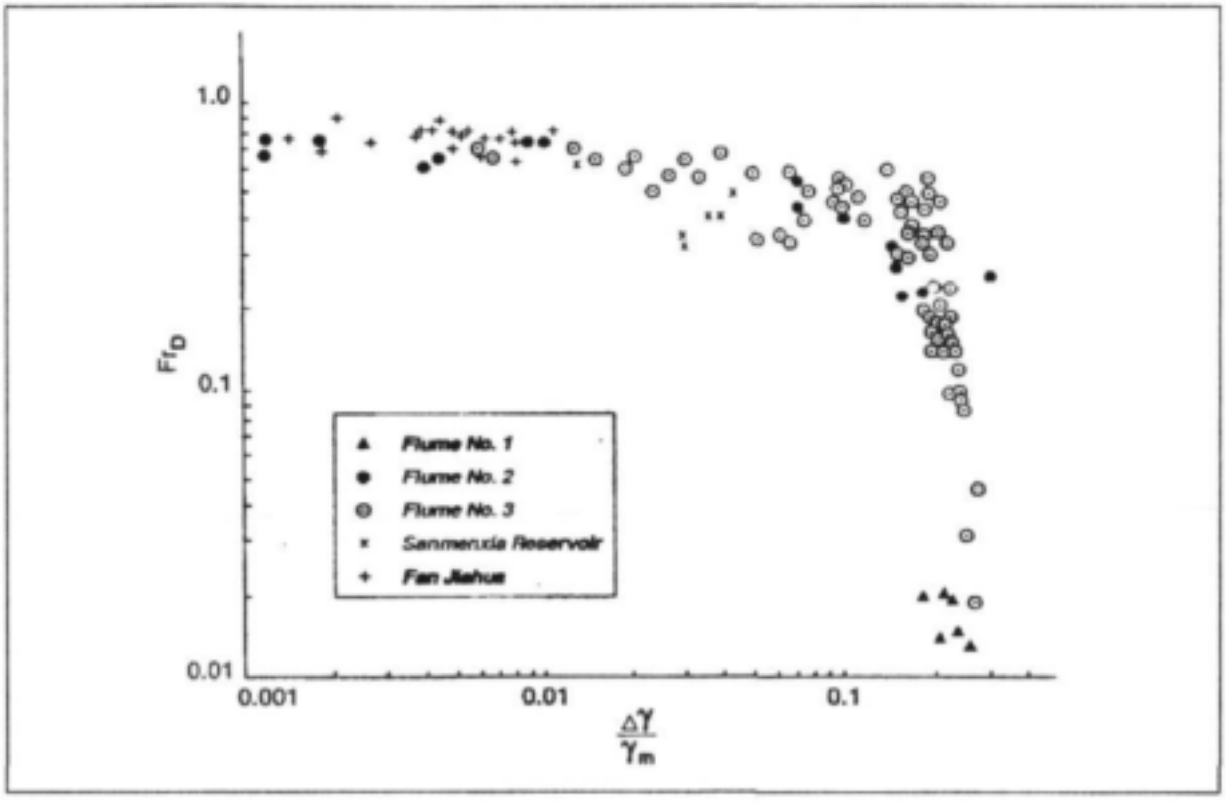

Figure 2.2-3 Densimetric Froude number and density difference ratio (Cao, 1992)

Previous studies dealt with sloping channels, rectangular cross-sections of constant width, or triangular shapes representing the reservoir geometry. Investigations of the formation of a density current based on the densimetric Froude number show considerable variation, as shown in Table 2.2-1.

Table 2.2-1 Densimetric Froude number at the plunge point

Reference	Fr_D
Ford and Johnson (1980)	0,1 to 0,7
Itakura and Kishi (1979)	0,54 to 0,69
Singh and Shah (1971)	0,30 to 0,80
Kan and Tamai (1981)	0,45 to 0,92
Fukuoka and Fukushima (1980)	0,40 to 0,72
Farrell and Stefan (1986)	0,66 to 0,70
Akiyama et al. (1987)	0,56 to 0,89

In this study a new theory based on minimum stream power is investigated which is believed should overcome the relatively inaccurate predictions of the widely used densimetric Froude number approach.

2.2.2 Minimum input stream power theory (Basson, 1996)

A flowing stream of water with a movable bed will always try to change the boundary conditions imposed on it until equilibrium conditions are reached. At equilibrium the energy dissipation per unit volume is minimized. In terms of applied stream power, $\left(\tau\frac{dv}{dy}\right)$ this means that the flow can adjust the values of the von Kármán coefficient (κ), bed roughness (k_s), flow depth (D), energy slope (s_f) and/or width of flow (B), in equation 2.2-4.

$$\tau\frac{dv}{dy}.B = \frac{\rho B(gs_f D.)^{1.5}}{\kappa.k_s} \qquad (2.2\text{-}4)$$

Minimization of stream power will also be the reason why a turbulent stream dives to the reservoir bed to be transported as density current through the reservoir. At the plunge point, input stream power for the density current should therefore become equal to our less than that of the turbulent inflow, assuming that the stream power in the upper reservoir layer is approximately zero as $v \rightarrow 0$ in the upper layer.

At the plunge point, from stream power continuity:

Stream power of turbulent inflow = stream power of density current

$$\int_0^D \rho g B_R v s_f dD = \int_0^d \Delta\rho g B_D v s_o dd \qquad (2.2\text{-}5)$$

with ρ = water density
s_f = energy slope
D = plunge point water depth
$\Delta\rho$ = water density difference
s_o = bed slope assuming a uniform density current
v = flow velocity
B_R = flow width of river
B_D = flow width of density current
d = density current flow depth

Therefore for a density current to form it is expected that:

$$\frac{B_{D}\Delta\rho g Q s_{o}}{B_{R}\rho g Q s_{f}} \leq 1 \qquad (2.2\text{-}6)$$

with Q = discharge,

and from flow continuity this simplifies to:

$$\frac{B_{D}\Delta\rho s_{o}}{B_{R}\rho s_{f}} \leq 1 \qquad (2.2\text{-}7)$$

Equation 2.2-7 indicates that for a density current to form, the ratio $\frac{\Delta\rho}{\rho}$ should be small, which is usually the case with $\frac{\Delta\rho}{\rho}$ values in the order of 0.001 to 0.1. Furthermore the ratio $\frac{s_o}{s_f}$ should be as small as possible for a density current to form. Considering the typical $\frac{\Delta\rho}{\rho}$ ratios and assuming the same flow widths in the river and density current, typical $\frac{s_o}{s_f}$ ratios should be less than 10 to 1000. This means that s_0 should be 10 to 1000 times larger than the river energy slope s_f at the plunge point, for example if s_f =1:10000, s_0 should be 1:1000 to 1:10 at the plunge point, which is relatively steep for many South African rivers. The flat energy slope s_f is created by the backwater of the reservoir.

If the flow widths are considered the same in the river and in the density current, then equation 2.2-8 is obtained:

$$\frac{\Delta\rho s_{o}}{\rho s_{f}} \leq 1 \qquad (2.2\text{-}8)$$

Equation 2.2-8 is tested against laboratory data in Chapter 3. From total stream power balance, an equation similar to equation 2.2-7 can also be derived in terms of applied stream power.

2.2.3 Minimum applied stream power theory

Following the same reasoning as in paragraph 2.2.2, it follows that:

Applied stream power of turbulent inflow = applied stream power of density current.

Assuming applied stream power at the bed equals the total applied stream power, then from the minimum energy principles, a density current should form when:

$$\frac{\tau \dfrac{dv}{dy_D}.B_D}{\tau \dfrac{dv}{dy_R}.B_R} \leq 1 \qquad (2.2\text{-}9)$$

with $\tau \dfrac{dv}{dy}$ = applied stream power at the bed

Subscript D = density current variable

Subscript R = river variable

From equation 2.2-4, it is possible to rewrite equation 2.2-9:

$$\frac{30(\rho_D - \rho_w) g s_o d.B_D \dfrac{\sqrt{g.s_o.d}}{\kappa_D k_{sD}}}{30\rho\ g s_f D\ .B_R \dfrac{\sqrt{g s_f.D_R}}{\kappa_R.k_{sR}}} < 1 \qquad (2.2\text{-}10)$$

or

$$\frac{\Delta\rho_D}{\rho_R}.\frac{s_o^{1.5}}{s_f^{1.5}}.\frac{d^{1.5}}{D^{1.5}}.\frac{\kappa_R k_{sR}}{\kappa_D k_{sD}}.\frac{B_D}{B_R} < 1 \qquad (2.2\text{-}11)$$

with g = gravitational acceleration

κ = von Kármán coefficient

s_f = energy gradient of inflowing river at the plunge point

s_o = energy slope of the density current, assumed equal to the reservoir bed slope

k_s = bed roughness

ρ_D = density current density

ρ_w = clear water density

ρ_R = River water density

Equation 2.2-11 is tested in Chapter 3 against laboratory flume data, and is considered as possible alternative to equation 2.2-8. The benefit of equation 2.2-11 is that it contains all the fundamental hydraulic variables such as bed roughness and in dimensionless form.

3. CONFIRMATION OF THEORY AGAINST LABORATORY DATA

3.1 Introduction

Basson and Rooseboom (1997) have verified the minimum input stream power theory (equation 2.2-8) successfully against laboratory data of Akiyama and Stefan.(1987). The data of Akiyama and Stefan. were however obtained from temperature induced density currents, and it was therefore necessary to investigate sediment induced density currents in this study.

3.2 Temperature induced density current formation data of Akiyama and Stefan (1987)

3.2.1 Minimum input stream power

As a preliminary test of the prediction accuracy of equation 2.2-8, laboratory data of Akiyama and Stefan. (1987) in which the density differences were created by temperature differences, were used. Verification of equation 2.2-8 to test for density current formation does indeed show that less stream power is used by the density current than by the turbulent open channel inflow in most cases, as shown in Figure 3.2-1. The data are attached in Appendix A. The data points should plot below the 1:1 line for a density current to form if the theory is correct. An assumption had to be made on the bed roughness of the flume, assumed to be 0.002 m. Most of the densimetric Fr values (see graph), are between 0.6 and 0.8, a relatively wide range of values.

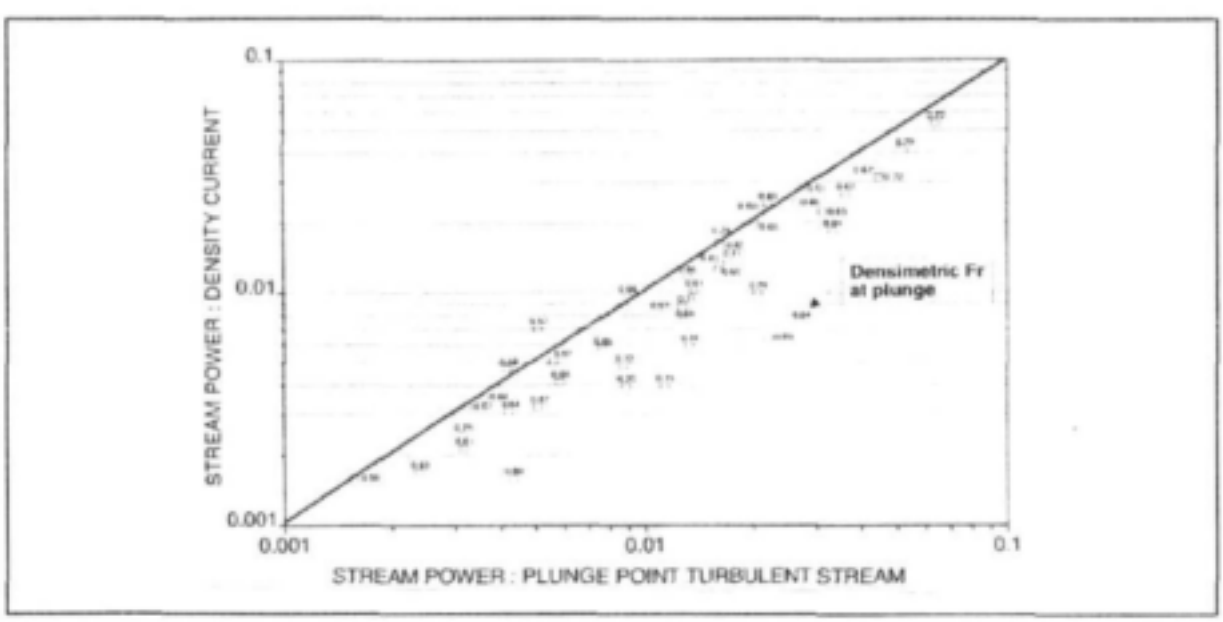

Figure 3.2-1 Density current formation and minimum input stream power

3.2.2 Minimum applied stream power

The three dimensional minimum applied stream power equation 2.2-10, has also been verified to some extent against the data of Akiyama and Stefan. (1987), as shown in Figure 3.2-2. In this case only 63 % of the data points plot below the line.

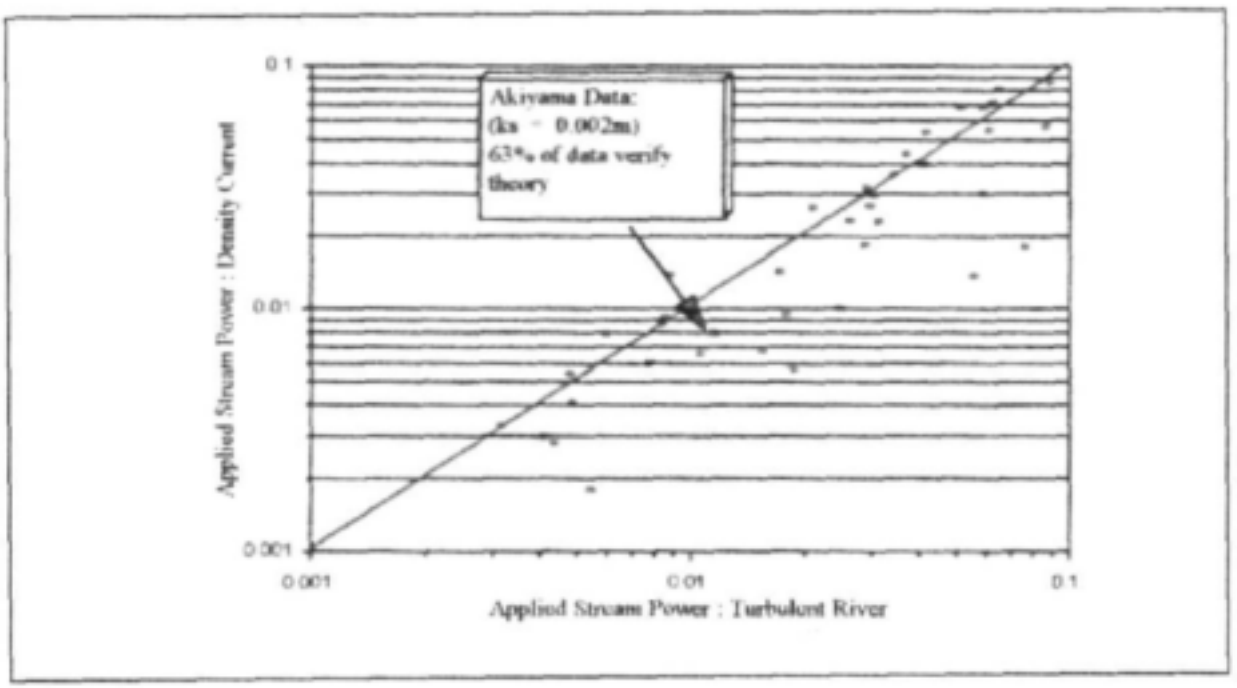

Figure. 3.2-2 Density current formation and minimum applied stream power using data of Akiyama and Stefan (1987)

Certain assumptions had to be made with regards to the data of Akiyama and Stefan.:

- bed roughness was assumed equal to 2 mm (k_s), for the turbulent inflow and the density current, and was also used in the calculation of the energy slope s_f at the plunge point.
- the von Kármán coefficient was taken equal to 0.4, for the inflow and density current.

The minimum applied stream power theory however needs to be tested further with sediment induced density current data before a conclusion can be reached whether this theory should be used for water resources planning.

3.2.3 Evaluation of proposed theory

Conditions that will favour the formation of a density current are:

- Equation 2.2-8 states that at the plunge point a steeper approaching turbulent flow slope s_f will create more favourable conditions for density current formation as the river meets the water mass in the reservoir. This might be due to the high momentum of the inflowing river which enables it to dive underneath the water mass, and once near the bed the density difference creates the density current flow and prevents a hydraulic jump of the submerged flow, (with consequent turbulent suspended sediment transport through the reservoir). On the other hand, the bed slope downstream of the plunge point needs to be steep enough for the propagation of the density current.

- A greater width B, reduces the turbulent sediment transport capacity, enabling the turbulent river to deposit large sediment particles at the plunge point more effectively. A narrower width B of the density current relative to the river width will however help to form the density current since it minimizes the stream power.

- The ratio of density current depth to turbulent river depth, should be as small as possible, from equation 2.2-10.

In this chapter two theories: minimum input and minimum applied stream power, have been tested against data by Akiyama and Stefan (1987), with temperature difference induced density currents. The theory looks promising, but assumptions had to be made on the bed roughness to determine the applied stream power. The effect of sediment transport in the formation of density currents is considered in more detail in section 3.3.

3.3 Laboratory investigation of sediment induced density current formation

3.3.1 Introduction

The minimum input and applied stream power relationships derived in Chapter 2 have been tested against temperature induced density current data in section 3.2. Sediment induced density current data are however also required as final verification of the new theory. Such tests have been carried out at the Hydraulic Laboratory of the University of Pretoria during 1998 to 1999.

3.3.2 Methodology

A 15 m flume, with cross-sectional dimensions of about 0,5 m x 0,5 m, and adjustable slope, has been used for the sediment induced density current formation tests. At the downstream end of the flume a hinged flume extension 5 m in length, was added. The extension represented the reservoir, while the flume acted as the inflowing river. The flume extension could be adjusted vertically from a horizontal position to a slope as steep as 1:5 (vertical: horizontal). Furthermore the flume extension diverged from the flume width of 0,5 m, to a width of 2,0 m, at adjustable divergence angels of 7½°, 15° and 30°. The idea with the extended flume was to investigate various three dimensional flow patterns, which might occur in the vicinity of the plunge line. The flume is shown in Figure 3.3-1 with a schematic layout of the facility in Figure 3.3-2 and Appendix B.

Figure 3.3-1 Sediment induced density current test flume

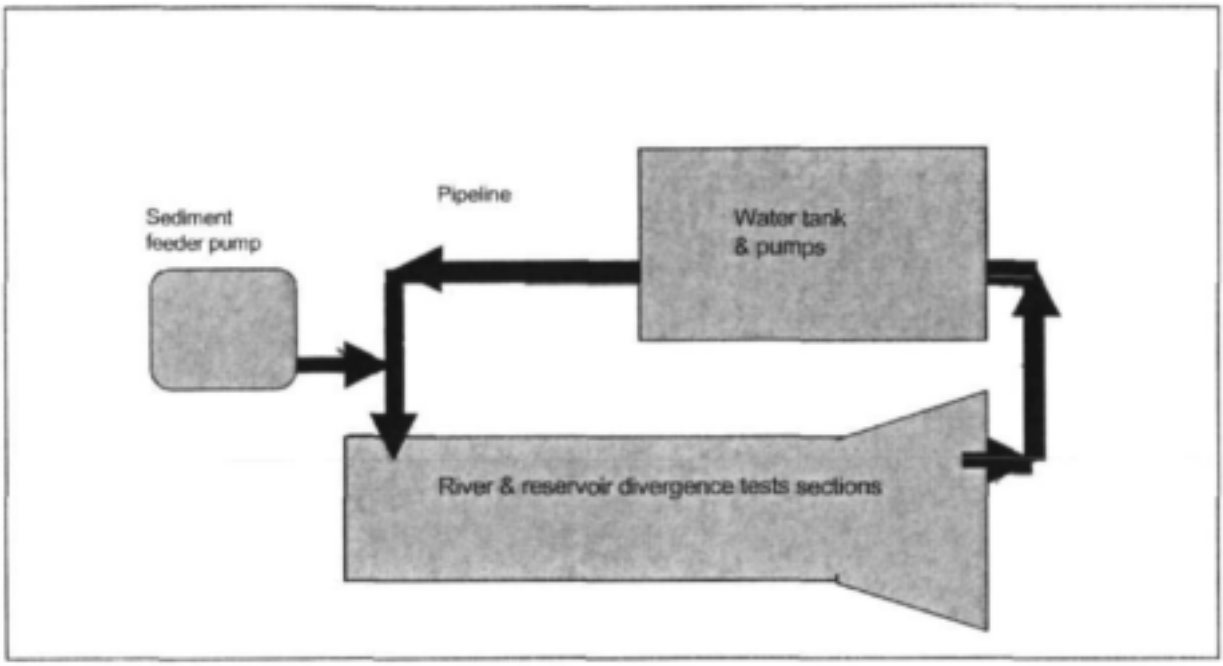

Figure 3.3-2 Schematic plan layout of test facility

Discharge was measured at a 90° v-notch at the outflow of a small canal, after spillage from the flume.

The test procedure was to determine for a specific bed slope, inflow and sediment concentration, whether a plunge point and density current formation would occur. Steady flow conditions were first achieved (which took several hours and permitted typically only one test per day), whereafter sediment was added at the upstream end of the flume and visual inspection of the sediment transport through the glass walled flume indicated the formation of a density current or not. A whole range of tests was carried out in order to verify the minimum stream power relationships with variables: bed slope, discharge, flow depth and inflow suspended sediment concentration.

The downstream water level was controlled by vertical sluice gate, with bottom opening across the full width of the extended flume of 2 m width.

Initial sediment supply was through a gravity system placed at the upstream end of the flume, with a water-sediment mixture discharge controlled by a valve. The volume of sediment and experimental runtime was however found to be too short, and a modification was carried out. Suspended sediment input was through a separate pumping unit (Figure 3.3-3) which discharged at the upstream end of the flume. A sediment-borehole water (same water as in the flume) mixture was added to the mixing tank to obtain the required

suspended sediment concentration. After stabilization of clear water conditions in the flume, the test commenced with the pumping of the sediment–water mixture into the flume. The sediment mixture therefore added extra flow which created unsteady conditions as it moves through the flume, but this additional discharge was small and measurements were only carried out after steady conditions returned after density current formation with sediment transport.

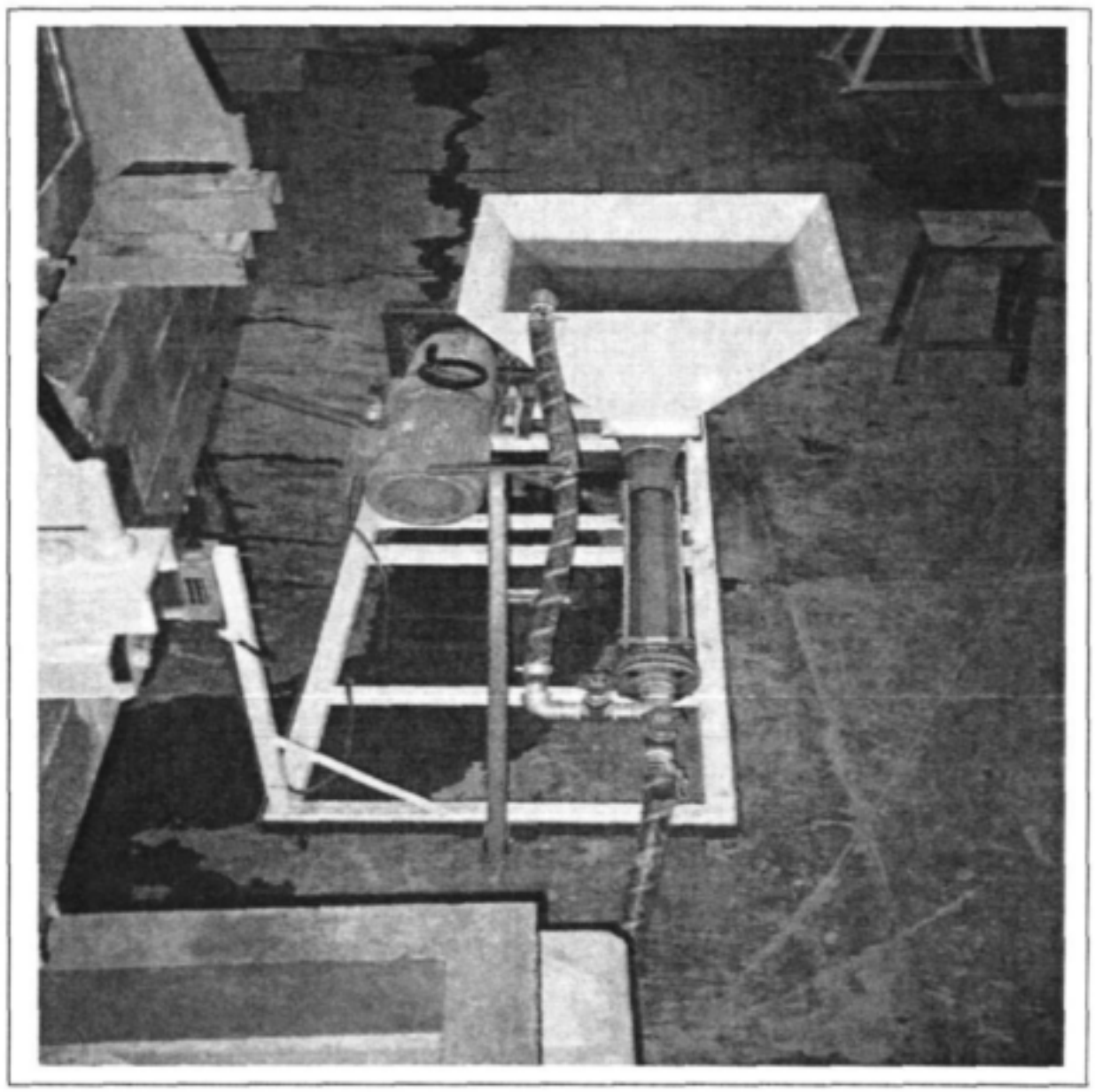

Figure 3.3-3 Suspended sediment mixing and pumping unit

3.3.3 Evaluation of data

Several very interesting observations were made in the laboratory:

- Sediment was first obtained using the finest sand fraction commercially available obtained from a wind cyclone process from sand suppliers. No density currents could be formed, and most of the sediment deposited in the upstream "river" part of the flume. Laboratory analysis of the sediment particle size distribution indicated that the sediment contained very little fractions of less than 0,03 mm, the typical silt and clay fractions, which are normally associated with density current formation in the field at reservoirs.

- New sediment was obtained from Centurion Lake, near Pretoria, and right from the first test density currents were forming. This sediment has a high percentage of silt and clay fractions and was used throughout all tests. The density current nose as observed during a test is shown in Figure 3.3-4.

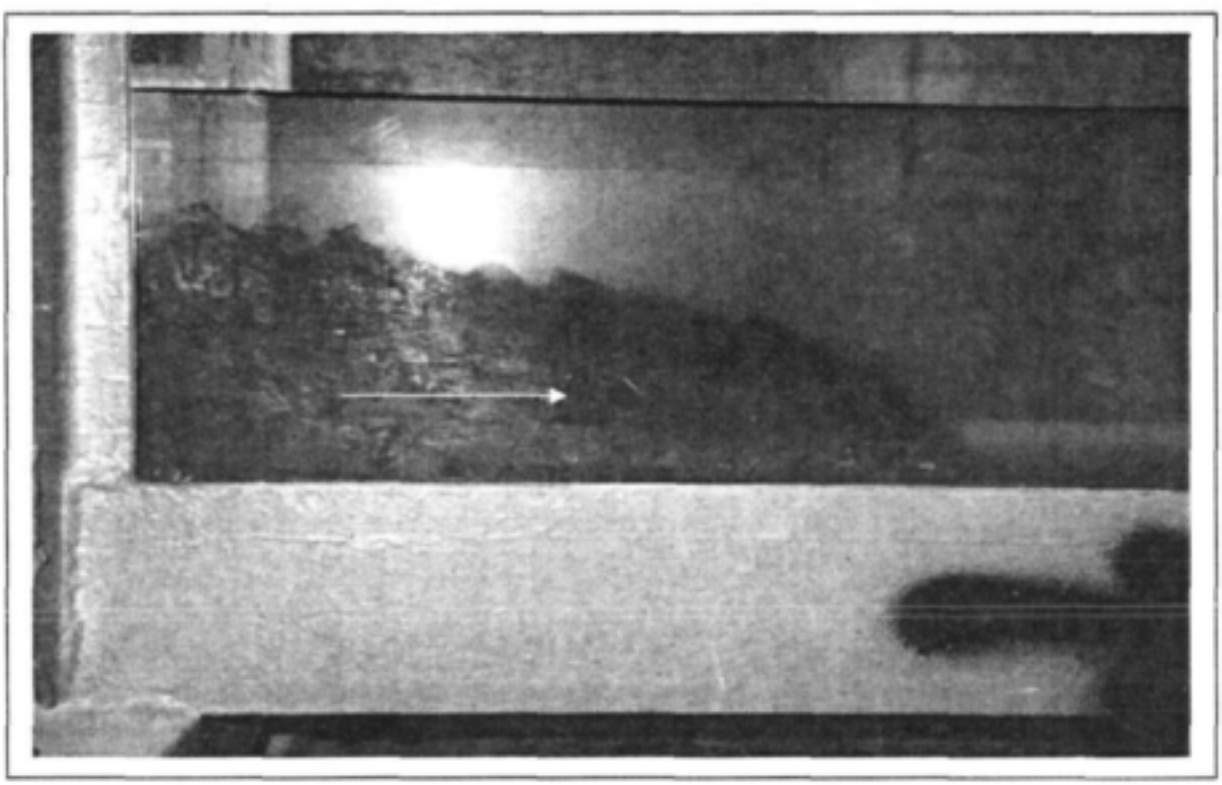

Figure 3.3-4 Density current nose

- Verification of the plunging phenomenon as described by the proposed new theory of minimum stream power also required conditions where density currents are not forming. Using the Centurion Lake sediment, however, seems to be forming density currents under a wide range of slope, discharge, depth and suspended sediment concentration conditions, without failure. Further tests were therefore required to specifically test under which conditions the density current would not form:

  a) Input sediment concentrations were firstly reduced and it was found that at about 250 mg/ℓ, no plunging occurs but sediment is only transported as a murky mixture, as turbulent suspension.

  b) High turbulence conditions were also tested in order to try and break up the stable plunge line conditions. This was successful and is described in greater detail in section 3.4.

- During tests the plunge line was observed under clear water conditions on the water surface, without any sediment input This plunge line has a curved form in plan, similar to the velocity distribution at the surface. It has a definite width of about 0.5 to 1 cm in the direction of flow. Viewed from above and the side, dust particles on the water surface seems to momentarily stop dead at the plunge line, before continuing downstream. Downstream of the plunge line, the water surface close to the flume walls (up to about 0.1 m away on each side), showed slowly rotating upstream movement.

The only explanation for the observed plunge line phenomena is the formation of a stagnation point (or stagnation line) on the surface. A stagnation point has also been associated with rivers flowing into the ocean, with the density current created by the salt water density difference. From the energy equation, if the surface flow velocity = 0 at the plunge point, the water surface level immediately upstream of the line would be lower than at the plunge line, as indicated by equation 3.3-1.

$$y_1(1+\frac{Fr_1^2}{2}) \leq y_2 \qquad (3.3\text{-}1)$$

with y_1 and y_2 water depths immediately upstream and downstream of the plunge line respectively;

Fr_1 = Froude number of the upstream "river", and assuming a horizontal bed between sections 1 and 2.

For typical values tested in the flume of say $y_1 = 0{,}2$ m and $Fr_1 = 0{,}1$, y_2 could be 1 mm higher than just upstream (y_1) of the plunge line.

Tests were carried out consequently to check specifically whether his observed clear water plunge line is indeed the plunge line where the density current forms. This was established and in all cases the plunge line was at the beginning of the diving density current.

- The observation of the clear water plunge line does not make the minimum stream power predictors irrelevant, but it certainly seems as if the plunge line could be described from hydraulic principles only, without the need of density differences caused by the inflowing sediment. An envisaged calculation procedure could therefore determine the following, in the given order:

a) clear water plunge line formation

b) availability of fine sediment at concentrations above a minimum suspended sediment concentration to create a density difference.

c) minimum input or applied stream power conditions in the inflowing river or reservoir density current.

d) possible extreme turbulence hydraulic conditions which could break up the stable plunge line and density current.

Additional tests were therefore conducted to establish hydraulic conditions for points (a) and (d) mentioned above.

- Due to the scope of testing which changed with more tests on the clear water plunge line, only a limited number of three dimensional tests were carried out with the plunge line forming at the hinge between the "river" and "reservoir" parts of the flumes and only at a diverging horizontal angle of 15 degrees. Most of the tests were carried out with plunging occurring in the "river" section of the flume.

When the plunging was established at the downstream end of the "river" section of the flume, the following was observed:

a) the water surface plunge line was visible, but not near the flume walls.

b) it was not possible to form the plunge line in the "reservoir" part of the flume, as the line seems to remain in the vicinity of the hinge (or slightly downstream). This does not mean that the plunge line would not form in a wider section, but it is believed that the line moved from the hinge downstream out of the flume to the downstream boundary.

3.3.4 Minimum input stream power theory verification

Verification of equation 2.2-8 against sediment induced density current data obtained in this study is shown in Figure 3.3-5. For this graph equation 2.2-8 has been rewritten in the dimensionless format $\frac{s_0}{s_f} < \frac{\rho}{\Delta\rho}$, in order for a density current to form, based on minimum input stream power. All of the data points (except one that is close to the line), fall below the 1:1 line, indicating that density currents would form, as was indeed found in the experiments.

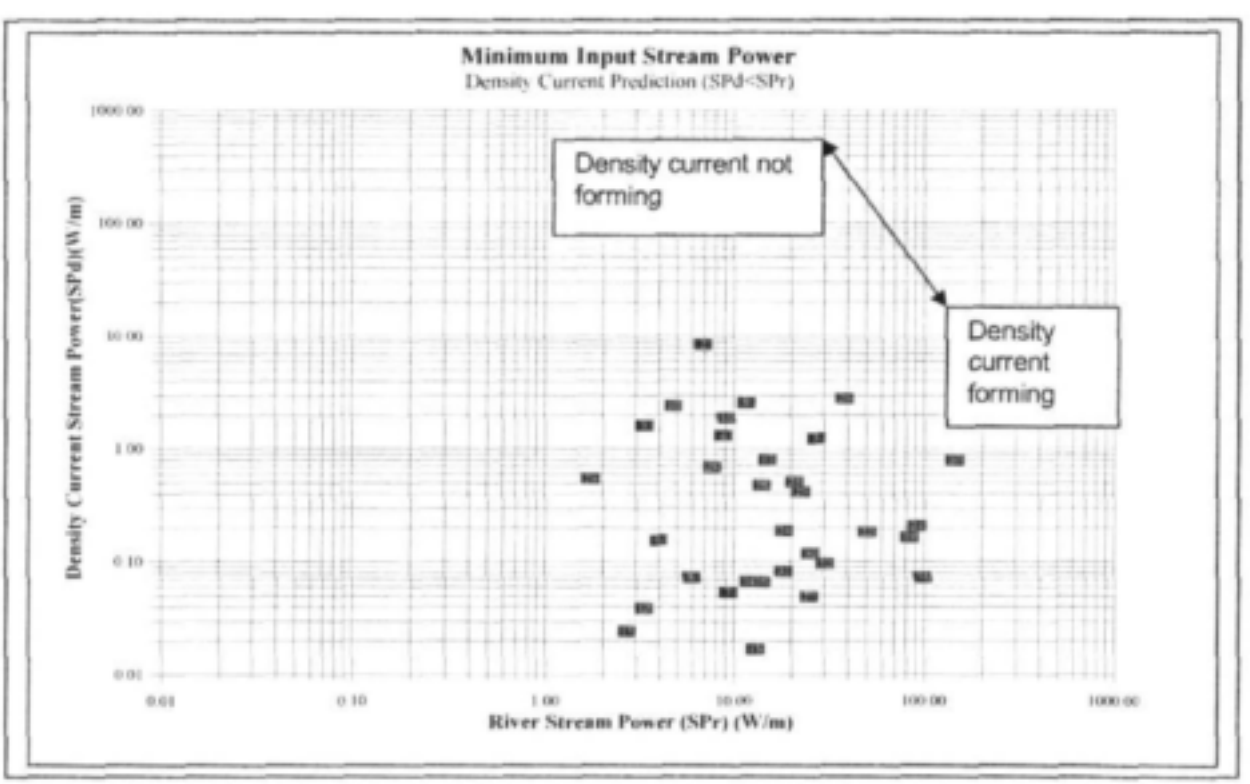

Figure 3.3-5 Sediment induced density current formation and minimum input stream power

In some of the tests, density currents did not form, however, but this can be attributed to suspended sediment concentrations in the inflow of less than 250 mg/ℓ, the critical minimum concentration found necessary for a density current to form (if the reservoir water has a low sediment concentration).

- the flume bed slope and related energy slope was found to play a major role in establishing a definite plunge line and strongly forming density current. This also confirmed the minimum input stream power theory:

$$\frac{\Delta\rho s_o}{\rho s_f} < 1$$

for a density current to form, which states the s_f value (of the river) should be as large as possible.

The test data are attached in Appendix B.

3.3.5 Minimum applied stream power theory verification

Equation 2.2-11 has been derived as alternative to equation 2.2-8. When the laboratory data of this study (Appendix B) tested by Oosthuizen is used to test equation 2.2-11, it is found that 35 % of the points plot above the 1:1 line which theoretically means that the density current should not have formed (Figure 3.3-6). A number of assumptions had to be made, however, such as assuming the same bed roughness, von Karman coefficient and flow width in the river and density current.

The minimum applied stream power theory is also based on the assumption that the total power can be described by the applied power at the bed. The applied power theory therefore seems to be less accurate than the input stream power theory, and is not considered further in this study. However, the densimetric Froude number approach is investigated in greater detail in the next section with data obtained during this study.

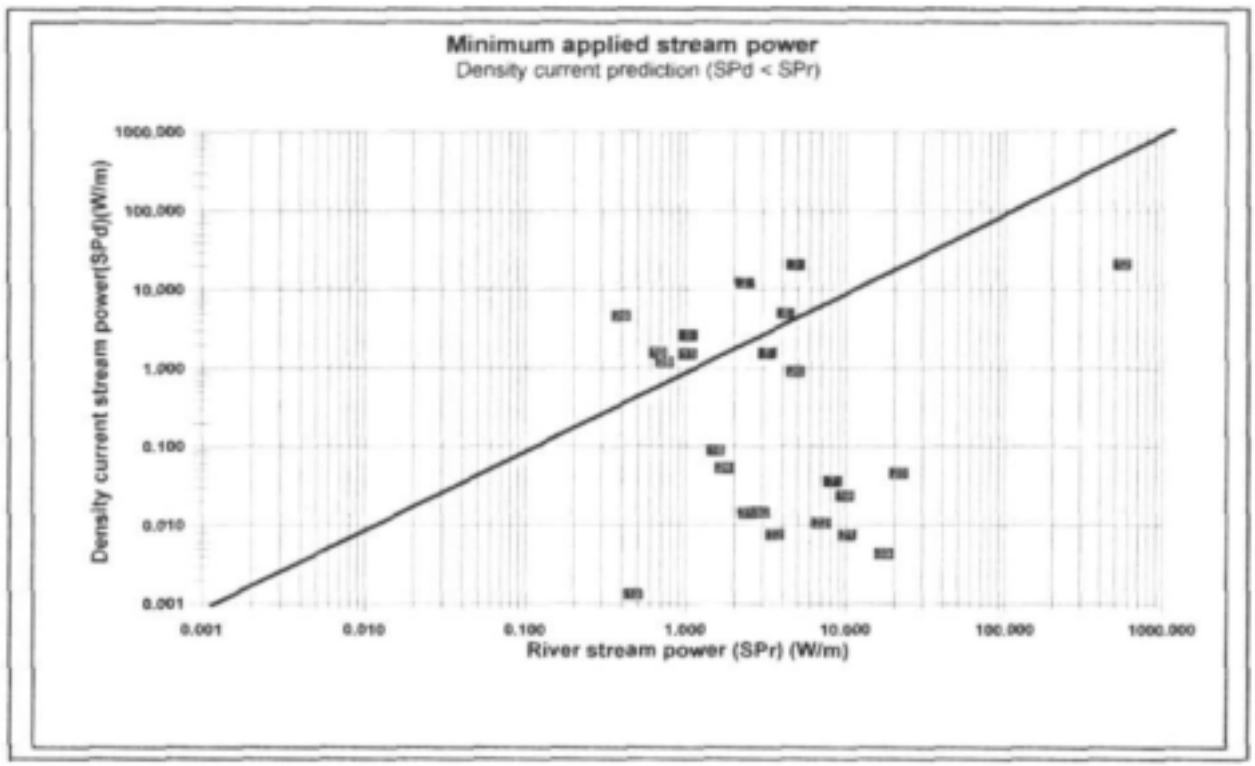

Figure 3.3-6 Sediment induced density current formation and minimum applied stream power

3.3.6 Densimetric Froude number

The prediction accuracy of the densimetric Froude number methodology was also tested using the newly obtained sediment flume data. Conditions at the plunge point as measured in this study are plotted on a graph, Figure 3.3-7. The original Fr_1, relationship proposed by Fan (1960) is also shown in Figure 3.3-7 and it is clear that it was derived from a very narrow range of data. The data obtained in this study at higher flow velocities indicate no correlation between velocity and the plunge point depth-gravitational acceleration relationship (x-axis).

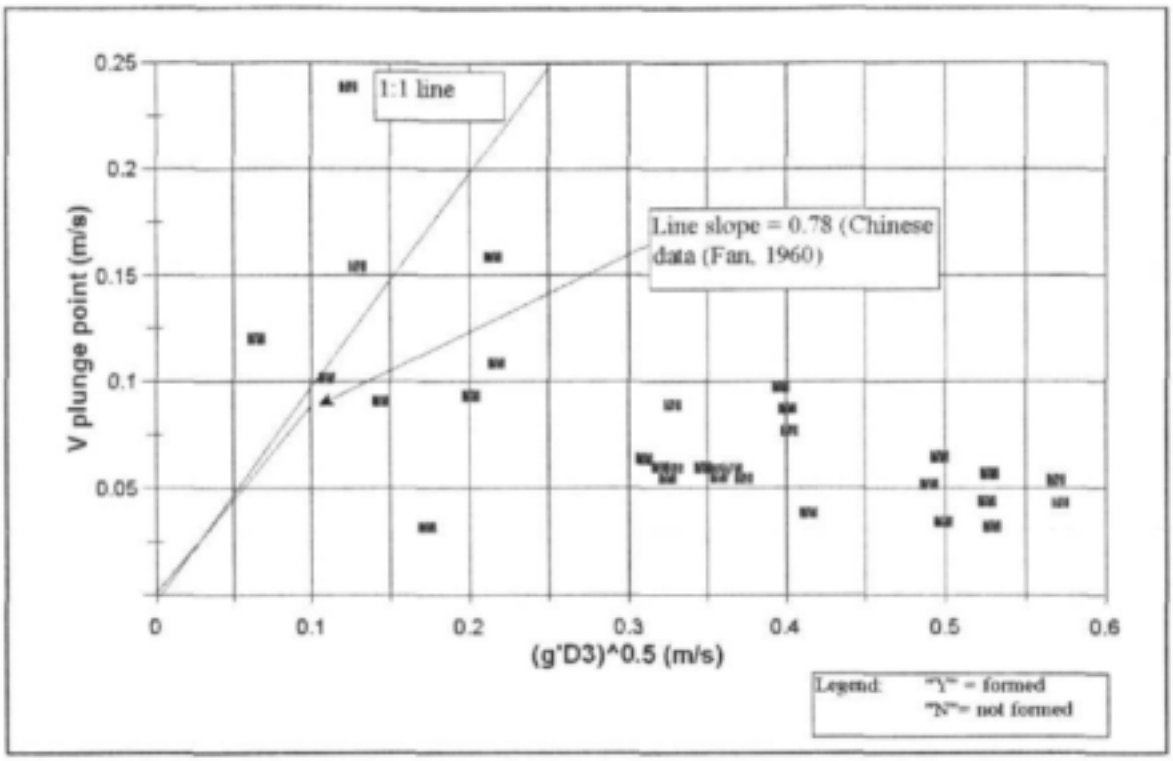

Figure 3.3-7 Densimetric Froude number and density current formation

Cao (1992) published a relationship between Fr_{1}, and the density difference ratio and indicated that at concentrations of less than 40 kg/m³, Fr_{1} is about 0.78, but at higher concentrations it decreases drastically as shown in Figure 3.3-8. The data obtained in this study shows a similar trend.

Akiyama and Stefan (1987) found an approximate average densitimetric Froude number of 0.68 at plunging. The Fr_{1} was only weakly related to the inflow densimetric Froude number of the river. When the data obtained in this study are plotted as shown in Figure 3.3-9 the finding of Akiyama of weak correlation is confirmed at high Fr_{1} values. At Fr_{1} values of say less than 0.2, however, there is a direct relationship between the river densimetric Froude number and the plunge point Fr_{1}.

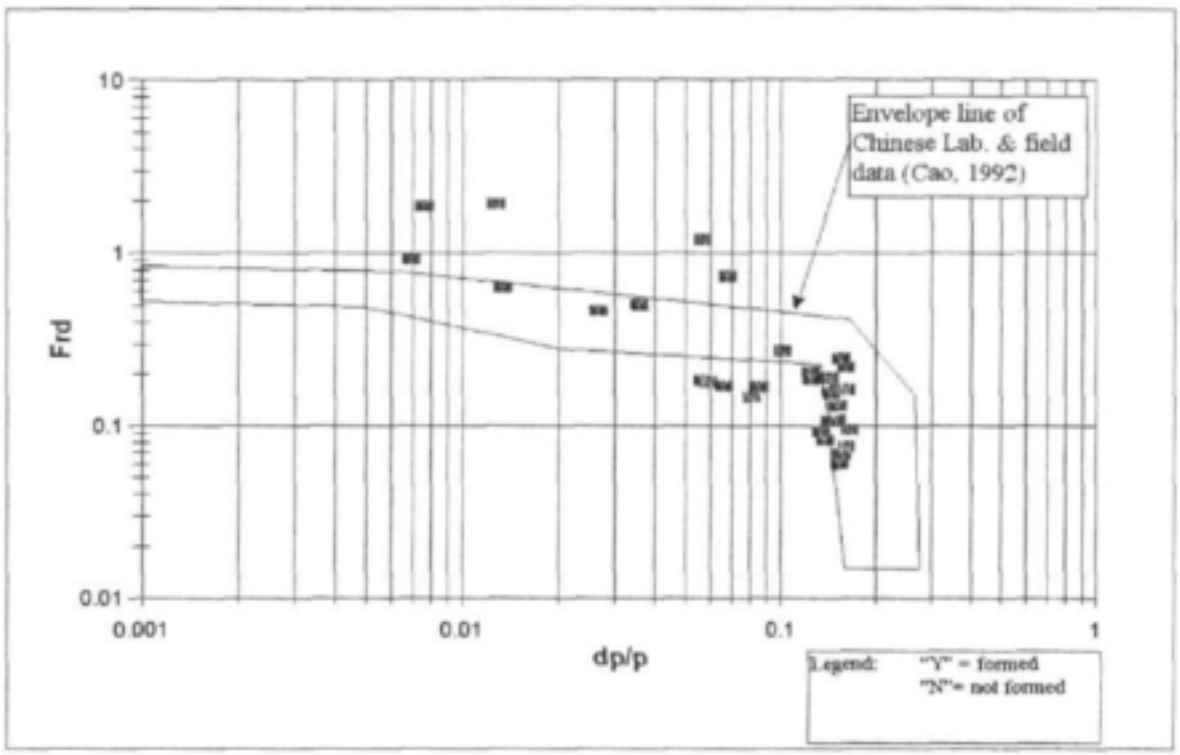

Figure 3.3-8 Densimetric Froude number and density difference ratio

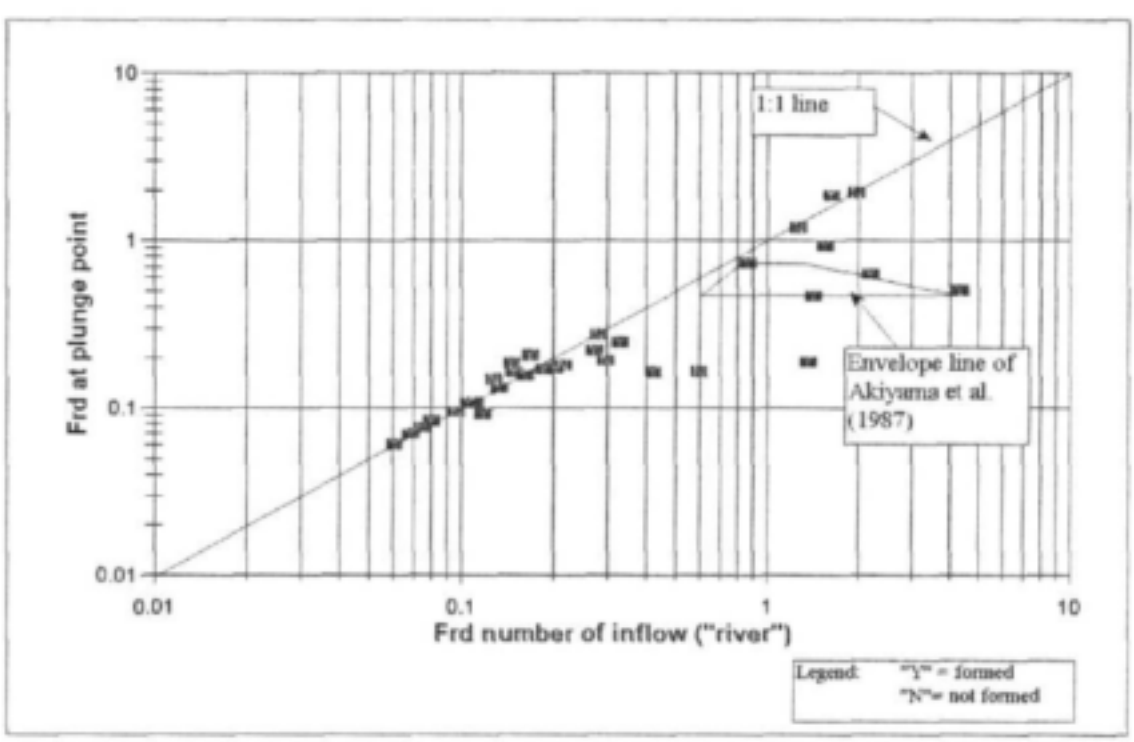

Figure 3.3-9 Densimetric Froude number relationship between river and plunge point

The data in Figure 3.3-9 show a wide scatter and relatively poor correlation with the value proposed by Fan (1960). It is clear from these graphs that the densimetric Froude number is not a reliable accurate predictor of density current formation under the wide range of possible hydraulic and sediment transport conditions.

3.4 Critical hydraulic conditions preventing stable plunge line formation

The facts that the plunge line is observed in clear water conditions and that the plunge line is directly related to the formation of a density current once suspended sediment is transported, should make it possible to predict the line without considering sediment transport. Since a more dominant plunge line formed when the flume (river) slope was steep, a critical energy slope (s_f) at the plunge line might be a good predictor of the range of formation of a plunge line. Other variables were however also investigated such as input steam power (vs), Froude number (F_r) and a s_e/s_f ratio. Some of these relationships are shown in Figures 3.4-1 and 3.4-2. The figures show the data of Oosthuizen (with sediment) and tests by van der Walt (clear water). In some cases high turbulence broke up the stable plunge line, and in other cases a density current did not form due to the low inflow suspended sediment concentration.

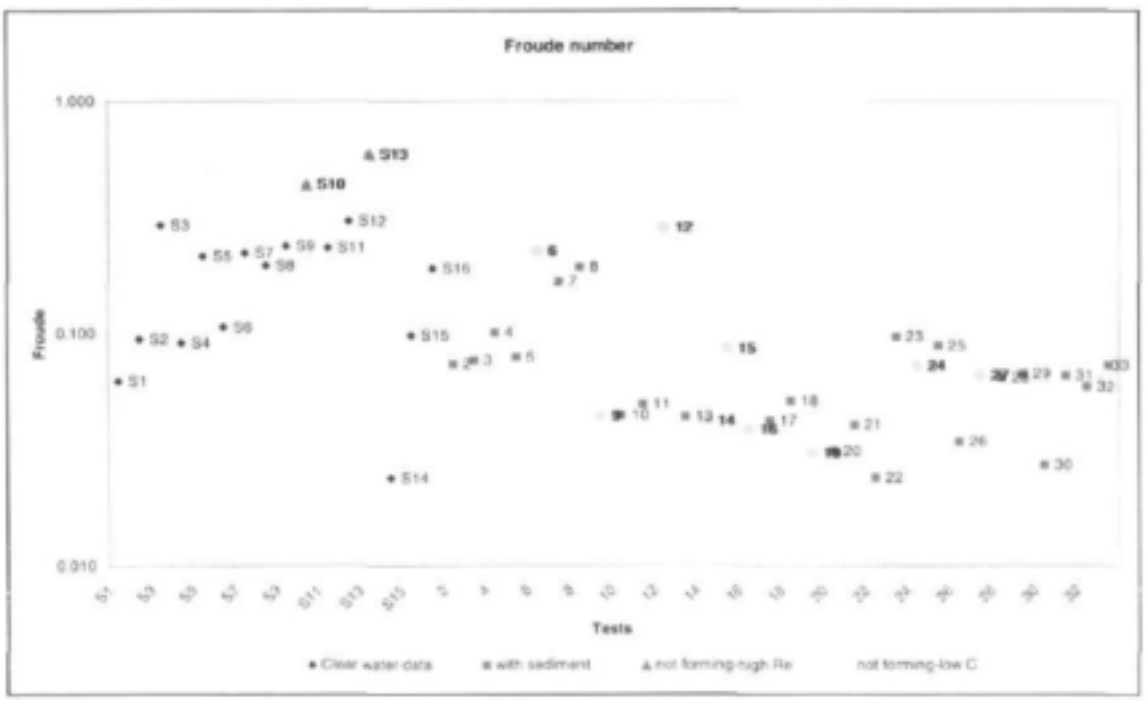

Figure 3.4-1 Froude number at the plunge point

3.5 Velocity distribution measurements at the plunge line

3.5.1 Laboratory setup

This study was conducted in the adjustable gradient flume of the hydraulic laboratory of the University of Stellenbosch by Wicht.

It is important to note that the presence of sidewalls can influence the flow and it is for this reason that it was decided to try to limit the width-depth ratio to three, where the effect of the walls is then negligible. An attempt was also made to ensure that the plunge line would occur as far away from the tailgate as possible to ensure that all measurements that were taken, occurred only as a result of the plunge line itself.

All runs of the experiment were tested with clear water. Figure 3.5-1 shows the flume as it was used during the study. The flume is 20 m long and 0.6 m wide. The flume was set at a gradient of 1:192 for the duration of the tests. The study was run using clear water from the main pump system of the laboratory.

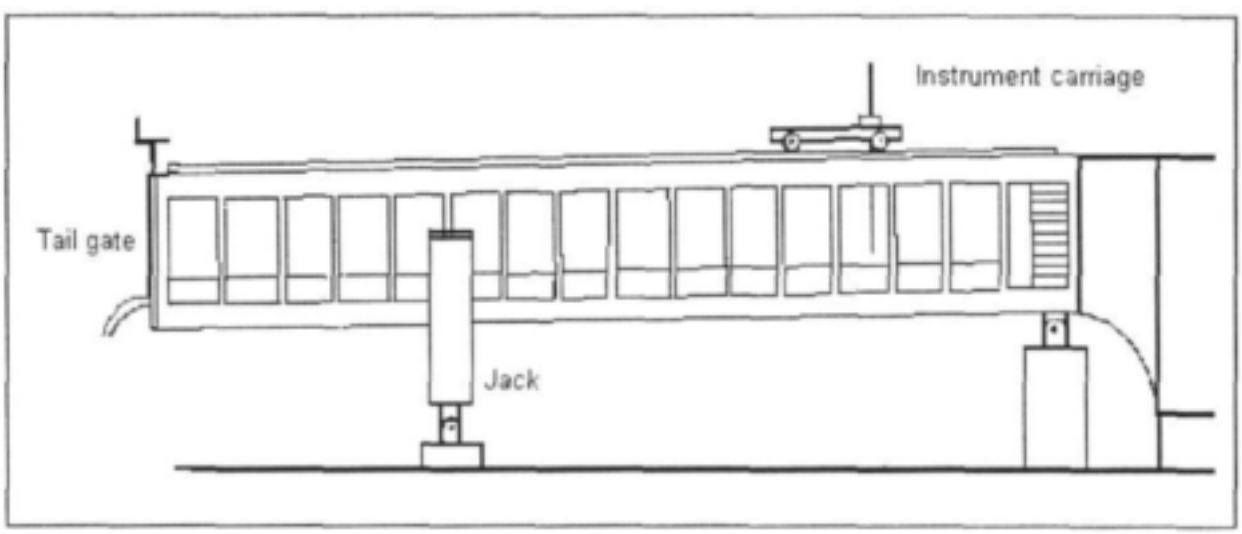

Figure 3.5-1 The set-up of the flume

The study consisted of eight different tests, with discharges ranging from approximately 3 l/s to 20 l/s. Stable flow was established, with the tailgate lowered into the flowing water so that reservoir-like conditions exist at the end of the flume, with absolutely no turbulence visible on the water's surface. It was then possible to see a U-shaped plunge line on the water's surface.

For experimental accuracy, it was preferable that the plunge line did not occur at the end of the flume, near the tailgate, where secondary effects may come into play. With the higher discharges this was more difficult. Care was also taken to ensure that the water level remained constant and was not rising or falling. This meant that the flow had to stabilise for some time before measurements were taken. The lower the rate of flow, the longer it took to stabilise.

Due to the sensitivity of the phenomenon, the utmost care was taken with the accuracy of the measurements. The following data were collected:

- Initial bed slope
- Discharge
- Depth of flow
- Three dimensional velocity profile
- Water surface slope

a) Initial Bed Slope

The initial bed slope was measured using the point gauge that runs on rails above the flume. Depths were measured at fifteen points along the flume, at 1.25 m spaces. Point one was at the shallower head of the flume, while point fifteen was at the deeper tail end, approximately 1.5 m from the tailgate of the flume. Readings at each measurement point were compared to a still water level. Assuming that the last measurement point in the flume (point fifteen) was at a height of 0 m, the elevations of all the other points could be determined relative to each other. A trend line was plotted through these points and the average bed slope was determined as shown in Figure 3.5-2.

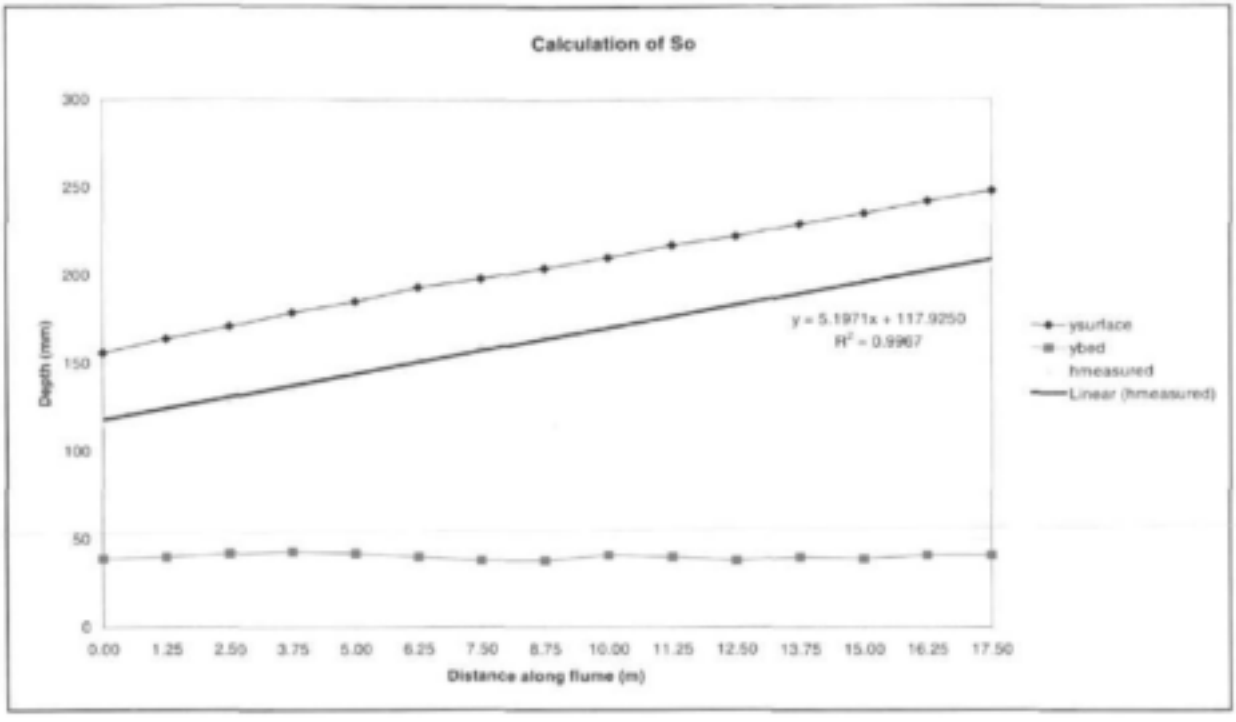

Figure 3.5-2 Calculation of average flume bed slope

b) Discharge Measurement

Flow was measured using an orifice meter, with a 162.9 mm diameter orifice plate in the 300 mm diameter pipeline in the laboratory.

c) Depth of Flow

All depths were measured at the points described using a point gauge on the instrument carriage that runs on rails above the channel. At all points both the surface reading and the actual position on the flume was recorded. The bed readings were taken as well to ensure that the needle gauge had not moved in between testing periods. At least two readings were taken at each point, up to a maximum of four, depending on the stability of the flow, and a statistical average was calculated to ensure accuracy. All depth measurements were recorded to the nearest millimetre, as this was the most accurate reading possible.

d) Velocity Profile Measurement

In order to investigate the plunge-line in three dimensions, the velocity profile had to be measured across the section of the flume. Readings were taken at intervals of fifty, one hundred, two hundred and three hundred millimetres from the edge of the flume and at five set depths according to the actual depth of flow. These readings were taken at different points in relation to the plunge line. The first position was at the point were the plunge line started at the edge of the flume. The second position was just downstream of the plunge line and the third was a further metre downstream as shown in Figure 3.5-3.

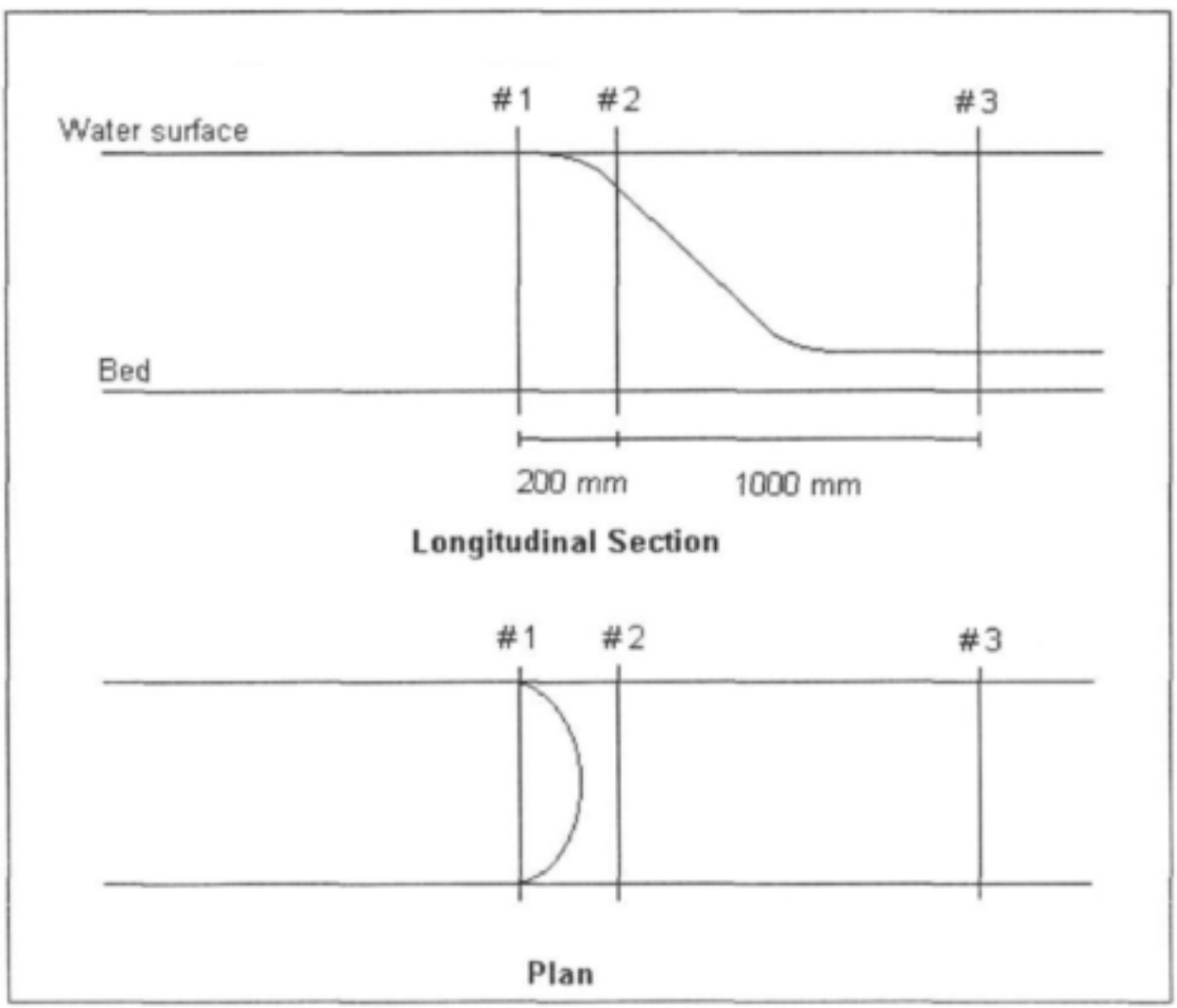

Figure 3.5-3 Positions of point velocity measurements in relation tothe plunge line

All point velocity readings were taken using an "A.OTT Kempton" propeller meter and a number 11356-2 propeller shown in Figure 3.5-4. Due to the actual time involved in taking each of the readings, it was decided to take only one reading at each point, but to allow the propeller to run for approximately a minute in each case in an attempt to compensate for the accuracy lost. Unfortunately, it was not possible to change the lubricant in the hub of the meter, and as such accurate readings for low flow rates were not possible. Also, due to the size of the actual propeller, it was not possible to take readings closer than forty millimetres from the edge or bottom of the flume or from the water's surface.

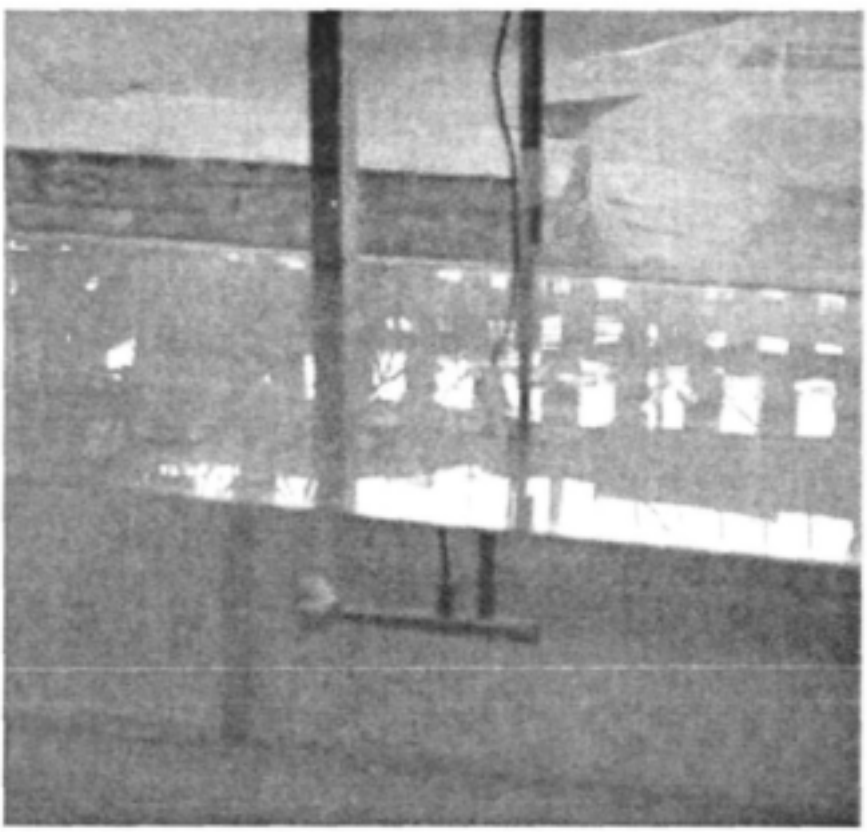

Figure 3.5-4 Photograph showing velocity measurements with a current meter

e) Average Water Surface Slope

During the calculation of the average bed slope, it was also possible to determine the elevations of each measurement point. Once the depth of flow readings were known, it was then possible to calculate the water surface slope by correlating the depths with the elevations. Due to the low flow velocities in relation to the depths, the kinetic energy (velocity head) when calculated, was less than one millimetre and can thus be considered negligible, with the average water surface slope equated with the average energy slope.

It is important to note that due to the very flat gradients involved, and with the depth readings taken to the nearest millimetre over the relatively short distance of the flume, a discrepancy in just one of the readings can change the average slope substantially.

3.5.2 Data analysis

Eight tests were run in total. All data as collected during the course of the experiments, along with all the graphs plotted, can be found in Appendix C in electronic format.

The first four tests were conducted with no point velocity measurements, as this was not the original intention of the study. It soon became apparent though, that these measurements were important if the plunge line was to be studied in depth. It is also important to note, however, that the measurement of point velocities for the first four tests would most probably not have been possible with the instrumentation available due to the low flow velocities involved.

All tests, except the last, included depth of flow measurements along the length of the flume. Test eight did not include this data as it was run only as an attempt to obtain more information on the three dimensional velocities near the plunge line. Calculations were done at different points in relation to the plunge line as shown in Figure 3.5-3 and also in some cases at set distances of fifty, one hundred, two hundred and three hundred millimetres from the walls of the flume.

The following calculations were done with all the data collected:

- Average hydraulic roughness, ks, calculated from average surface slope across the whole flume.
- Energy slope at specific points in relation to the plunge line using the calculated roughness.
- Energy slope as above, but using an assumed roughness of one millimetre.
- The ratio of bed slope to energy slope.
- The Froude and Reynolds numbers.
- For the tests where point velocities were also measured, values for the energy slope at points at set distances from the edge of the flume and at set positions in relation to the plunge line were calculated using equations for laminar and turbulent flows.

The following graphs were plotted using an Excel spreadsheet for the tests run:

- All measurement point depths recorded (including the average depth calculated) versus the distance along the flume.
- Total energy (showing potential energy, average depth of flow and velocity head) versus the distance along the flume, including a linear trend line of the total energy.
- Average velocity at each measurement point versus distance along the flume.

For the tests where point velocities were measured the following graphs were also plotted:

- Contour lines showing the cross sectional velocity distribution at set points in relation to the plunge line.
- Longitudinal sections showing the relationship between the ratio of depth to total depth and velocity at set positions in the flume and in relation to the plunge line including theoretical turbulent and laminar velocity distributions.
- The same longitudinal sections as above, but with the depth ratio scale logarithmic in an attempt to compare slopes.

3.5.3 Brief Description of Test results

a) Test One

The first test was completed using a discharge of 8.7 litres per second. This was a relatively low flow rate and thus took some time to stabilise. The low flow rate also meant that the plunge line was less distinct than for the larger flows. As can be seen from the recorded data, the measurement needle on the instrument carriage shifted slightly during the course of the experiment, but this is thought to have had no negative effect on the final results.

A calculated average flume roughness of over a metre gave the first indication that the average observed energy slope was not accurate enough for the purposes of calculation.

b) Test Two

This test had the lowest discharge (3.8 l/s) where the plunge line could be located. (An attempt was made to form a plunge line with a discharge of 3.2 l/s but this was not possible. It is presumed that the plunge line in this case could not be seen (as opposed to not forming), either due to the fact that it was too unstable and moved out of the flume, or it was too feint to be noticeable.) As can be seen from the variability in recorded depth results, the flow was still rather unstable and depth measurements were abandoned after the second set was recorded.

Graphs were plotted with the data that was recorded before the run was stopped, and one can see that the observed average energy slope was positive (i.e. the total energy was increasing along the flume). This is of course not possible. It is thought that these results were obtained due to the instability of the low flow rate. Calculations with an estimated roughness gave a very flat energy slope gradient

c) *Test Three*

Run also at a relatively low flow rate of twelve litres per second, it can be seen that the flow, as in test two, was not quite stable. It would appear that for low discharges, a much longer time is needed for flow to stabilise, that is assuming that the flow would ultimately reach a stable state (both tests two and three were given more than an hour to stabilise before any readings were taken). Once again, calculations with an estimated roughness gave a very flat energy slope gradient.

d) Test Four

It was realised that for accurate depth readings with low discharges (test four had a discharge of fourteen litres per second) at least four depth measurements had to be taken. This lead to much more satisfactory results when it came to plotting the observed average energy slope. The calculated roughness using this observed energy slope was ten millimetres, which was the smoothest of all tests completed.

e) Test Five

Test five was the first test where point velocities were measured. Even though the discharge was at almost eighteen litres per second, the propeller meter did not at times run smoothly. As this was only really a trial run with the velocity measurements, no actual pattern was followed during the recording of data. Although velocity contour graphs have been plotted with the results, not enough measurements were taken for an accurate picture to be drawn.

f) Test Six

Test six was run at nineteen litres per second with the flow much more stable than for other tests. Only two depth readings were taken at each measurement point. From the experience gained from velocity measurement in test five, a more ordered measurement collection pattern was devised. It was decided to collect data at fixed positions in relation to the plunge line and at a fixed number of depths (see figure 4.4).

g) Test Seven

At a discharge of just over seventeen litres per second, flow was once again stable enough to warrant only two depth readings at each measurement point. Point velocity readings were once again taken, using the same method as test six.

h) Test Eight

Test eight was run only to confirm the velocity contours just downstream of the plunge line at position two. As such, no longitudinal section with depth of flow measurements across the whole flume was measured. As was expected, one can see a broadening and flattening of the velocity contours, and a favourable comparison between the measured velocity profile and the calculated turbulent profile.

A typical velocity distribution through the flume of test 5 is shown in Figure 3.5-5.

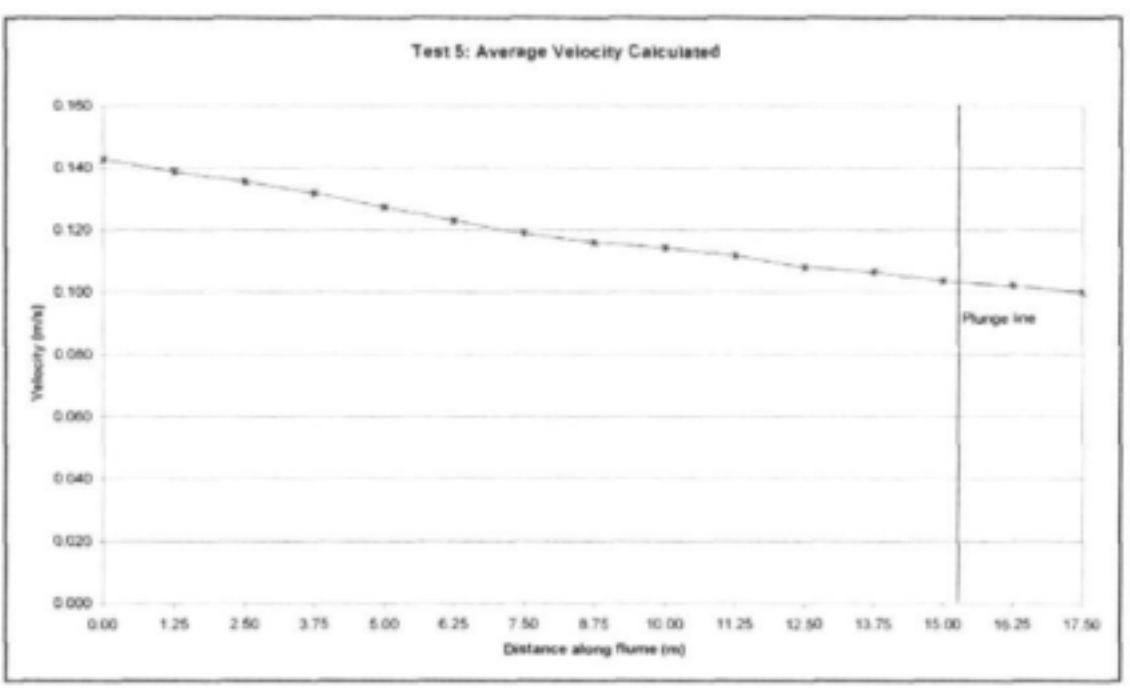

Figure 3.5-5 Example of changing velocities along the flume

3.5.4 Velocity distribution at cross-sections

Where point velocities were recorded with the propeller meter it was possible to plot the point velocities and to interpolate the velocity contours. As can be seen from Figures 3.5-6 and 3.5-7, taken from test seven, the flow velocity contours appear to broaden and flatten near the bottom from position one to position two (refer to Figure 3.5-3), while the maximum velocity area seams to become smaller to compensate for these broader contours. This was the case for all the runs where point velocities were recorded, although it was more visible in some than others. It also appeared that the changed flow pattern did not stay like this, but reverted back to normal within a metre, because the measurements taken at point three were similar in appearance to those at position one. This can be seen most clearly in Figures 3.5-8 and 3.5-9, taken from test six, where the graphs are very similar at position one and three. All graphs plotted with three-dimensional velocities showed the same tendencies, but the ones shown here are the clearest. All graphs plotted are enclosed in electronic format in Appendix C.

It is thought that the flow reverts back to its original pattern because it does not have the momentum to plunge all the way to the bottom, and is thus broken up by turbulence. A plunge line that is carrying a high enough sediment load is able to plunge to the bottom as a result of this increased density and thus momentum.

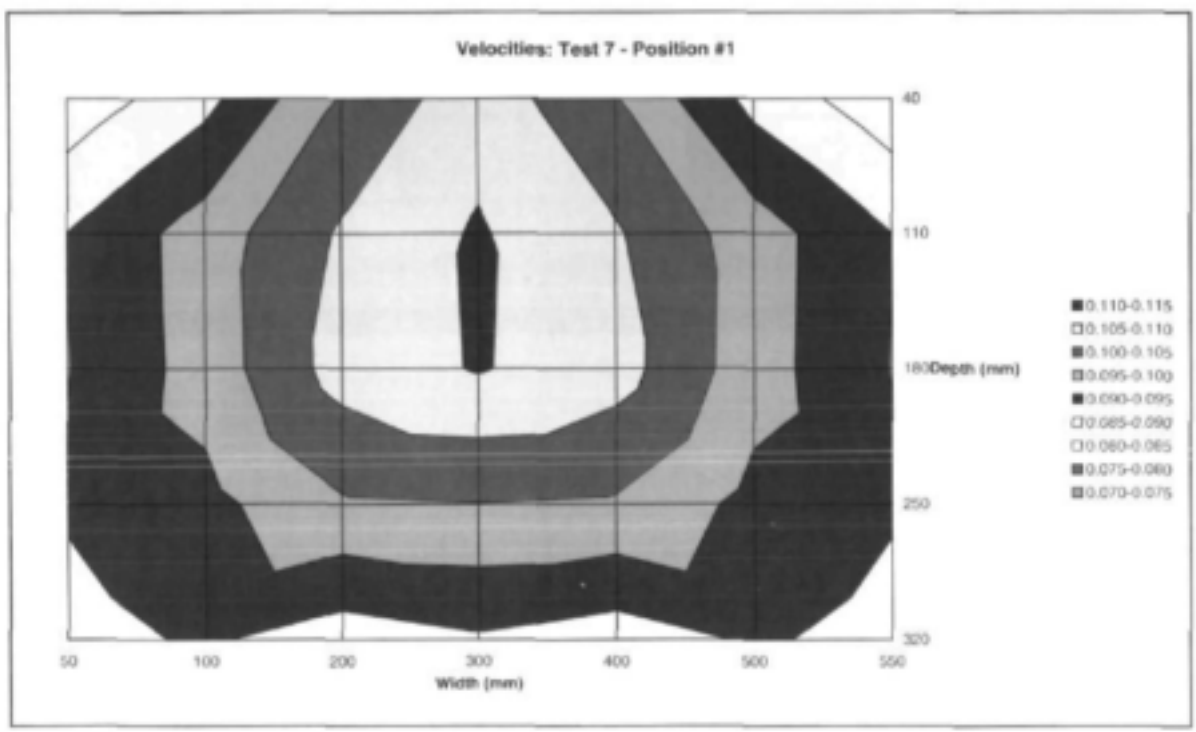

Figure 3.5-6 Velocities at start of plunge line for test seven

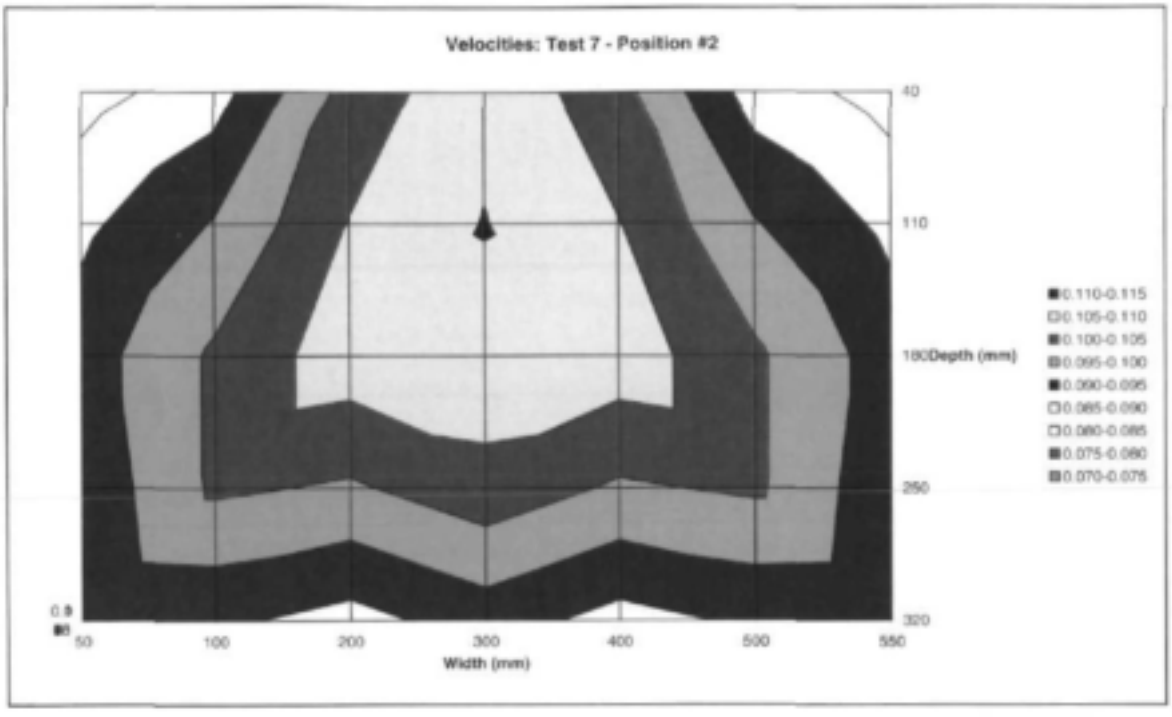

Figure 3.5-7 Velocities 200 mm past start of plunge line for test seven

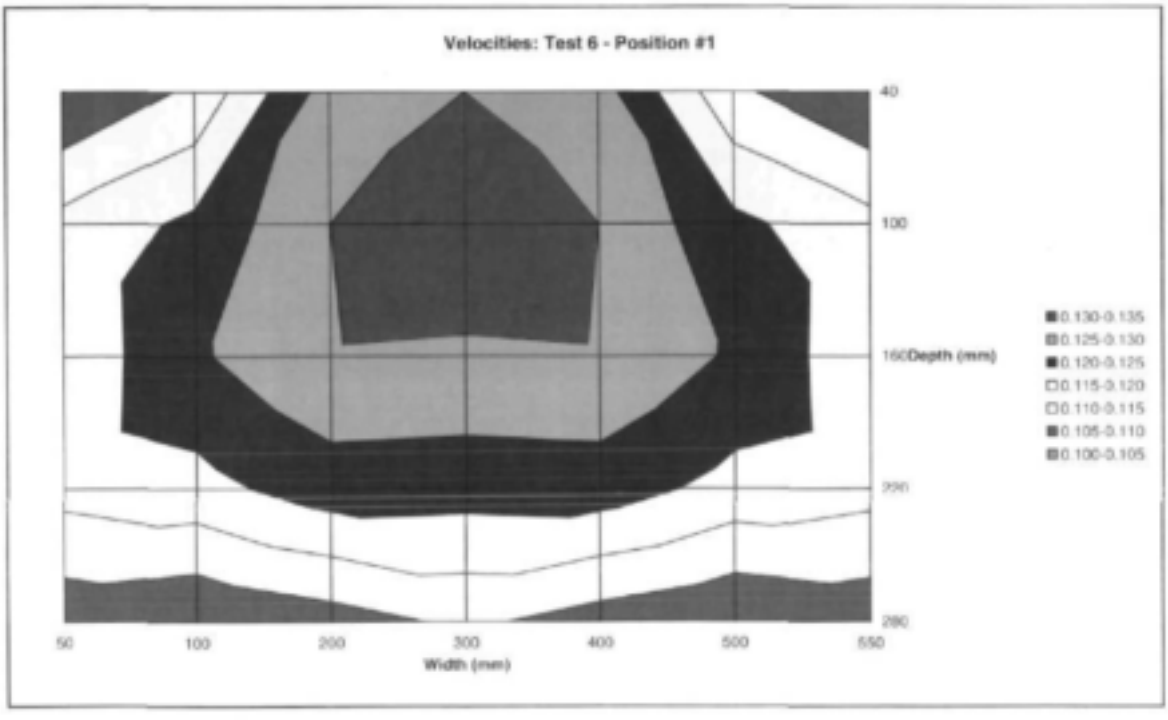

Figure 3.5-8 Velocities at start of plunge line for test six

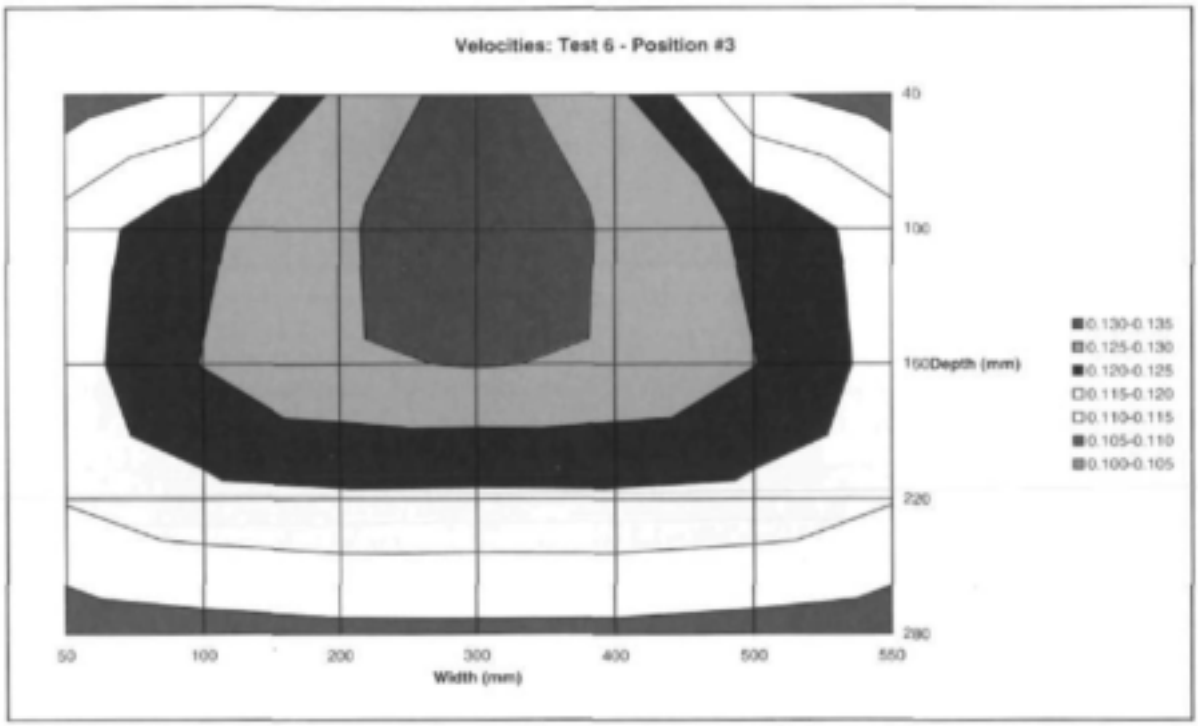

Figure 3.5-9 Velocities 1200 mm past start of plunge line for test six

3.5.5 Vertical velocity distribution

Longitudinal sections showing the velocity profiles fifty, one hundred, two hundred and three hundred millimetres from the edge of the flume and at different positions in relation to the plunge line were plotted and compared to laminar and turbulent velocity profiles (Figures 3.5-10 to 3.5-13). It can clearly be seen that the flow is turbulent.

The laminar energy slope and velocity profile were calculated using the following equation (Rooseboom, 1975):

$$v = \frac{\rho g s_f}{2\mu}(2Dy - y^2)$$

with v = point velocity at a specific depth

D = total depth

y = point depth

The energy slope was calculated first using the maximum point velocity of all three and its corresponding depth. This was in order to calculate a velocity profile that was of a similar magnitude to those observed.

The turbulent energy slope and velocity profile were calculated using the following equation (Rooseboom, 1975):

$$v = \sqrt{2\pi . gDs_f}\ \ln\left(\frac{y}{k_s/30}\right)$$

The same graphs were plotted with a logarithmic depth to total depth ratio so that one can compare the slopes (Figure 3.5-14). It can be seen that the slopes of the observed velocity profiles and the calculated velocity profiles for turbulent flow are quite similar, especially when measured futher from the flume wall. The theoretical velocity distribution can however not determine the low flow velocities near the surface accurately.

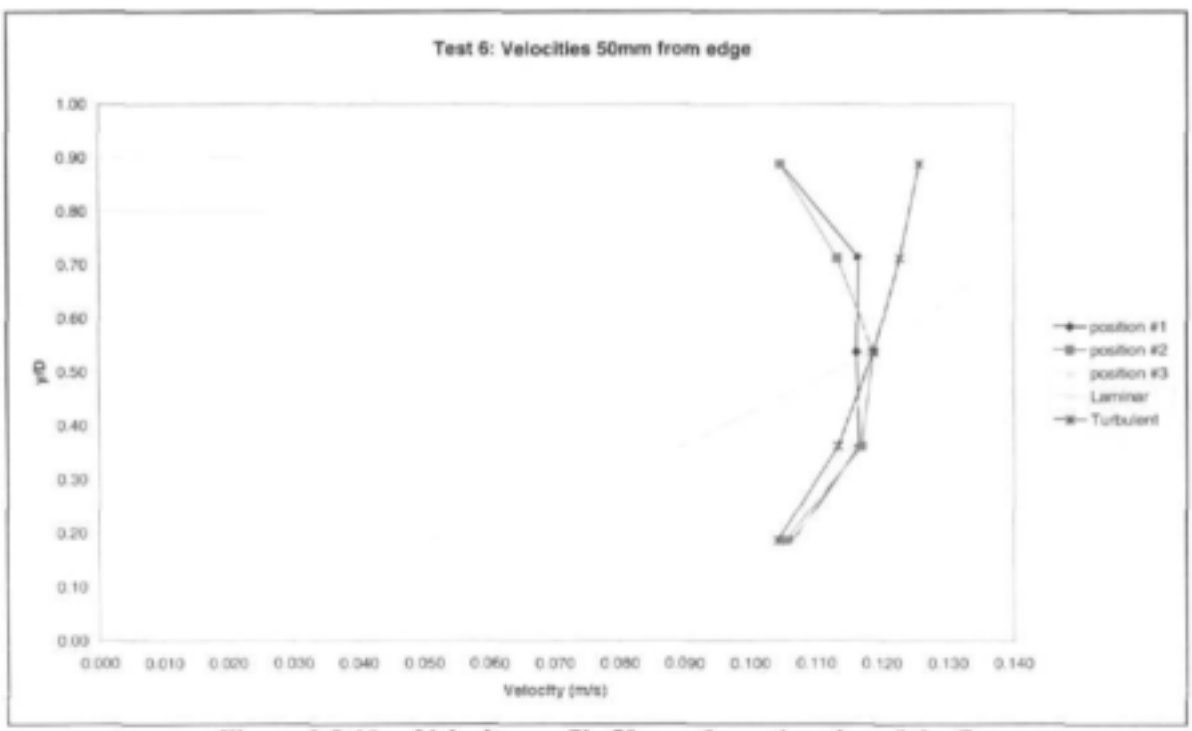

Figure 3.5-10 Velocity profile 50 mm from the edge of the flume

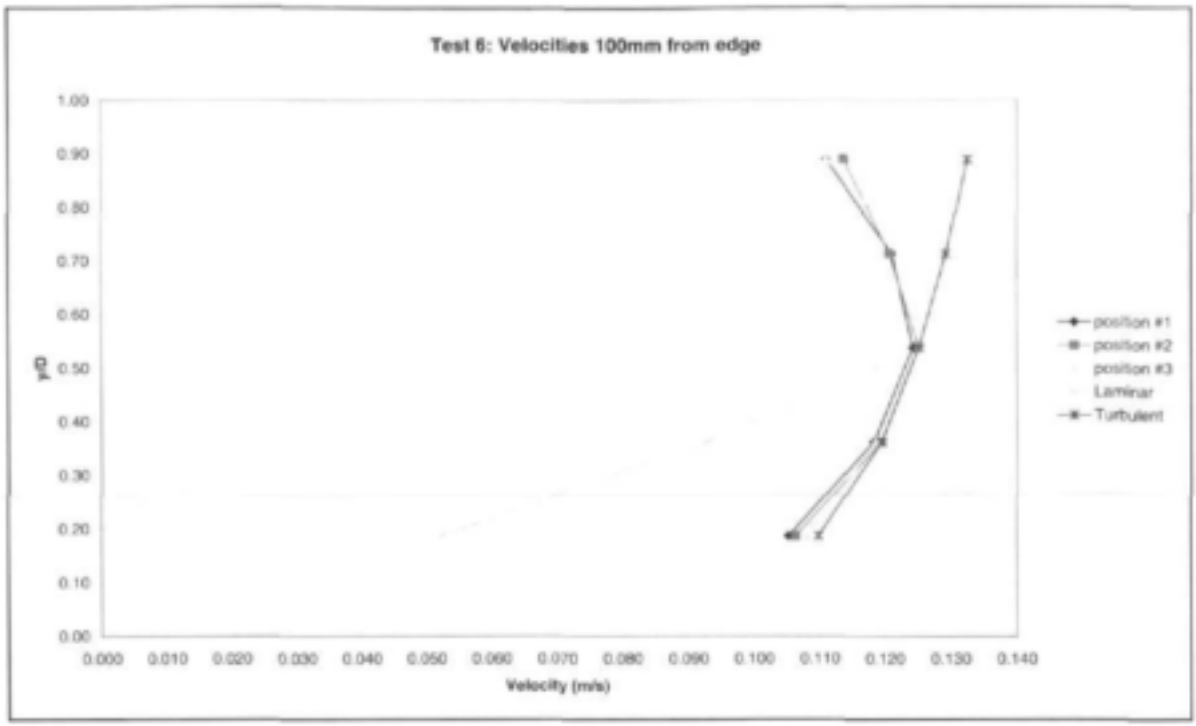

Figure 3.5-11: Velocity profile 100 mm from the edge of the flume

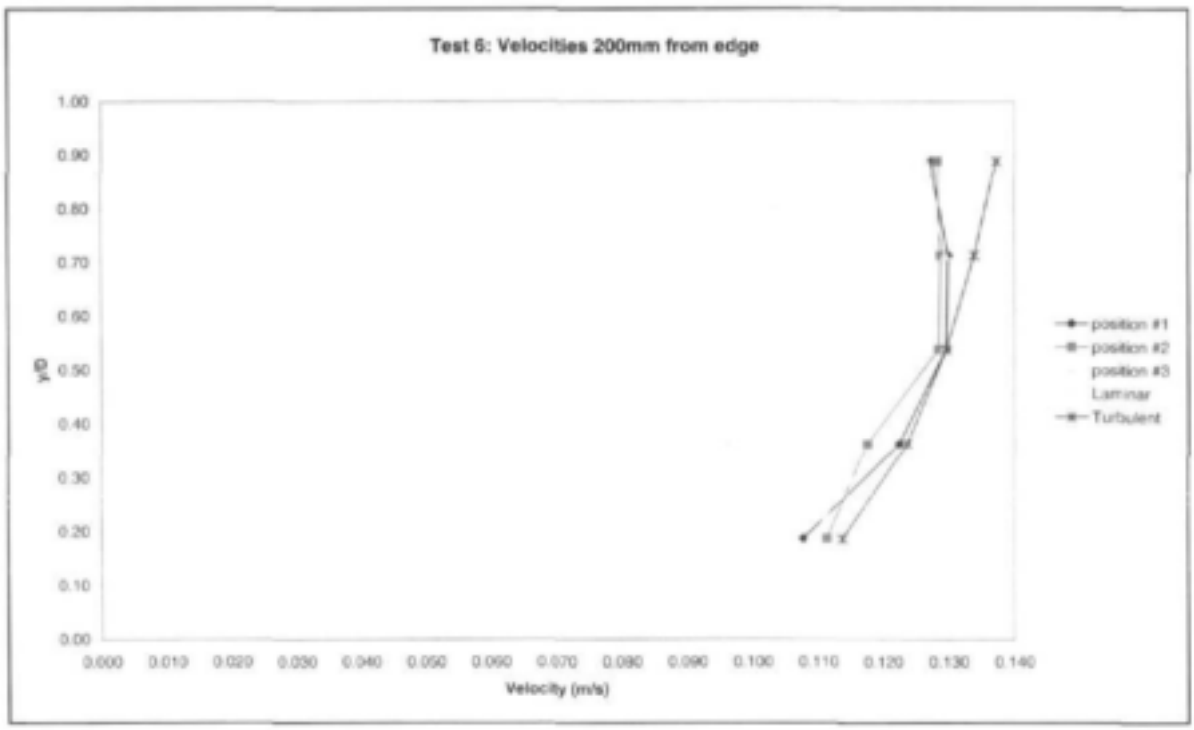

Figure 3.5-12: Velocity profile 200 mm from the edge of the flume

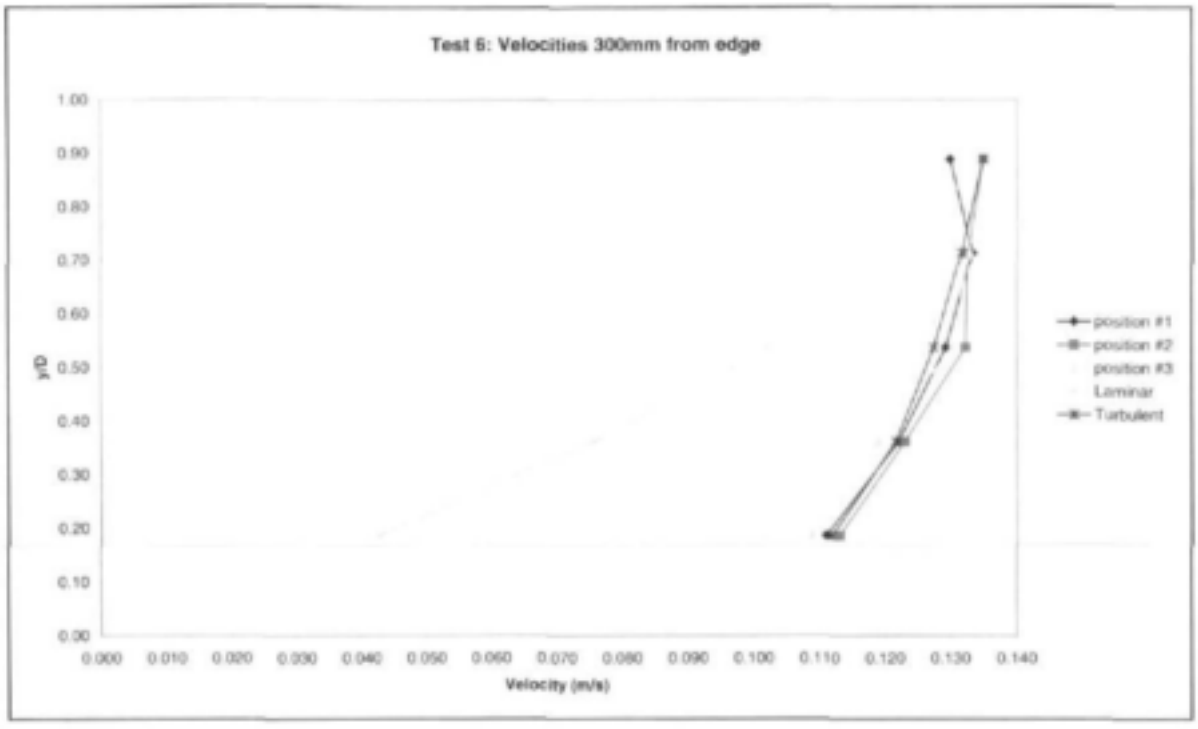

Figure 3.5-13 Example of the velocity profile in the middle of the flume

Figures 3.5-10 to 3.5-13 show how the velocity profile changes from close to the edge of the flume, to the middle. The velocities at the edge are much slower, with the surface and bed velocities similar in magnitude, while the velocity profiles for the centre are more curved from the surface to the bed. One can also see a higher velocity at a greater depth for the edge profiles, which is also what was seen with the three dimensional graphs where the contours became broader and flatter near the bed.

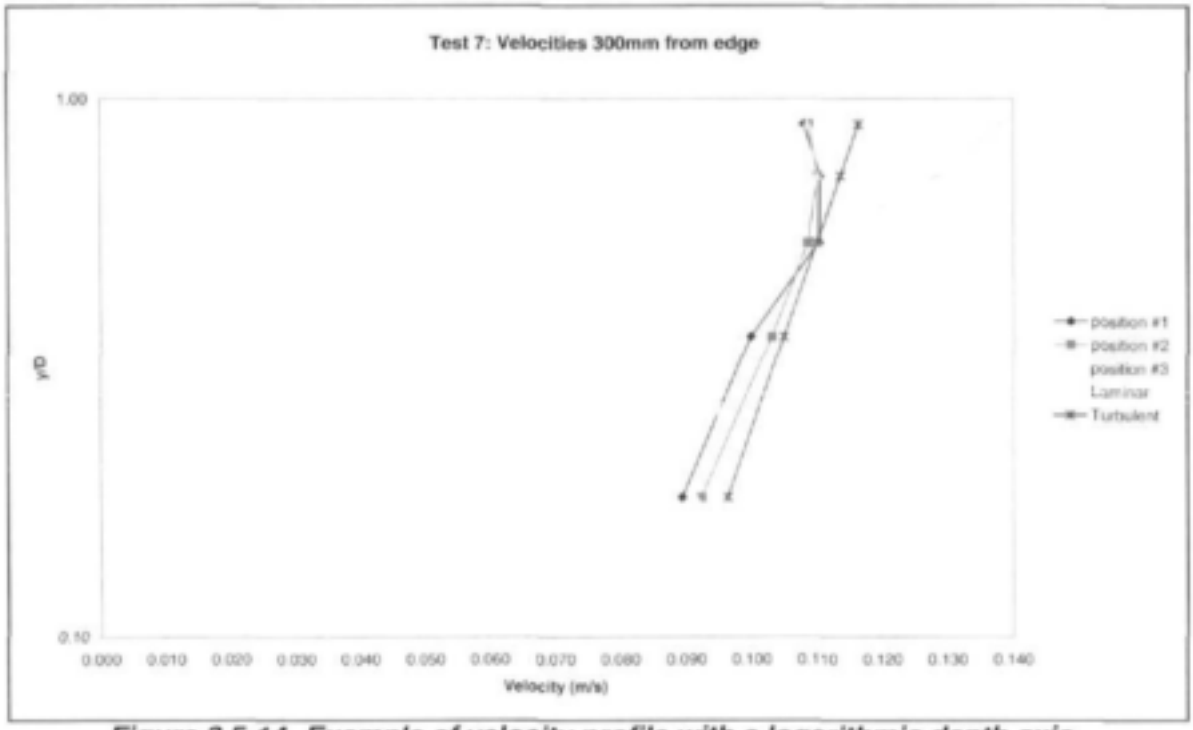

Figure 3.5-14 Example of velocity profile with a logarithmic depth axis

3.5.6 Summary of Results

Table 3.5-1 gives a summary of tests and data analysed by Wicht

Table 3.5-1 Summary of results recorded in all tests by Wicht

Test number	1	2	3	4	5	6	7
Discharge (l/s)	8.69	3.84	11.97	14.28	17.78	18.94	17.11
Across flume:							
Average velocity (m/s)	0.032	0.017	0.060	0.135	0.117	0.104	0.079
Observed energy slope	8.7E-05	n/a	n/a	5.9E-05	4.4E-05	5.5E-05	8.1E-06
Calculated roughness (m)	2.865	n/a	n/a	0.010	0.034	0.144	0.440
Energy slope from k=1mm	4.9E-07	1.8E-07	2.6E-06	2.9E-05	1.4E-05	8.5E-06	4.1E-06
Froude number	0.0150	0.0090	0.0335	0.1029	0.0744	0.0599	0.0375
Reynolds number	14486	6403	19949	23807	29630	31561	28510
At plunge line:							
Average velocity (m/s)	0.031	0.016	0.057	0.113	0.103	0.093	0.073
Energy slope from k_{calc}	7.0E-05	n/a	n/a	3.2E-05	2.8E-05	3.7E-05	4.1E-05
Energy slope from k=1mm	4.4E-07	1.6E-07	2.2E-06	1.6E-05	9.0E-06	6.0E-06	3.2E-06
Froude number	0.0142	0.0083	0.0309	0.0785	0.0612	0.0508	0.0375
Reynolds number	14486	6403	19949	23807	29630	31561	28510

Note: n/a applies to runs with positive observed gradients or non-recorded data

From the Reynolds and Froude numbers one can see that the flow is both fully turbulent and strongly subcritical. None of the Froude numbers come even close to the value suggested for the break-up of the plunge line.

Although depth readings were not accurate enough to calculate the exact energy slope, a clear picture of plunge lines has been formulated through the three-dimensional velocity analysis. It is clear that the plunge line is not only a surface effect, but that it changes the vertical and lateral velocity distribution. Although the clear water plunge line is an indicator of where the density current will plunge, it is clearly not enough for density current formation. This can be seen by the way that the change in velocity profile does not continue downstream, but rather reverts back to its original state. A density current will only form in conjunction with a relatively high density difference between the inflow and stored water. This higher density gives the inflow the momentum needed to plunge all the way to the bed and to stay there.

4. VERIFICATION OF NEW THEORY AGAINST FIELD DATA

4.1 Introduction

Sediment induced density currents formation have been observed at many reservoirs across the world. Information and data of Lake Mead (Hoover Dam, USA), Sanmenxia and Guanting reservoirs, China, are used here to test the prediction reliability of the minimum stream power and densimetric Froude number approaches. Gariep Reservoir data, RSA, are also used as a case where a density current did not form, although field data indicate possible formation conditions.

4.2 *Gariep Reservoir, Orange River*

4.2.1 Background

Gariep Dam (Figure 4.2-1) was constructed on the Orange river and commissioned in 1974.

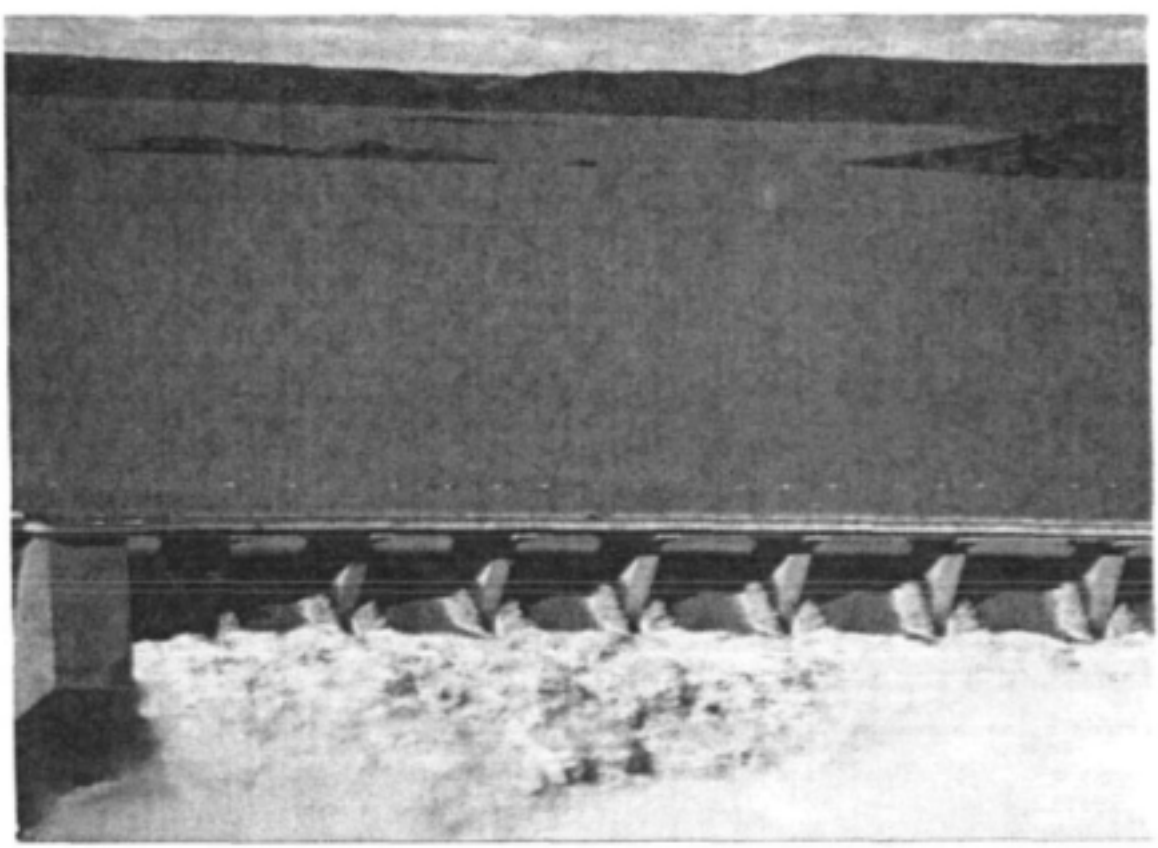

Figure 4.2-1 Gariep Dam on the Orange River

Observed field data of suspended sediment discharge and hydraulic conditions have been obtained during floods in 1974. The field data indicated that a density current did not form and turbulent suspended sediment transport dominated through the reservoir, as shown in Figure 4.2-2, according to Rooseboom (1975).

The minimum stream power relationships which have been successfully verified in Chapter 3 against temperature and sediment induced density currents, can now be applied on the Gariep Reservoir data.

4.2.2 Minimum input stream power

The turbulent flow and density current flow input stream power have been calculated at several cross-sections where hydraulic field conditions from the 1974 data are known. The bed slope (s_o) at each selected cross-section was taken as the average along the reservoir basin: $s_o = 64/74000 = 1/1156$. The energy slope (s_f) is calculated from the stream power calculated by Rooseboom (1975).

For a density current not to form (as in the case of Gariep Reservoir), the river turbulent stream power should be less than that of a possible density current if it should form.

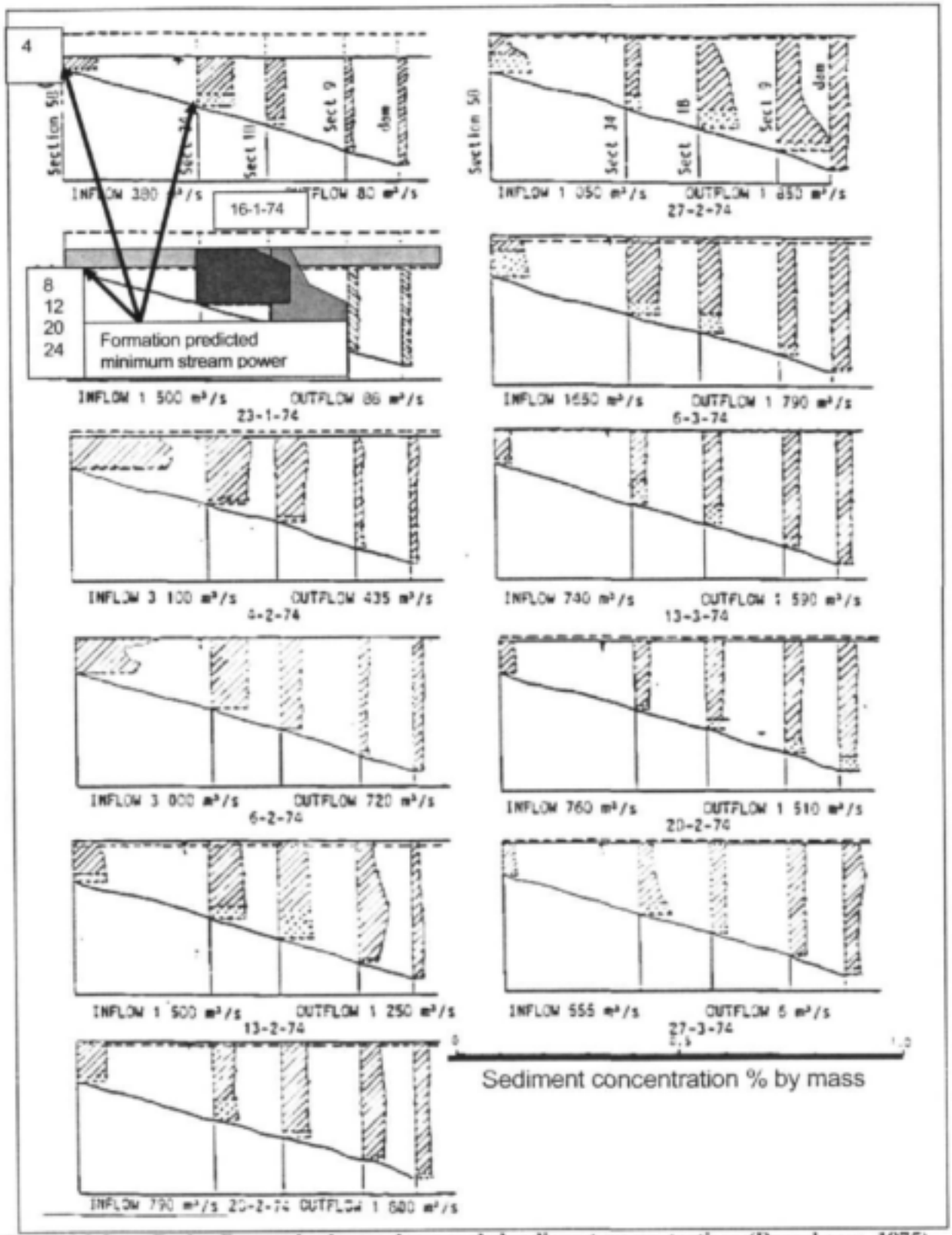

Figure 4.2-2 Gariep Reservoir observed suspended sediment concentrations (Rooseboom, 1975)

Verification of equation 2.2-8 with Gariep Reservoir data is shown graphically in Figure 4.2-3.

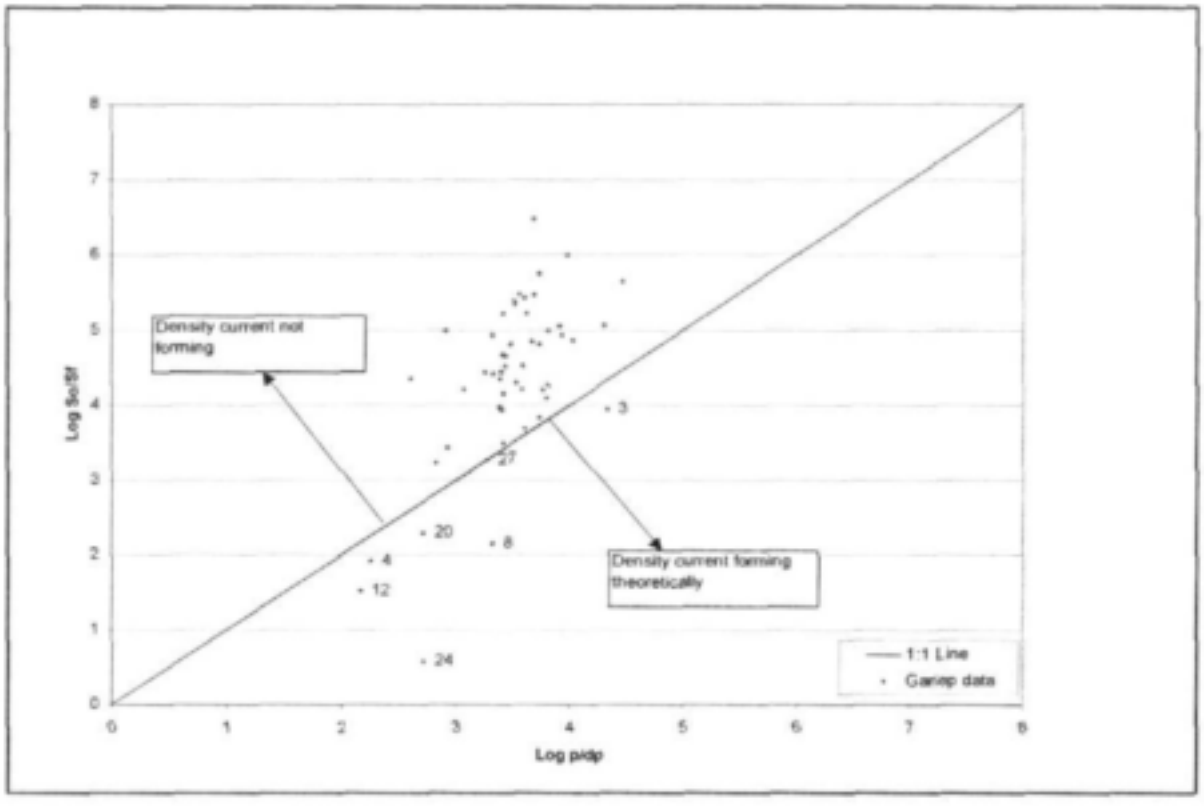

Figure 4.2-3 Minimum input stream power theory verification against Gariep Reservoir data

Figure 4.2-3 indicates clearly that at most of the data sets a density current would not be forming, as was observed in the field. According to the minimum input stream power theory prediction, a density current should be forming at section 58 which is at the upstream end of the reservoir. At this section the observed sediment concentrations were indeed higher at the bed than at the surface on 16/01/1974 (Figure 4.2-2). This could possibly be attributed to deposition of coarser particles with a higher bed load as the river enters the reservoir, or indeed density current formation. The events where density current formation are predicted by the theory are indicated in Figure 4.2-3 and Figure 4.2-2.

Figure 4.2-4 shows the observed discharge and sediment outflow from a bottom outlet at Gariep Dam during 1978. The maximum outflow sediment concentration was 0.075 percent at the start of the flushing operation and the concentration remained higher than the spillway sediment concentration for a period of 20 days. At the same time as the bottom outlet was opened the dam was spilling with observed concentrations of maximum 0.028 %. If the bottom outlet was only scouring and flushing previously deposited sediment immediately upstream of the gates, the sediment availability would have become limited. The data however shows 20 days of concentrations above that of the surface water and if turbulent

sediment transport was the mechanism then one would expect a uniform vertical distribution in the concentration due to the fine character of the sediment. The indications therefore are that the high sediment concentrations released through the bottom outlets were because of density current sediment transport and venting through the reservoir.

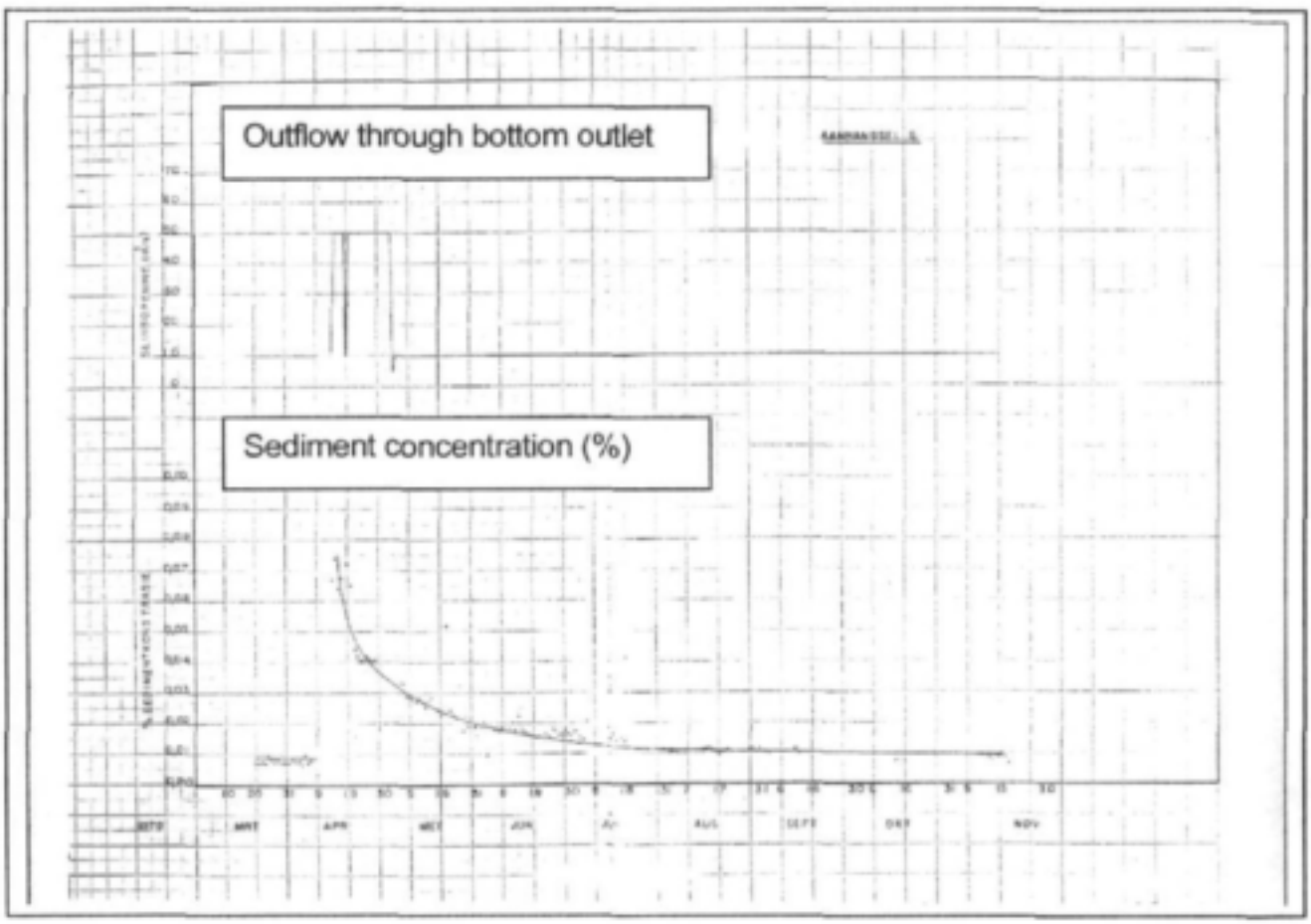

Figure 4.2-4 Gariep Dam observed bottom outlet discharge and sediment venting during 1978

4.3 Lake Mead, Colorado River, USA

4.3.1 Background

Hoover Dam, forming Lake Mead, was completed in 1935 (Figure 4.3-1).

Figure 4.3-1 Hoover Dam and Lake Mead

During the first years of operation, several sediment induced density currents have been observed. The characteristics of these density currents were:

- A very definite plunge line formed in the narrow upper reaches of the reservoir, where floating debris was trapped (Figure 4.3-2).

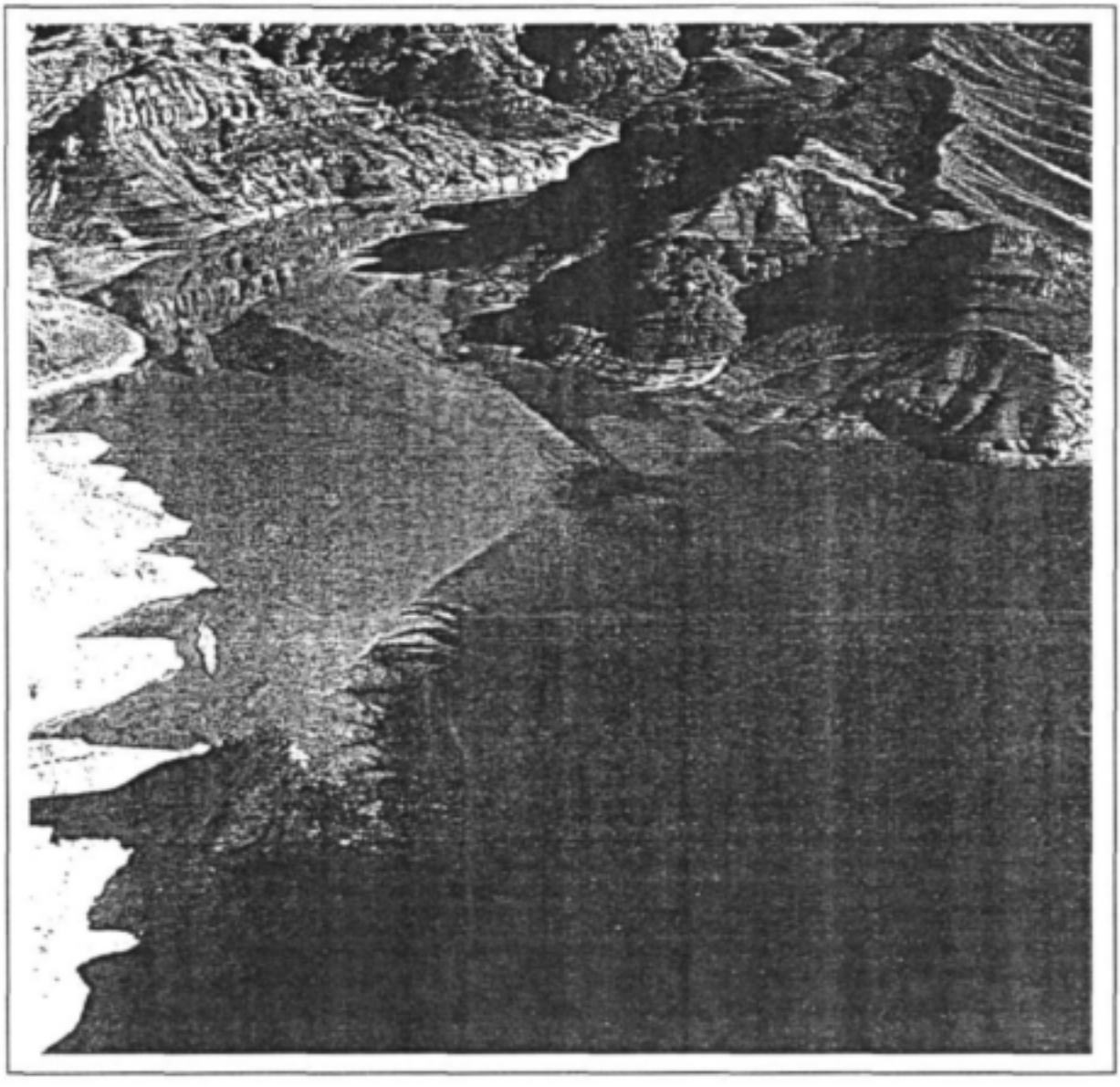

Figure 4.3-2 Plunge line at Lake Mead

- Density currents formed, even at very low density differences.

- Only fine sediment was transported by the density current, while coarser sediment was deposited at the plunge point, forming a delta. (Figure 4.3-3).

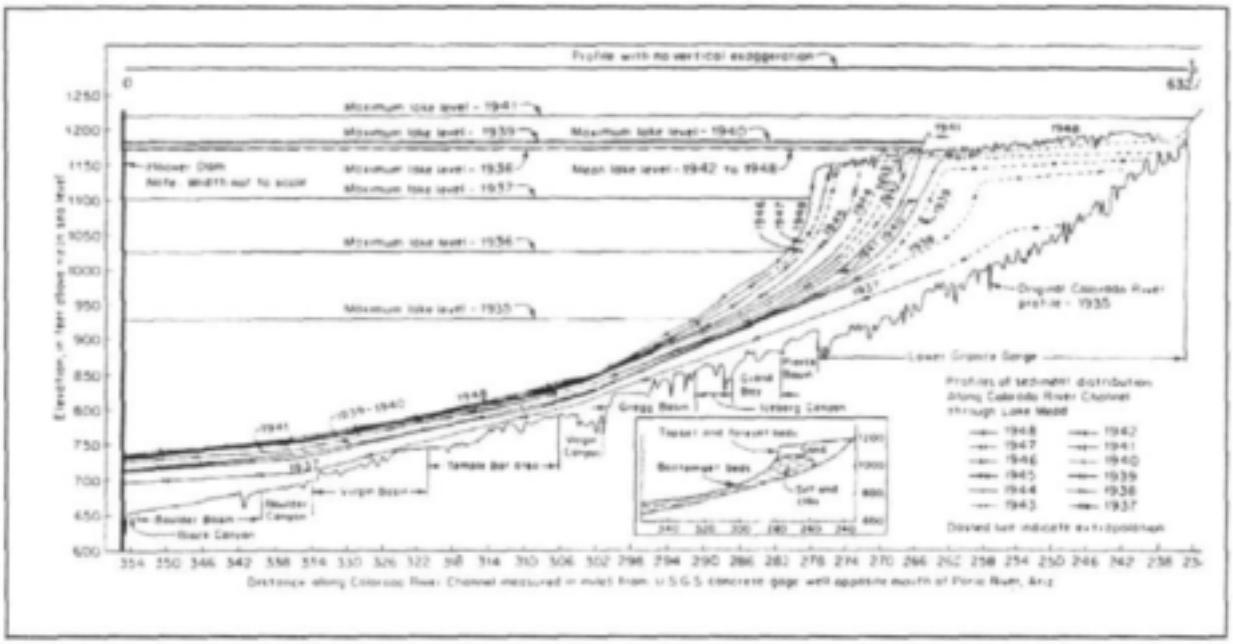

Figure 4.3-3 Lake Mead delta (Smith et al., 1960)

4.3.2 Minimum input stream power

Data on the inflow and sediment load when density currents were observed, were obtained for two flood events: 1935 and 1948. The density current which formed during 1935 occurred when the reservoir was still filling and the water level was relatively low, with relatively little sedimentation. In 1948 however, the water level was near the full supply level and sedimentation had formed a large delta in the upper reaches of the reservoir. For this study hydraulic conditions have been determined where the river meets the lake (1935), and at the downstream end of the delta topset during the 1948 event, assuming that this would be at the plunge line locations described in literature and as shown in photographs.

Results of the minimum input stream power approach for the two density current events, are shown in Figure 4.3-4. The methodology predicts the formation of the density currents correctly. The data used in this calculation is however not as detailed and reliable as that obtained for Chinese reservoirs described in par. 4.4.

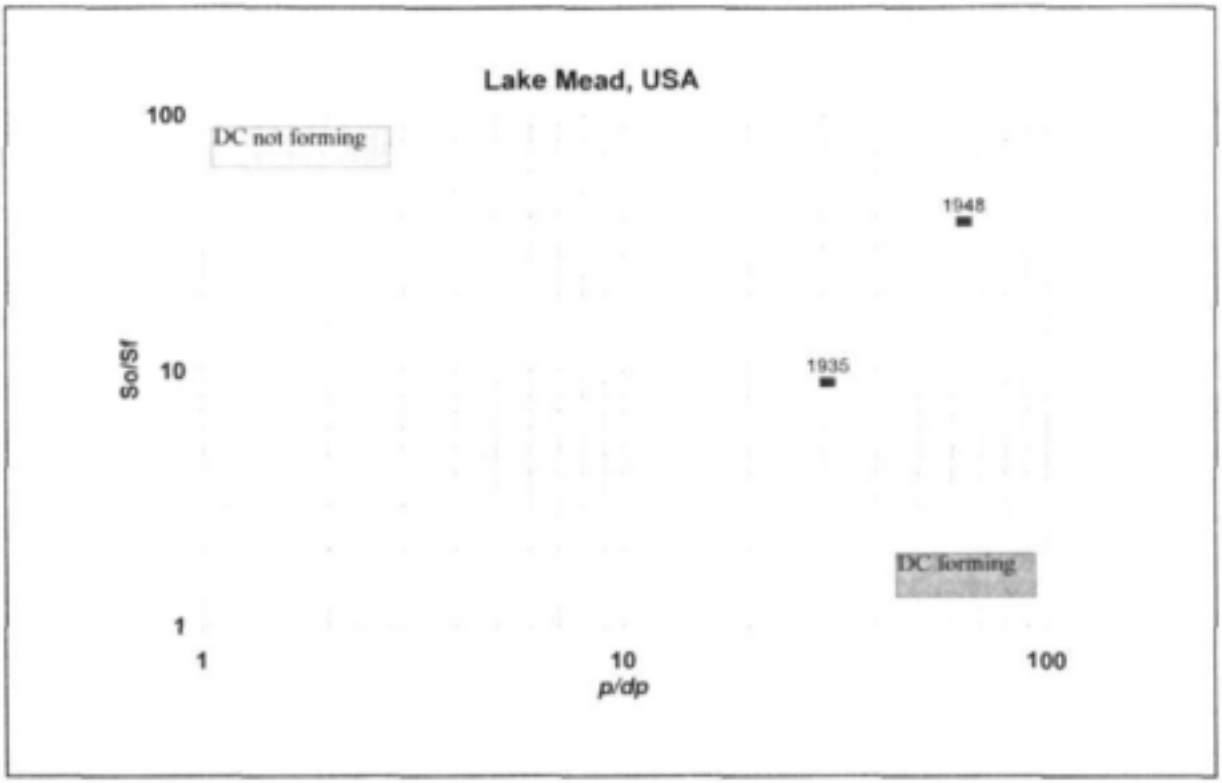

Figure 4.3-4 Lake Mead density current formation by minimum input stream power

4.4 Sanmenxia Reservoir, China

4.4.1 Background

Sanmenxia Dam, on the Yellow River, China, was completed in 1960. During 1960 a density current was surveyed at several cross-sections in the reservoir basin, from 51 km upstream of the dam. A view of the dam from downstream is shown in Figure 4.4-1.

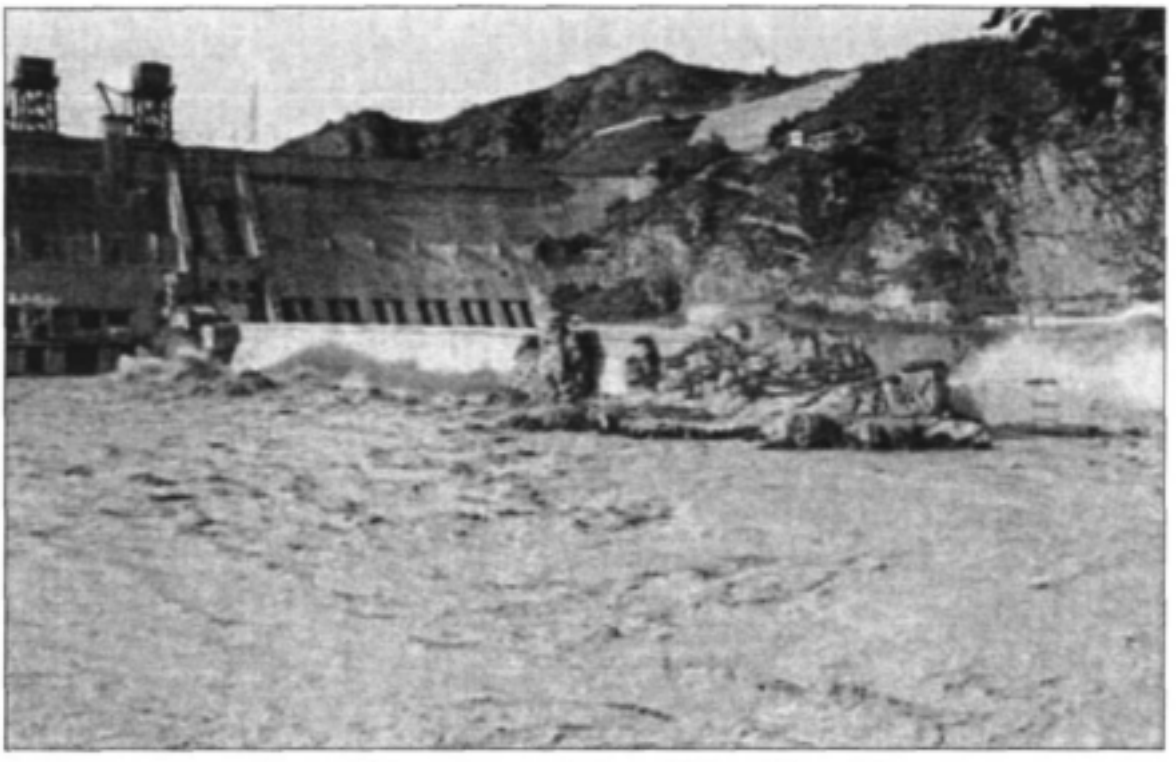

Figure 4.4-1 Sanmenxia Dam, Yellow River, China

4.4.2 Minimum input stream power theory at Sanmenxia Reservoir

Field data (Figure 4.4-2), with measured velocity (Figure 4.4-3) and suspended sediment vertical distribution, have been used to verify the minimum input stream power methodology. The result of the theoretical verification is shown in Figure 4.4-4.

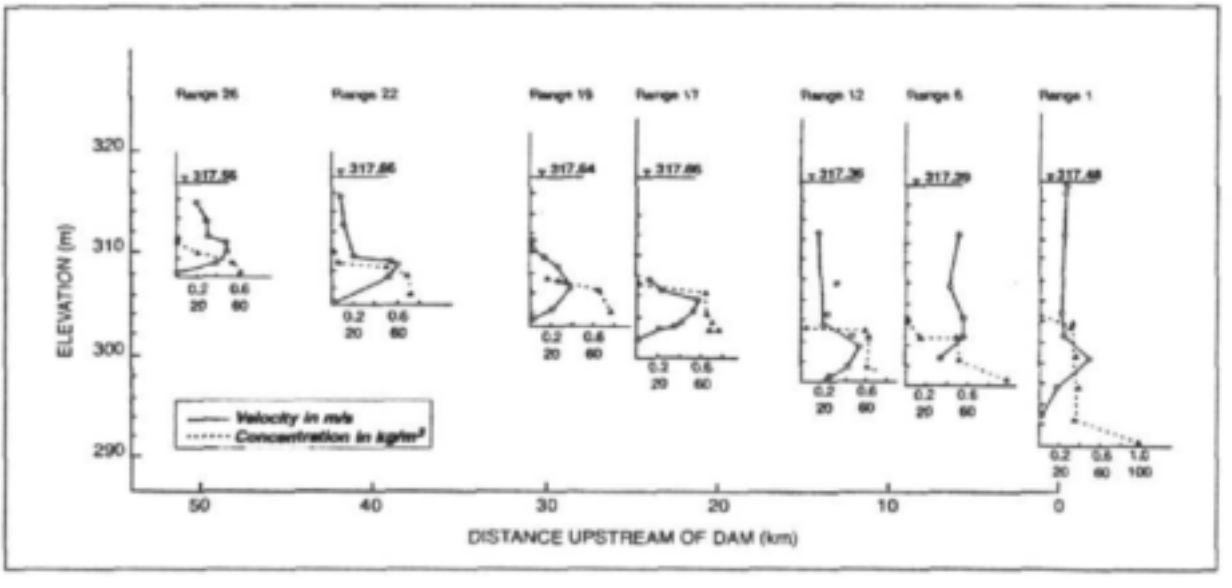

Figure 4.4-2 Observed density current in Sanmenxia reservoir

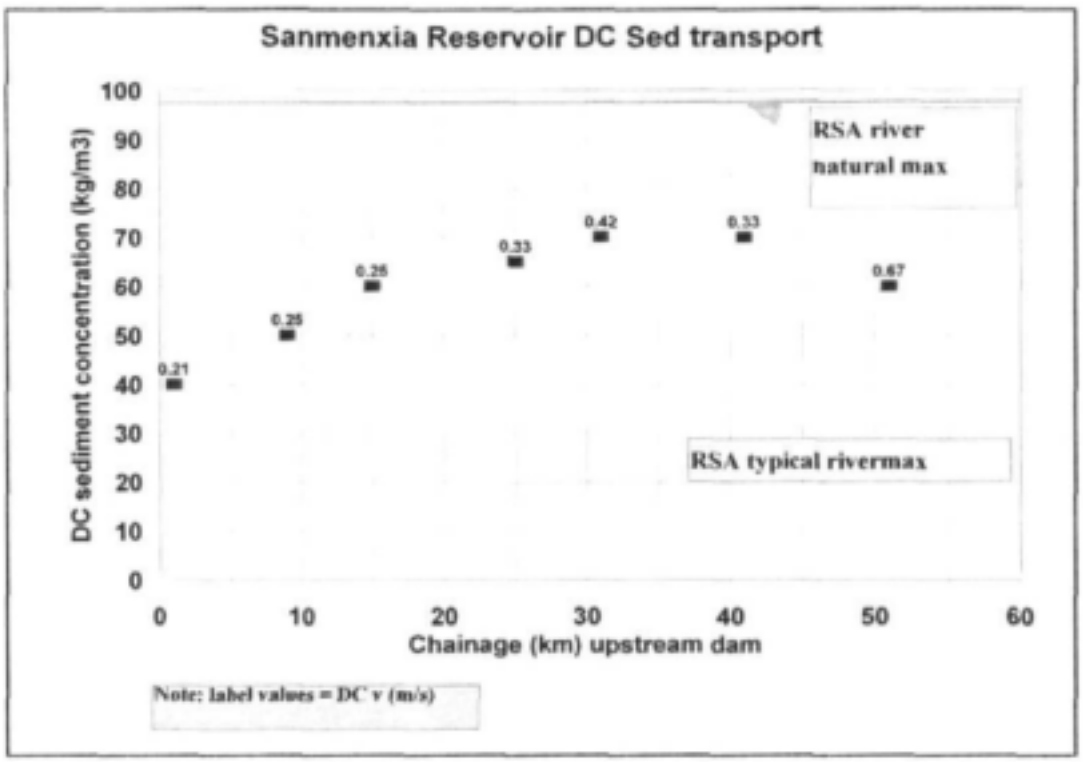

Figure 4.4-3 Sanmenxia Reservoir density current sediment concentrations

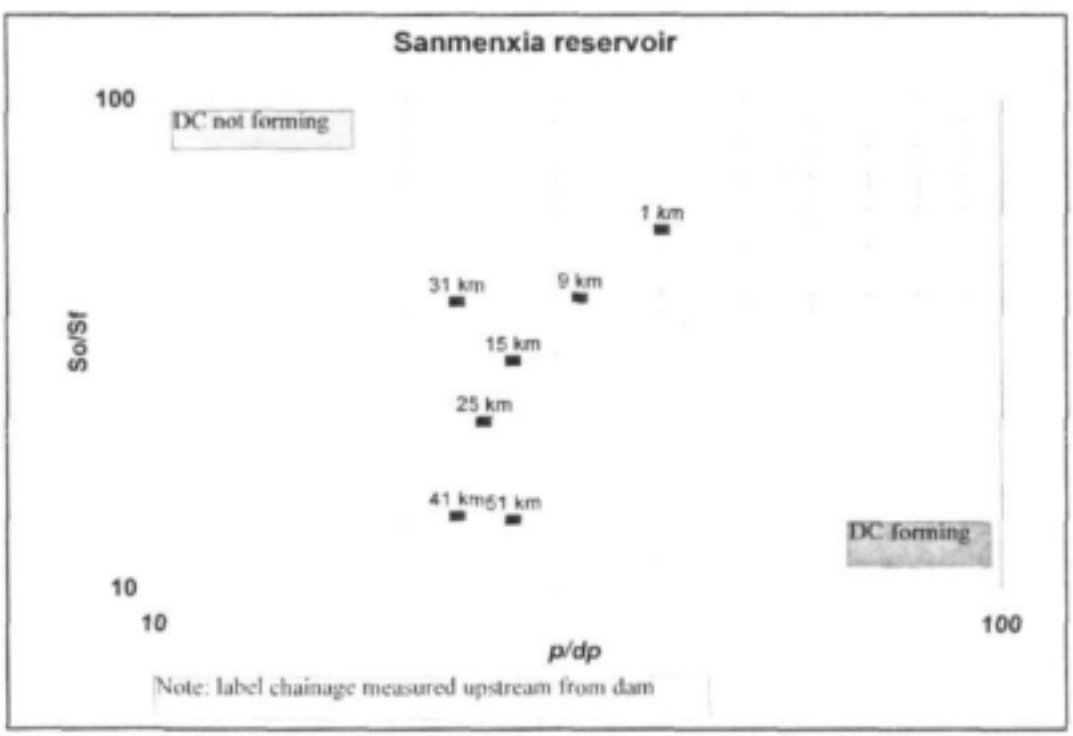

Figure 4.4-4 Sanmenxia Reservoir density current formation prediction by minimum input stream power

At the upstream end of the reservoir basin where the field data show plunging starts to occur at chainage 51 km, with fully developed density current at chainage 41 km, the minimum stream power concept predicts accurately formation of a density current. Four other data sets of chainages 1 km (at the dam) to 31 km, predicts that a density current would not be forming at those locations, with chainage 25 km very close to the line The minimum input stream power relationship therefore seems accurate in predicting density current formation as well as its location.

Figure 4.4-5 indicates the densimetric Froude numbers, with a value of 0.27 where formation was observed, which is much less than the 0.78 proposed by Fan (1960).

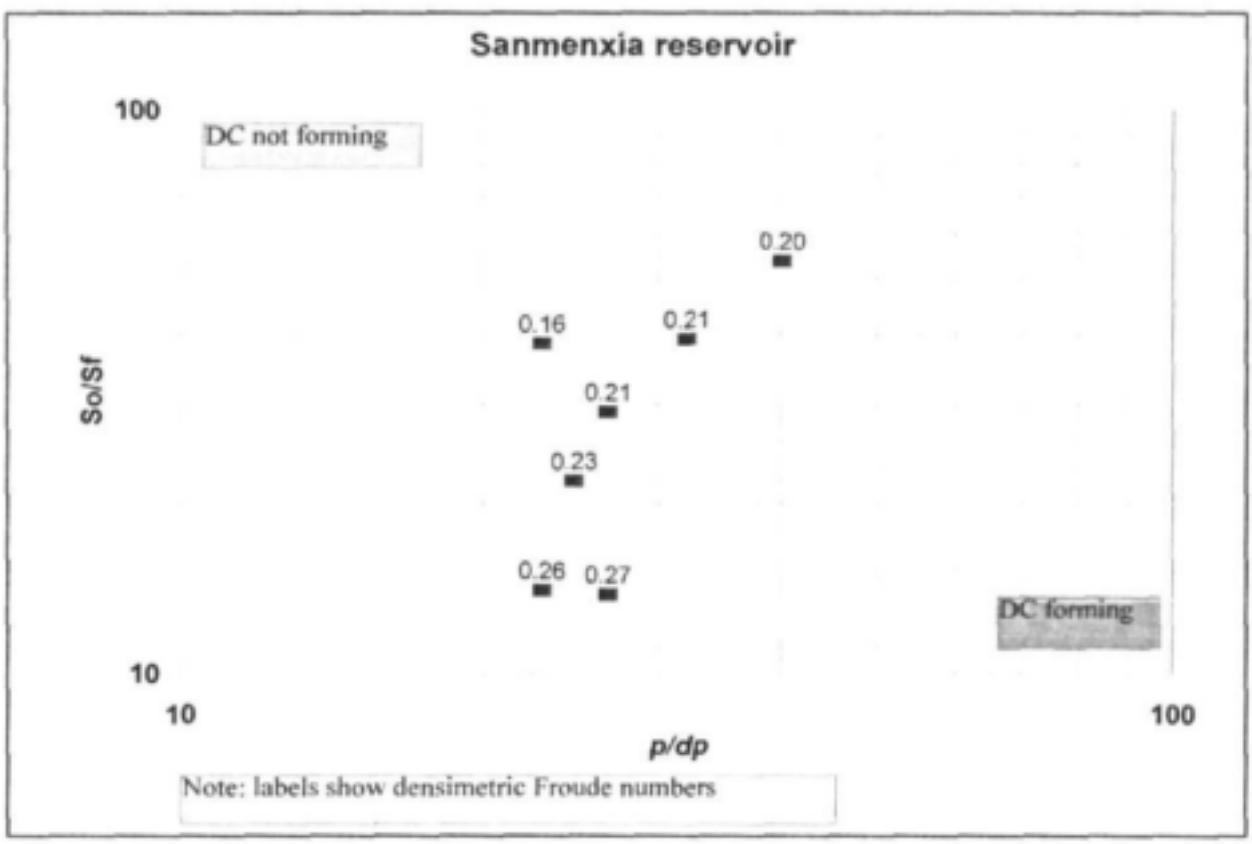

Figure 4.4-5 Sanmenxia Reservoir densimetric Froude numbers

4.5 Guanting Reservoir, China

4.5.1 Background

Guanting Dam in China, was completed in 1953.

4.5.2 Minimum input stream power

A density current was monitored in the field from 13 to 15 October 1954, and flow velocity and suspended sediment distribution were obtained at 10 reservoir cross-sections (Figure 4.5-1). Figure 4.5-2 shows observed density current concentrations in the reservoir that are compared with typical South African river concentrations. The three data sets (one for each day) have been used to verify the minimum input stream power methodology successfully, as shown in Figure 4.5-3. Density current formation is calculated at the upstream reaches of the reservoir, as indeed observed in the field.

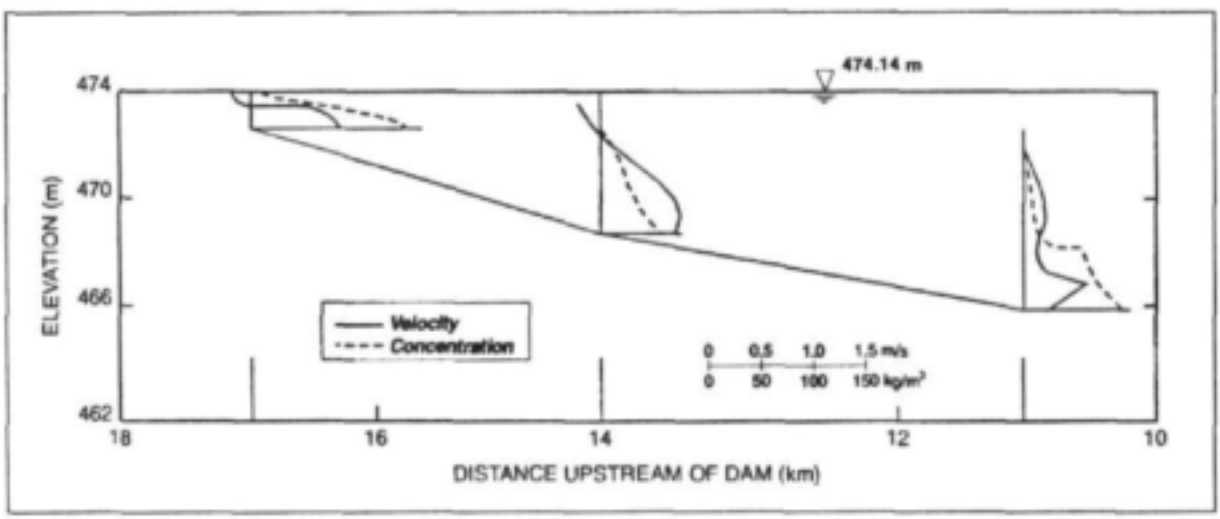

Figure 4.5-1 Observed density current in Guanting Reservoir, China

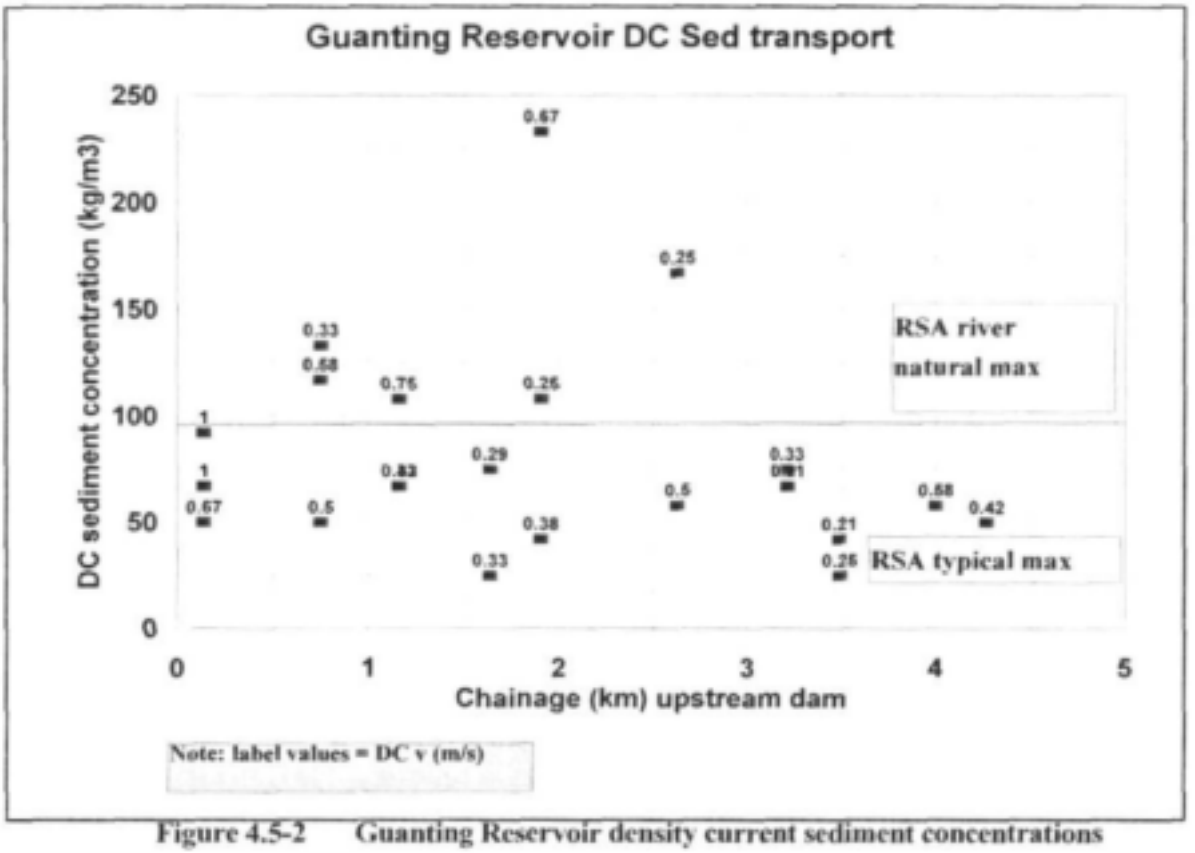

Figure 4.5-2 Guanting Reservoir density current sediment concentrations

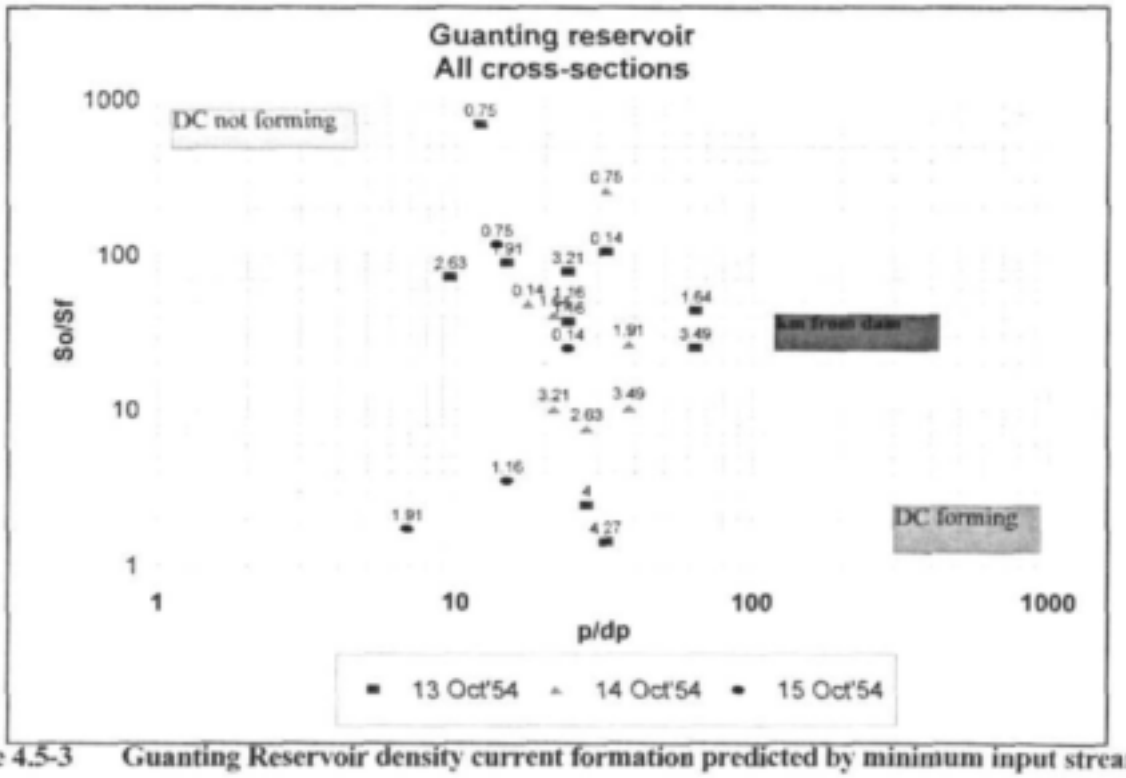

Figure 4.5-3 Guanting Reservoir density current formation predicted by minimum input stream power

For the cases with density current predicted by minimum input stream power, Figure 4.5-4 shows the corresponding densimetric Froude number: a range of 0.45 to 1.07, which is very wide.

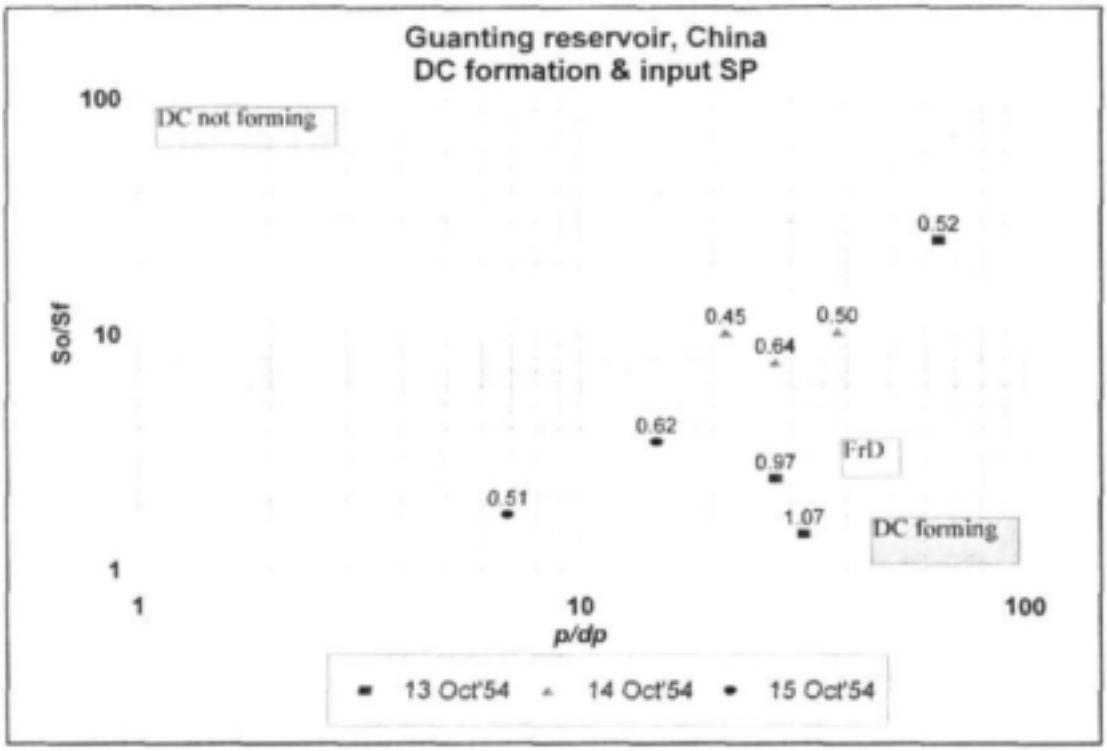

Figure 4.5-4 Guanting Reservoir densimetric Froude numbers

5. DENSITY CURRENT SEDIMENT SIZE REQUIREMENTS

From field and laboratory data on sediment transported by density currents through reservoirs, it is clear that only the finest particle sizes are transported. It is therefore a requirement for a density current that the river flowing into the reservoir should transport fine sediment at a concentration above at least 250 mg/ℓ if the reservoir water is clear (as obtained from laboratory experimental work in this study).

Typical observed density current sediment particle sizes are shown in Table 5-1.

Table 5-1 Observed suspended sediment sizes transported by density currents

d_{50} (micron)	Description
< 20	Graf (1983)
40	Jammersdrift, Caledon River (1978/78)
9.5 to 10.5	Welbedacht Reservoir, 1995, at end of flushing (Basson and Rooseboom, 1997)
1.65 (d_{90} = 60)	Lake Mead, USA (Smith et. al., 1960)
2 to 2.5 (d_{97} = 40)	Guanting Reservoir, China (Fan, 1960)
14	Aliwal North, Orange River (1978)
1.9	Gariep Dam bottom outlet gates (1978)

Typical inflow suspended sediment grading analyses of Welbedacht Reservoir on the Caledon River indicate data as shown in Table 5-2. This data were obtained during February 1994.

Table 5-2 Inflow suspended sediment size distribution at Welbedacht Reservoir

Discharge (m^3/s)	**% clay (< 2 micron)**	**% silt (2 to 50 micron)**	**% fine sand (50 to 150 micron)**
500	49	45	6
550	36	56	5

The fine characteristics of the Caledon River sediment explains why a density current could be observed at Welbedacht Dam after flood flushing in 1995. Limited data on suspended sediment particle sizes observed over the years at many rivers, are available from the Department of Water Affairs and Forestry.

The ratio of density current sediment outflow to inflow is a factor of the availability of fine sediments and the density current sediment transport capacity. Typical ratios are given in Table 5-3.

Table 5-3 Observed ratio of density current sediment outflow to inflow during floods (Bruk, 1985)

Reservoir	Reservoir Length (km)	Sediment outflow to inflow ratio
Heisonlin	2	0.16 to 0.59
Fengjiashan	12-14	0.23 to 0.65
Guanting	4.8 – 8.5	0.19 to 0.34
Guanting	10.1-16.8	0.20 to 0.29
Sanmenxia	80 (during 1961)	0.18 to 0.21
Lake Mead	128	0.18 to 0.39

From practical experience (Table 5-3), it seems realistic to use an outflow to inflow sediment discharge ratio of about 0.20, for realistic conservative long-term planning.

6. FORCED DENSITY CURRENT FORMATION AS MEANS OF RESERVOIR SEDIMENTATION MANAGEMENT

Flume tests by others (described in Basson and Rooseboom, 1997) show that if a turbid stream is flowing directly into the bottom of the reservoir, a density current would transport the fine sediment under most conditions. This is achieved by vertical sluice gate with a bottom opening.

At the Eril Emda reservoir, Algeria, tests have been carried out (Duquennois, 1956) to investigate density current formation when bed sediment is resuspended mechanically to create a density difference. Plunging did occur but the density current moved only a short distance. Density current formation and/or sediment transport conditions were therefore not ideal.

South African reservoir water levels vary considerably from season to season and spatial sediment distribution in the basin is quite dynamic, which would make it difficult to locate a permanent structure. Furthermore, where a density current forms, large sediment particle (sand and gravel) deposition occurs, which would complicate the flow conditions, suitable for density current formation.

Forcing of density current formation is therefore not considered feasible due to the many boundary conditions which play a role in the natural formation of a sediment induced density current.

7. CALCULATION PROCEDURE TO DETERMINE DENSITY CURRENT FORMATION IN A RESERVOIR

The following calculation procedure is proposed to determine density current formation in a reservoir:

- Obtain a sediment load-discharge rating curve of the river flowing into the reservoir, based on suspended sediment sampling.
- Use the rating curve to determine the long-term sediment load time series flowing into the reservoir
- Obtain a representative reservoir inflow time series of 20 years with at least daily time steps (shorter time steps may be required depending on flood flow variability), preferably from a flow gauging station, adjusted for future development scenarios if required.
- Carry out level pool routing of the reservoir at say hourly time steps over the 20 year period, considering rainfall, evaporation, inflow(s), spillage, environmental flow releases and water firm yield, to obtain the reservoir operational water levels at the dam.
- Use a computational model to simulate the backwater profile, with boundary conditions the water level at the dam and the 20 year inflow record upstream.
- Simulate the sediment transport through the reservoir assuming turbulent sediment transport conditions. The bed load and suspended sediment particle size distribution in the river flow should be known from field observations. A density current typically transports sediment particles smaller than 10 micron in diameter and therefore the river should transport a high percentage of fine sediment (clay and silt) during floods for a density current to form.
- Starting from the upstream end of the reservoir, test for density current formation by using the minimum input stream power approach, equation 2.2-8:

$$\frac{\Delta\rho s_a}{\rho s_f} \leq 1$$

- For the density difference to be sufficient for formation, it is suggested that the suspended sediment concentration upstream of the possible plunge point should be at least 1000 mg/l, and the sediment concentration difference between the river and reservoir should be at least 250 mg/l.
- At locations where plunging are calculated, check for high turbulence conditions that could break up the plunge line. If the above conditions for density current formation are met, the Froude number should also be less than 0.3 and the energy slope at the plunge line should be less than 0.0002.

- Use the densimetric Froude number approach as follows as an alternative to the minimum input stream power approach:
    - For density difference ratio $\frac{d\rho}{\rho}$ range of 0.001 to 0.01, use $Fr_{1,1}$ values of 0.6 to 0.9;
    - For a density difference range of 0.01 to 0.15, use decreasing $Fr_{1,1}$ values from the above range to a range of 0.2 to 0.6 at $\frac{d\rho}{\rho} = 0.15$
    - Do not use the $Fr_{1,1}$ approach at density difference ratios larger than 0.15

  The above recommendations on the use of the densimetric Froude number approach is based on data by Cao (1992) and data of this study (refer to Figure 3.3-8).
- It is not possible at this stage to say which of the two methods to determine density current formation: minimum input stream power or densimetric Froude number, are more accurate than the other.
- If formation of a density current is established based on the conditions set out above during a specific time step, establish whether the formation conditions at a specific location would still be stable during subsequent time steps. Do this for the 20 year simulation period and establish where and when density current formation is predicted.
- Once formation has been established, use a density current sediment transport equation to predict the sediment transport through the reservoir to the dam (Basson and Rooseboom, 1997). Sediment scour from the bed and deposition processes can be included with sediment mass balance.
- Simulate sediment venting operation through bottom outlets. Consider different discharges and timing of releases to maximize sediment outflow with minimum water loss from the reservoir. Determine the long-term density current sediment outflow to river sediment inflow relationship, based on realistic reservoir management rules.

8. CONCLUSIONS AND RECOMMENDATIONS

Flume tests carried out in this study to form sediment induced density currents indicate the following:

a) The inflowing river should transport a relatively high concentration of fine sediment, with particle diameters < 10 to 20 micron in size. Only the fine sediment would be transported by the density current.

b) From the laboratory analysis, density currents did not form at suspended sediment inflow concentrations below 250 mg/ℓ. In field conditions the reservoir suspended sediment concentrations are not zero as analysed in the laboratory, but could be as high as 500 mg/ℓ. Inflow sediment transport at international reservoirs indicated relatively high suspended sediment concentrations in the rivers, and for practical use therefore it is recommended that the river suspended sediment concentration for density current formation should be at least 1 000 mg/ℓ, for Southern African conditions. The difference between river and reservoir sediment concentrations should be at least 250 mg/ℓ.

c) The proposed minimum input stream power principle has been verified successfully against temperature and sediment induced density current laboratory and field data of Gariep, Lake Mead, Guanting and Sanmenxia Reservoirs. The methodology to predict the formation of a density current:

$$\frac{s_o}{sf} < \frac{\rho}{d\rho}$$

has been confirmed and also provides an indication of the formation locality. A density current would form when it would require less stream power (or rate of energy dissipation is less) than that of turbulent suspended sediment transport.

c) The densimetric Froude number does not seem to be not an accurate predictor of density current formation, due to the typical wide range of values from say 0.2 to 0.9. It is however recommended that the densimetric Froude number approach is used as alternative to the minimum input stream power theory, with Fr_1 related to the density difference ratio as proposed in Chapter 7.

e) A plunge line was observed on the water surface under clear water (no sediment transport) conditions. Closer inspection revealed that this plunge line is a stagnation point at the water surface where the horizontal reservoir water surface meets the inflowing river. Since the plunge line formed under clear water conditions and it could be related to where the density current starts to plunge, it should be possible to describe the plunge line without considering the sediment transport. Critical conditions to break up he plunge line have therefore been investigated in the laboratory. Plunge line break up occurred when: $F_r > 0{,}3$ and $S_f > \frac{1}{5000}$ at the plunge line location, and can be used for practical application. The vertical and lateral velocity distribution at the plunge point was investigated and it was found that immediately downstream of the plunge line, the maximum flow velocity is higher at a deeper location than at the plunge line. This downward local diving effect in the flow helps to form a stable density current if the density difference created by the sediment transport is sufficient

f) Forced density current formation have been evaluated and the conclusion is that while it is possible to identify the hydraulic conditions for formation, in general reservoir water levels and spatial sedimentation are too dynamic to propose a specific fixed structure for practical use.

g) From field experience, due to fine sediment availability, the typical sediment outflow to inflow ratio by density currents during floods is 0.20. Ratios up to 0.6 have however also been experienced internationally. About eighty percent of sediments are therefore still trapped in the reservoir if it is a large storage operated reservoir, but the long-term life of a reservoir could be extended by about 25% if the mode of storage operation with density current venting through bottom outlets is adopted.

h) The minimum input stream power methodology can be used with the densimetric Froude number approach, to predict the formation of a density current at a reservoir or turbulent sediment transport through a reservoir. This information can be used to determine the sediment distribution in the reservoir basin for water yield analysis, the sedimentation at and design of outlets, and for the design and operation of density current venting.

Recommended future research:

a) More tests should be carried out in the laboratory with steady density current formation and accurate water level measurements. These tests should be used to calibrate the densimetric Froude number and density difference ratio, and to verify the minimum stream power theory for a wider range of conditions.

b) Field observations should be carried out at a reservoir where theory indicates a high probability of density current formation. Density current venting through bottom outlets should also be monitored.

9. REFERENCES

Akiyama and Stefan, H.G. (1987). Onset of Underflow in Slightly Diverging Channels. *J. Hydr. Engrg. Am. Soc. Civ. Engrs*, 113 (7), pp. 825-844.

Basson, G.R. (1996). The Hydraulics of Reservoir Sedimentation. Ph.D. Dissertation, University of Stellenbosch.

Basson, G.R. and Rooseboom A. (1997). Dealing with Reservoir Sedimentation. South African Water Research Commission Publication No. TT91/97, ISBN 1 8684G 2557.

Bruk, S. (ed.) (1985). Methods of Computing Sedimentation in Lakes and Reservoirs. Unesco. Paris, IHP-11 Project.

Cao, R. (1992). Experimental Study on Density Current with Hyperconcentration of Sediment. *Int. J. Research*. 8 (1).

Dequennois, H. (1956) New Methods of Sediment Control in Reservoirs. *Water Power*, pp. 174-180.

Fan, J. (1960). Experimental Studies on Density Currents. *Scientia Sinica*, 9 (2), pp. 275-303.

Fan. J. (1986). Turbid Density Currents in Reservoirs. *Wat. Int.* 11 (3), pp. 107-116.

Farrell, G.J. and Stefan, H.G. (1986). Buoyancy Induced Plunging Flow into Reservoirs and Coastal Regions. St. Anthony Falls Hydraulic Laboratory, Univ. of Minnesota. Project Report No. 241.

Ford, D.E. and Johnson, M.C. (1980). Field Observations on Density Currents in Impoundments. In: Stefan, H.G. (ed.) Surface Water Impoundments, *Proc. of the symp.Am. Soc. Civ. Engrs.*, 2, Minneapolis, Minnesota, pp. 1239-1248.

Fukuoka, S. and Fukushima, Y. (1980). On Dynamic Behaviour of the Head of the Gravity Current in a Stratified Reservoir. *Proc. Second Int. Symp. on Stratified Reservoir*, Trondheim, Norway, 1, pp. 164-173.

Graf, W.H. (1983). The Hydraulics of Reservoir Sedimentation. *Int. Water Power and Dam Construction*.35, (4),pp. 45-52, April.

Itakura, T. and Kishi, T. (1979). Open Channel Flow with Suspended Sediments. *J. Hydr. Div. Am. Soc. Civ. Engrs.*, 106 (HY8).

Kan, K,. and Tamai, N. (1981). On the Plunging Point and Initial Mixing of the Inflow into Reservoirs. *Proc. 25th Japanese Conf. on Hydr.*, pp. 631-636 (In Japanese).

Rooseboom, A. (1975) Sediment Transport in Rivers and Reservoirs. D.Eng. dissertation, University of Pretoria, (In Afrikaans).

Singh, B. and Shah, C.R. (1971). Plunging Phenomenon of Density Currents in Reservoir. *La Houille Blanche*, 26 (1), pp. 59-64.

Smith, W.O., Vetter, C.P. and Cummings, G.B. (1960). Comprehensive Survey of Sedimentation in Lake Mead, 1948 – 1949. USGS Professional Paper 295, U.S. Government Printing Office.

APPENDIX A

DENSITY CURRENT LABORATORY DATA OF AKIYAMA 1987

Experiment No	Qinflow (cm3/s)	Dr (cm)	Br (cm)	dp (kg/m^3)	pd (kg/m^3)	dp/p	g' (m/s^2)	Dd/Dr	Br/Bd	Dd (cm)	Bd (cm)
1-1	324.76	15.5	6.2	1.897	1001.90	1.90E-03	0.019	0.65	0.86	10.08	7.19
2	473.67	15.4	9.3	1.927	1001.93	1.93E-03	0.019	0.87	0.91	13.40	10.23
3	346.24	16	7	1.693	1001.69	1.69E-03	0.017	0.81	0.90	12.96	7.78
4	542.35	16.1	9.3	2.202	1002.20	2.20E-03	0.022	0.84	0.91	13.52	10.23
5	646.21	16.1	9.7	2.608	1002.61	2.61E-03	0.026	0.78	0.91	12.56	10.67
6	480.57	15.8	9.6	2.012	1002.01	2.01E-03	0.020	0.91	0.93	14.38	10.37
7	363.3	14.7	12	0.854	1000.85	8.54E-04	0.008	0.78	0.94	11.47	12.83
8	553.02	14.8	7.7	3.635	1003.64	3.64E-03	0.036	0.84	0.89	12.43	8.62
9	408.23	14.8	5.9	2.934	1002.93	2.93E-03	0.029	0.80	0.87	11.84	6.78
10	378.7	13.1	6.9	3.498	1003.50	3.50E-03	0.034	0.83	0.89	10.87	7.80
11	546	12.9	9.3	3.6	1003.60	3.60E-03	0.035	0.77	0.92	9.93	10.14
12	607.44	12.9	10.9	4.155	1004.16	4.16E-03	0.041	0.77	0.93	9.93	11.77
13	607.44	13	12.8	3.297	1003.30	3.30E-03	0.032	0.88	0.95	11.44	13.45
14	383.48	12.3	5.8	4.549	1004.55	4.55E-03	0.045	0.73	0.87	8.98	6.67
15	383.48	12.3	6.5	4.203	1004.20	4.20E-03	0.041	0.80	0.89	9.84	7.34
16	573.06	12.3	10.1	4.097	1004.10	4.10E-03	0.040	0.83	0.94	10.21	10.80
17	381.56	14.3	11.5	1.202	1001.20	1.20E-03	0.012	0.86	0.94	12.30	12.20
18	477.55	14.4	13.8	1.261	1001.26	1.26E-03	0.012	0.72	0.93	10.37	14.90
19	326.58	14.8	7	1.369	1001.37	1.37E-03	0.013	0.81	0.91	11.99	7.70
20	624.94	15	13.2	1.533	1001.53	1.53E-03	0.015	0.80	0.94	12.00	14.12
3-1	509.6	14.8	7.5	2.231	1002.23	2.23E-03	0.022	0.86	0.83	12.73	9.08
2	374.96	15.8	12.6	0.511	1000.51	5.11E-04	0.005	0.80	0.91	12.64	13.86
3	417.2	15.9	7.9	1.056	1001.06	1.06E-03	0.010	0.65	0.80	10.34	9.88
4	627.52	16	9.5	1.737	1001.74	1.74E-03	0.017	0.86	0.76	13.76	12.45
5	427.77	15.2	14.4	0.46	1000.46	4.60E-04	0.005	0.85	0.86	12.92	16.71
6	479.05	16.2	9.2	1.381	1001.38	1.38E-03	0.014	0.83	0.80	13.45	11.50
7	496.27	15.9	13.9	0.781	1000.78	7.81E-04	0.008	0.83	0.83	13.20	16.83
8	588.6	15.4	13.1	1.326	1001.33	1.33E-03	0.013	0.85	0.86	13.09	15.20
9	584.08	15.5	10.9	1.542	1001.54	1.54E-03	0.015	0.81	0.81	12.56	13.41
10	676.14	16.6	23.6	0.52	1000.52	5.20E-04	0.005	0.86	0.92	14.28	25.74
11	696.61	16.6	17.9	0.826	1000.83	8.26E-04	0.008	0.82	0.89	13.61	20.23
12	509.6	14.8	9.5	1.647	1001.65	1.65E-03	0.016	0.70	0.86	10.36	11.11
13	540.43	14.9	6.7	3.182	1003.18	3.18E-03	0.031	0.71	0.81	10.58	8.24
7-1	632.75	14.5	9.4	2.167	1002.17	2.17E-03	0.021	0.77	0.56	11.17	16.91
2	632.75	14.5	16.7	1.071	1001.07	1.07E-03	0.011	0.77	0.71	11.17	23.55
3	298.35	14.7	10.4	0.554	1000.55	5.54E-04	0.005	0.75	0.60	11.03	17.33
4	365.93	14.8	13.2	0.649	1000.65	6.49E-04	0.006	0.70	0.69	10.36	19.27
5	550.22	14.9	9	1.457	1001.46	1.46E-03	0.014	0.73	0.55	10.88	16.48
6	365.05	13.9	9	1.126	1001.13	1.13E-03	0.011	0.68	0.55	9.45	16.48
7	575.23	13.9	15.4	1.202	1001.20	1.20E-03	0.012	0.71	0.69	9.87	22.32
8	579.62	13.8	21.5	0.714	1000.71	7.14E-04	0.007	0.86	0.81	11.87	26.67
9	476.65	12.7	11	1.691	1001.69	1.69E-03	0.017	0.66	0.56	8.38	19.57
10	476.65	12.6	12.7	1.459	1001.46	1.46E-03	0.014	0.78	0.65	9.83	19.57
11	599.29	12.8	14.8	1.559	1001.56	1.56E-03	0.015	0.73	0.65	9.34	22.95

APPENDIX B

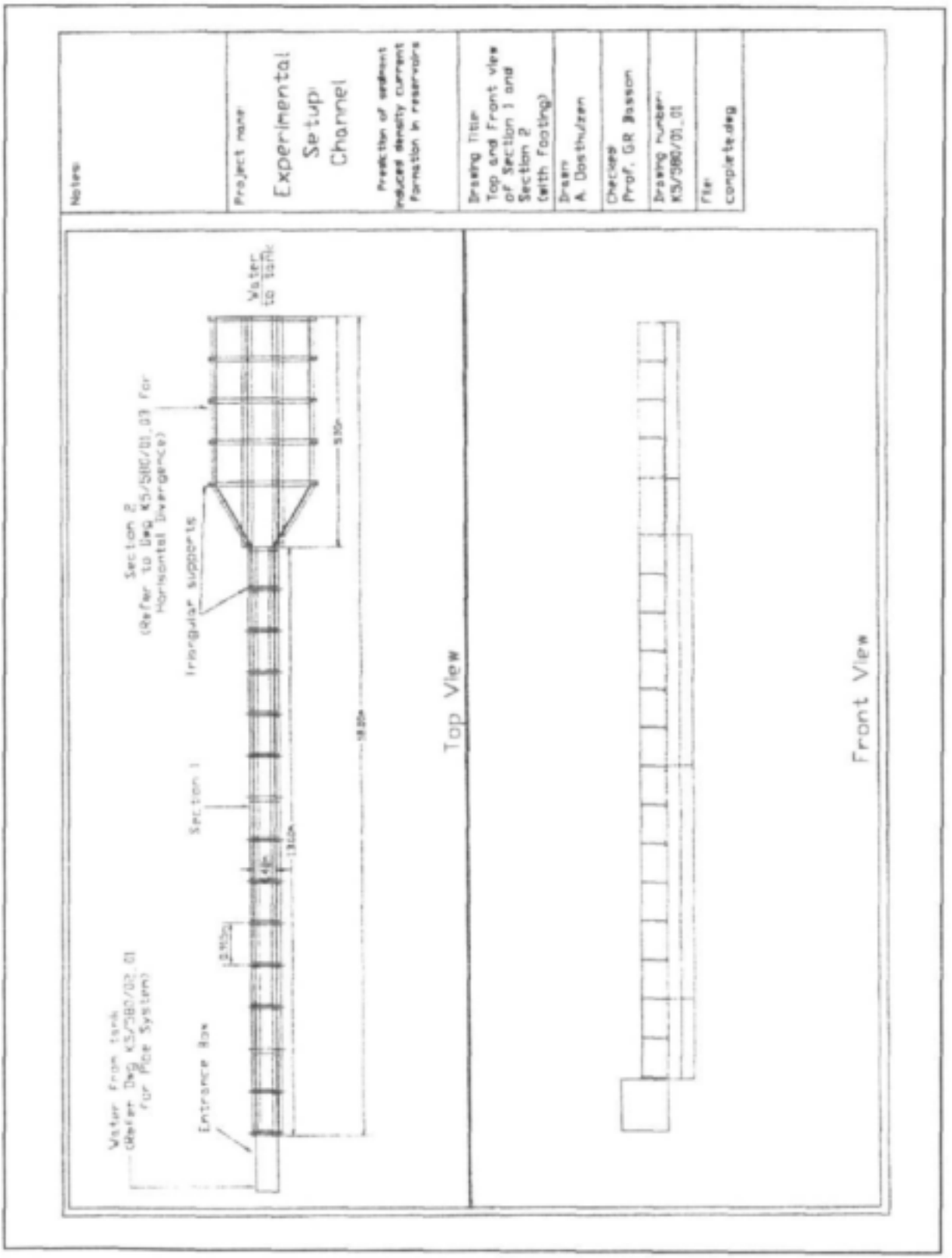
Notes:
Project name
Experimental Setup Channel
Prediction of sediment induced density current Formation in reservoirs
Drawing Title
Top and Front view of Section 1 and Section 2 (with footing)
Drawn
A. Dosthuizen
Checked
Prof. G.R Basson
Drawing number
K5/580/01_01
File
complete.dwg
Water to tank
Section 2
(Refer to Dwg K5/580/01_03 for Horisontal Divergence)
Triangular supports
Section 1
Water from tank
(Refer Dwg K5/580/02_01 for Pipe System)
Entrance Box
Top View
Front View

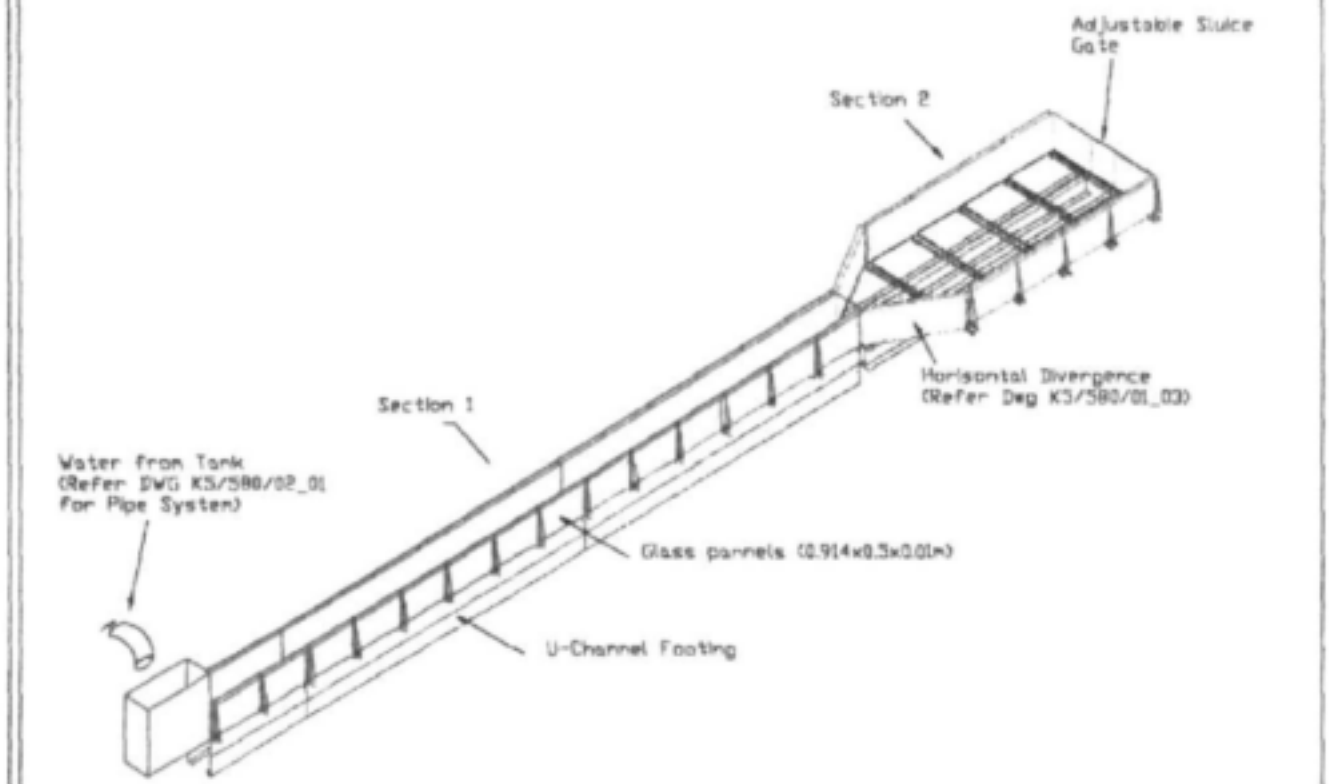

Isometric View

Notes:

Project name:

Experimental Setup: Channel

Prediction of sediment induced density current Formation in reservoirs

Drawing Title:
Isometric View Section 1 and Section 2 (without supports)

Drawn:
A. Oosthuizen

Checked:
Prof. G.R Basson

Drawing number:
K3/580/01_02

File:
dwg1_2.dwg

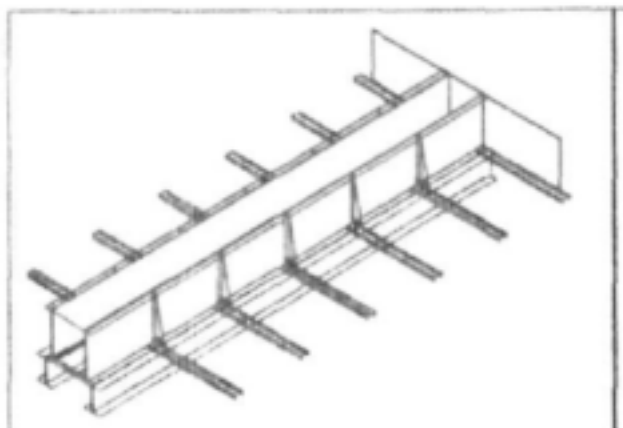

0° Horisontal Divergence

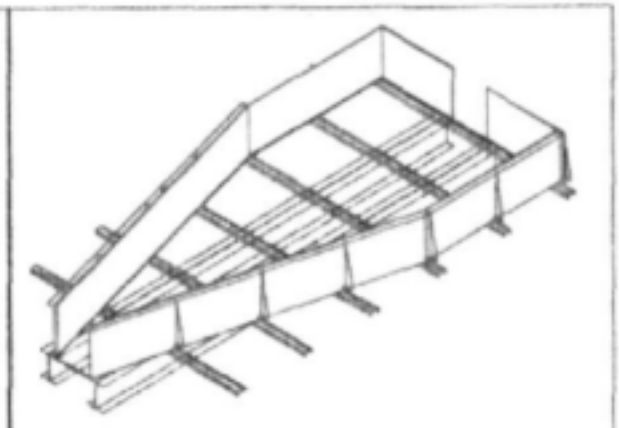

15° Horisontal Divergence

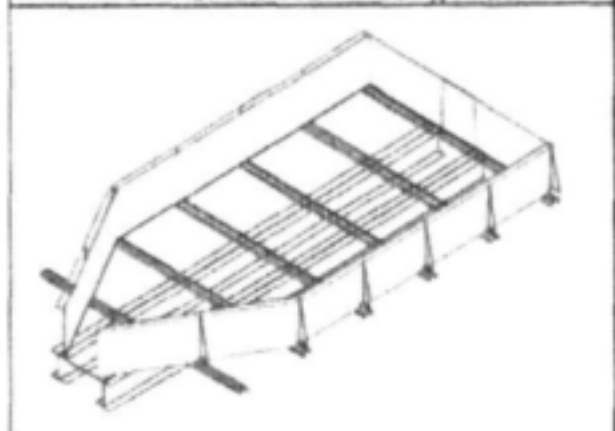

30° Horisontal Divergence

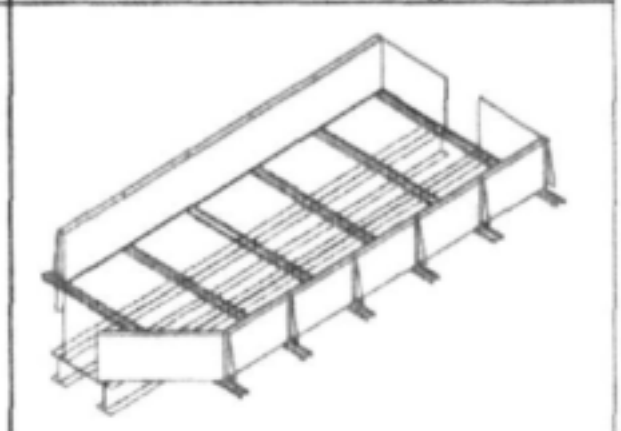

45° Horisontal Divergence

Notes:

Project name:

Experimental Setup: Channel

Prediction of sediment induced density current formation in reservoirs

Drawing Title:
0°-45° Horisontal divergence of section 2 (without supports)

Drawn:
A. Dosthulzen

Checked:
Prof. G.R Basson

Drawing number:
K5/380/01_03

File:
newsect2.dwg

LABORATORY EXPERIMENT DENSITY CURRENT LONGITUDINAL SECTIONS GRAPHS

LONG SECTION EXP. 14

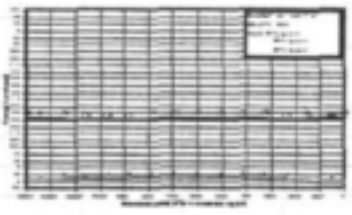

LONG SECTION: EXP. 15

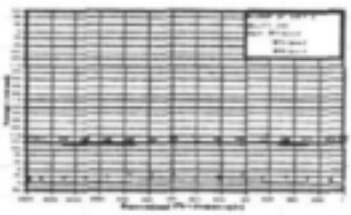

LONG SECTION EXP. 16

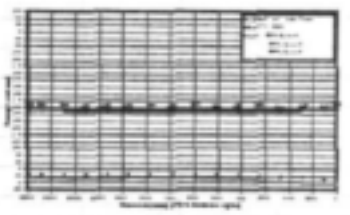

LONG SECTION: EXP. 17

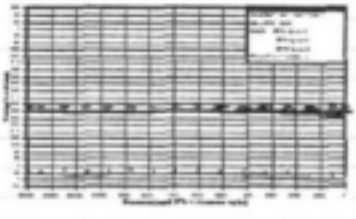

LONG SECTION: EXP. 18

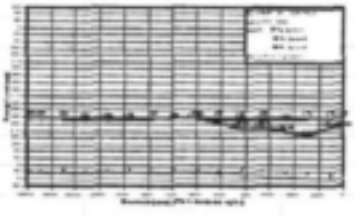

LONG SECTION: EXP. 19

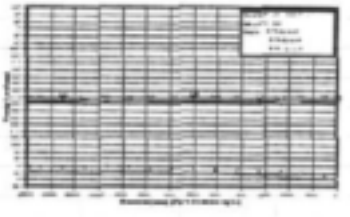

LONG SECTION: EXP. 20

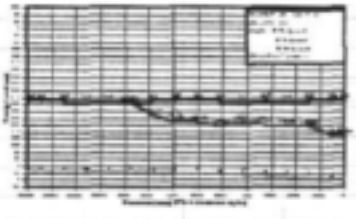

LONG SECTION: EXP. 21

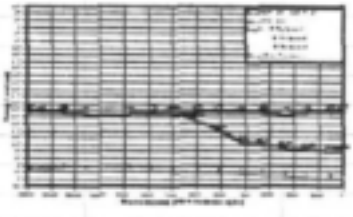

LONG SECTION EXP. 22

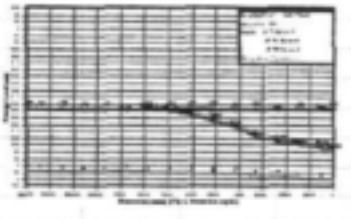

LONG SECTION: EXP. 23

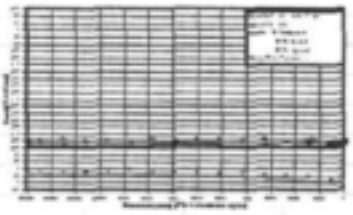

LONG SECTION: EXP. 24

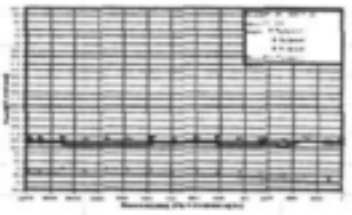

LONG SECTION: EXP. 25

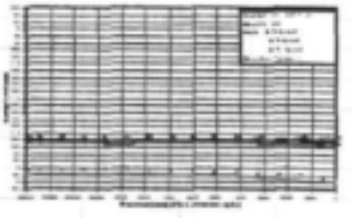

LABORATORY EXPERIMENT DENSITY CURRENT LONGITUDINAL SECTIONS

LONG SECTION EXP 26

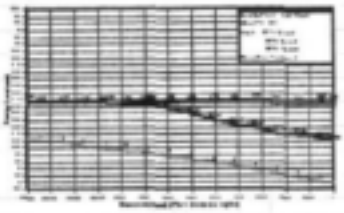

LONG SECTION: EXP. 27

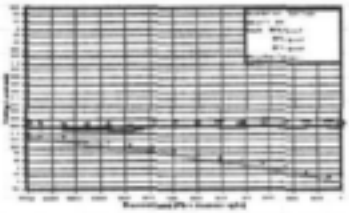

LONG SECTION EXP 28

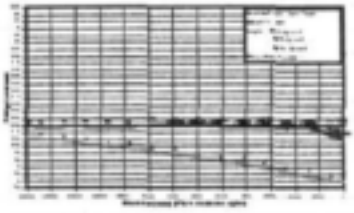

LONG SECTION: EXP. 29

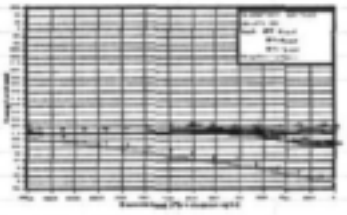

LONG SECTION: EXP. 30

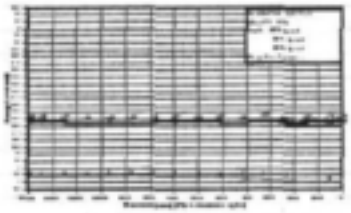

LONG SECTION: EXP. 31

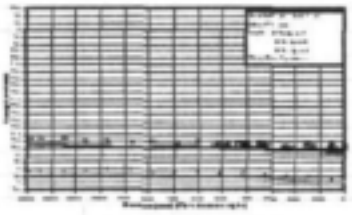

LONG SECTION: EXP. 32

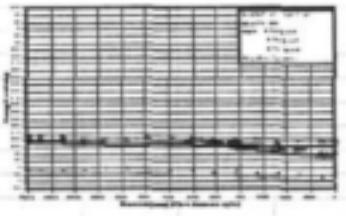

LONG SECTION: EXP. 33

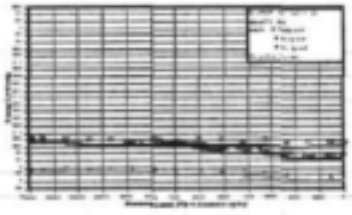

DENSITY CURRENT LABORATORY DATA OF BASSON & OOSTHUIZEN 1998/99

Main data:					Turbulent inflow river data:						Density current data								Reservoir data:		
Setup Type:	Experiment Nr:	Date: (dd/mm/99)	Time (hh:mm)	Q (l/s)	Di(pos2) (mm)	Bi(pos2) (mm)	ρr (kg/m^3)	kr (m)	kappa(r)	Si (p.p)	Formed (Y/N)	Dd (mm)	Bd (mm)	g' (m/s^2)	ρd' (kg/m^3)	hd (m)	kappa(d)	So	Di (mm)	Bi (mm)	ρr (kg/m^3)
C1-1	1	17/12/98	04:30 PM	8.54							N							1E-05			
C1-1	2	19/12/98	08:00 PM	6.57	147.5	454	1006.91	0.02765	0.4	0.0001	Y	85	454	0.12916	993.22	0.02765	0.4	0.01	174	1200	980.14
C1-2	3	20/12/98	01:30 PM	6.57	145	454	1022.89	0.0043	0.4	5E-05	Y	105	454	0.02435	1006.24	0.0043	0.4	0.01	185	1200	1003.7
C1-3	4	20/12/98	06:00 PM	6.57	117	454	1020.62	0.01574	0.4	0.0001	Y	110	454	0.01967	1015.34	0.01574	0.4	0.01	161	1200	1013.3
C1-4	5	8/01/99	11:30 AM	8.24	159	454	993.421	0.12711	0.4	0.0003	Y	250	454	0.01511	986.829	0.12711	0.4	0.01	315	1200	985.31
C3-5	6	13/01/99	03:30 PM	13.3	116.5	454	993.568	ERR	0.4	ERR	N	130	454	0.03521	992.563	ERR	0.4	0.0003	130	1200	989
C3-5	7	13/01/99	09:00 PM	3.06	55	454	989.97	0.00894	0.4	0.0003	Y	45	454	0.05311	987.525	0.00894	0.4	0.0003	64	1200	982.18
C3-2	8	14/01/99	03:00 PM	4.97	64.5	454	1049.45	ERR	0.4	ERR	Y	85	454	0.04171	1047.27	ERR	0.4	0.0003	100	1200	1042.8
C1-3	9	19/01/99	06:00 PM	4.97	170	454	1055.54	0.25358	0.4	0.0002	N	245	454	0.04936	1038.59	0.25358	0.4	0.01	286	1200	1033.4
C1-3	10	19/01/99	07:00 PM	4.97	170	454	1061.21	0.10217	0.4	9E-05	Y	100	454	0.04615	1045.66	0.10217	0.4	0.01	290	1200	1040.7
C1-3	11	20/01/99	02:30 PM	3.1	125	454	1065.5	0.2239	0.4	0.0003	Y	140	454	0.05731	1064.44	0.2239	0.4	0.01	255	1200	1058.2
C3-3	12	20/01/99	07:00 PM	2.1	29	454	1043.11	1.8E-05	0.4	0.0002	N	49	454	0.05323	1035.94	1.8E-05	0.4	0.0003	49	1200	1030.3
C3-3	13	21/01/99	05:30 PM	0.78	54	454	1066.47	0.18004	0.4	0.0003	Y	25	454	0.08954	1035.83	0.18004	0.4	0.0003	85	1200	1026.4
C3-3	14	25/01/99	09:00 PM	4.35	174	454	1091.27	ERR	0.4	ERR	N	174	454	0.04305	1059.64	ERR	0.4	0.0003	184	454	1055
C3-3	15	26/01/99	11:30 PM	4.35	105	454	1081.99	ERR	0.4	ERR	N	105	454	0.01071	1079.65	ERR	0.4	0.0003	118	454	1078.5
C2-3	16	27/01/99	02:30 PM	4.83	203	454	1143.76	ERR	0.4	ERR	N	214	454	0.01198	1143.66	ERR	0.4	0.001	214	454	1142.3
C2-3	17	27/01/99	03:30 PM	4.83	185	454	1136.82	ERR	0.4	ERR	Y	185	454	0.1469	1128.88	ERR	0.4	0.001	200	454	1112
C2-3	18	27/01/99	04:30 PM	4.83	164	454	1134.38	0.21689	0.4	0.0003	Y	150	454	0.08658	1130.53	0.21689	0.4	0.001	178	150	1120.6
C4-3	19	29/01/99	05:00 PM	4.02	202	454	1149.47	0.87406	0.4	0.0019	N	226	454	0.01786	1139.43	0.87406	0.4	0.002	226	454	1137.4
C4-3	20	29/01/99	05:00 PM	4.02	204	454	1118.33	0.95111	0.4	0.0033	Y	130	454	0.08817	1116.99	0.95111	0.4	0.002	230	454	1107
C4-3	21	31/01/99	06:30 PM	4.02	165	454	1131.53	0.72884	0.4	0.0021	Y	80	454	0.02283	1121.45	0.72884	0.4	0.003	193	454	1118.8
C4-3	22	03/02/99	06:00 PM	2.67	179	454	1140.01	0.89232	0.4	0.0017	Y	95	454	0.03021	1132.15	0.89232	0.4	0.002	205	454	1128.7
C4-3	23	03/02/99	08:20 PM	4.55	96	454	1164.7	ERR	0.4	ERR	Y	106	454	0.04916	1133.34	ERR	0.4	0.002	107	454	1127.7
C4-3	24	05/02/99	10:30 PM	4.01	92	454	1122.52	0.16082	0.4	0.0004	N	115	454	0.02082	1121.03	0.16082	0.4	0.002	115	454	1118.6
C4-3	25	05/02/99	11:00 PM	4.01	96	454	1142.49	ERR	0.4	ERR	Y	105	454	0.04546	1139.56	ERR	0.4	0.002	114	454	1134.3
C1-3	26	06/02/99	01:30 PM	2.26	123	454	1112.91	0.6447	0.4	0.0016	Y	125	454	0.11141	1112.33	0.6447	0.4	0.01	229	454	1099.7
C1-3	27	06/02/99	04:00 PM	2.26	65	454	1138.39	ERR	0.4	ERR	N	155	454	0.0019	1138.65	ERR	0.4	0.01	155	454	1138.4
C1-3	28	06/02/99	04:15 PM	2.26	61	454	1209.99	0.12542	0.4	0.0003	Y	130	454	0.02691	1131.26	0.12542	0.4	0.01	157	454	1128.2
C1-3	29	06/02/99	05:30 PM	2.26	47	454	1119.73	0.01765	0.4	7E-05	Y	100	454	0.02167	1103.56	0.01765	0.4	0.01	145	454	1101.1
C2-3	30	08/02/99	07:20 PM	2.5	157	454	1145.14	0.69906	0.4	0.0009	Y	160	454	0.04157	1135.34	0.69906	0.4	0.001	170	454	1130.5
C2-3	31	08/02/99	09:00 PM	2.26	84	454	1171.82	0.2331	0.4	0.0007	Y	90	454	0.032	1140.25	0.2331	0.4	0.001	96	454	1136.5
C2-3	32	08/02/99	09:30 PM	2.26	85	454	1127.13	0.34852	0.4	0.0012	Y	70	454	0.0379	1122.32	0.34852	0.4	0.001	102	454	1118
C2-3	33	08/02/99	10:00 PM	2.26	83	454	1115.19	0.40765	0.4	0.004	Y	65	454	0.02896	1103.31	0.40765	0.4	0.001	100	454	1100.1

Plunge line study by S van der Walt with no sediment

Test by			Plung lyn			ks = 0.002		Plunge	
	Toets	Q(m3/s)	D(m)	V(m/s)	Fr	Sf	V*Sf	line	R
vd Walt	S1	6.4	0.174	0.081017	0.062	3.3E-05	2.64E-06	Y	0.098499
vd Walt	S2	4.8	0.109	0.096997	0.094	4.3E-05	4.15E-06	Y	0.07364
vd Walt	S3	3.3	0.04	0.181718	0.290	0.00011	1.91E-05	Y	0.034007
vd Walt	S4	18.59	0.275	0.148899	0.091	5.6E-05	8.29E-06	Y	0.124353
vd Walt	S5	8.2	0.09	0.200685	0.214	9.3E-05	1.86E-05	Y	0.064448
vd Walt	S6	11	0.175	0.136452	0.106	5.6E-05	7.69E-06	Y	0.098818
vd Walt	S7	7.1	0.08	0.195485	0.221	9.3E-05	1.81E-05	Y	0.059153
vd Walt	S8	25.73	0.205	0.276459	0.195	0.00011	2.99E-05	Y	0.10772
vd Walt	S9	25.73	0.18	0.314856	0.237	0.00013	3.96E-05	Y	0.100393
vd Walt	S10	25.73	0.12	0.472283	0.435	0.0002	9.64E-05	N	0.078501
vd Walt	S11	15.52	0.13	0.262962	0.233	0.00011	2.94E-05	Y	0.082661
vd Walt	S12	15.52	0.109	0.313624	0.303	0.00014	4.34E-05	Y	0.07364
vd Walt	S13	15.52	0.07	0.488357	0.589	0.00024	0.000117	N	0.053502
vd Walt	S14	4.1	0.245	0.036861	0.024	1.4E-06	5.17E-07	Y	0.117828
vd Walt	S15	12.79	0.204	0.138097	0.098	5.4E-05	7.46E-06	Y	0.107443
vd Walt	S16	21.98	0.188	0.257522	0.190	0.0001	2.63E-05	Y	0.102834
Oosthuizen	2	6.57	0.158	0.091591	0.074	3.7E-05	3.43E-06	Y	0.093158
tests with	3	6.57	0.154	0.09397	0.076	3.9E-05	3.63E-06	Y	0.091753
sediment input	4	6.57	0.128	0.113058	0.101	4.8E-05	5.45E-06	Y	0.081848
	5	8.24	0.175	0.103713	0.079	4.2E-05	4.32E-06	Y	0.098818
	6	13.31	0.12	0.24431	0.225	0.00011	2.58E-05	N	0.078501
	7	3.06	0.055	0.122547	0.167	6.4E-05	7.89E-06	Y	0.044273
	8	4.97	0.069	0.158654	0.193	7.8E-05	1.24E-05	Y	0.052916
	9	4.97	0.185	0.059174	0.044	2.4E-05	1.39E-06	N	0.10193
	10	4.97	0.184	0.059496	0.044	2.4E-05	1.41E-06	Y	0.101625
	11	3.1	0.125	0.054626	0.049	2.3E-05	1.28E-06	Y	0.080611
	12	2.1	0.03	0.154185	0.284	9.8E-05	1.51E-05	N	0.026498
	13	0.78	0.054	0.031816	0.044	1.7E-05	5.34E-07	Y	0.043623
	14	4.35	0.175	0.054751	0.042	2.2E-05	1.2E-06	N	0.098818
	15	4.35	0.108	0.088718	0.086	3.9E-05	3.48E-06	N	0.073182
	16	4.831	0.198	0.053742	0.039	2.1E-05	1.14E-06	N	0.105755
	17	4.831	0.187	0.056904	0.042	2.3E-05	1.28E-06	Y	0.102534
	18	4.83	0.164	0.064871	0.051	2.6E-05	1.71E-06	Y	0.095212
	19	4.02	0.205	0.043193	0.030	1.7E-05	7.29E-07	N	0.10772
	20	4.02	0.202	0.043835	0.031	1.7E-05	7.53E-07	Y	0.106886
	21	4.02	0.17	0.052086	0.040	2.1E-05	1.09E-06	Y	0.097204
	22	2.67	0.184	0.031962	0.024	1.3E-05	4.06E-07	Y	0.101625
	23	4.55	0.103	0.097301	0.097	4.3E-05	4.23E-06	Y	0.070852
	24	4.01	0.115	0.076805	0.072	3.3E-05	2.57E-06	N	0.07633
	25	4.01	0.101	0.087451	0.088	3.9E-05	3.43E-06	Y	0.069899
	26	2.264	0.13	0.03836	0.034	1.6E-05	6.25E-07	Y	0.082661
	27	2.26	0.084	0.059262	0.065	2.8E-05	1.65E-06	N	0.061312
	28	2.261	0.085	0.05859	0.064	2.7E-05	1.6E-06	Y	0.061843
	29	2.261	0.083	0.060002	0.066	2.8E-05	1.69E-06	Y	0.060777
	30	2.5	0.162	0.033991	0.027	1.4E-05	4.7E-07	Y	0.094535
	31	2.261	0.084	0.059288	0.065	2.8E-05	1.65E-06	Y	0.061312
	32	2.261	0.09	0.055335	0.059	2.6E-05	1.41E-06	Y	0.064448
	33	2.261	0.078	0.063848	0.073	3E-05	1.95E-06	Y	0.058052

+

Other related WRC reports available:

Dealing with reservoir Sedimentation – Dredging

Basson GR • Rooseboom A

Reservoir sedimentation causes an average annual loss in storage capacity of 130 million m^3 in South Africa. With the high water stress in most catchments, reservoir sedimentation remedial measures such as flushing are usually not feasible due to the lack of excess water. Density current venting, a sedimentation management technique, was investigated in this research project. In density current venting high river sediment loads can be transported through a reservoir and released to the downstream river through bottom outlets, without water level draw-down of over-year storage reservoirs.

A theoretical formulation of minimum stream power at the plunge point is used in this study to predict the formation of the density current. Laboratory application and an assessment of local case studies are used to test the theory and develop recommendations for general practice. An investigation of the cost implications of alternative reservoir sedimentation remedial measures concludes this study.

Report Number: TT 110/99 **ISBN: 1 86845 493 2**

TO ORDER: Contact **Publications** - Telephone No: 012 330 0340
Fax Number: 012 331 2565
E-mail: publications@wrc.org.za

1770050 71X

Water Research Commission
Private Bag X03, Gezina, 0031, South Africa
Tel: +27 12 330 0340, Fax: +27 12 331 2565
Web: http://www.wrc.org.za